

Infocommunications Journal

A PUBLICATION OF THE SCIENTIFIC ASSOCIATION FOR INFOCOMMUNICATIONS (HTE)

September 2020

Volume XII

Number 3

ISSN 2061-2079

MESSAGE FROM THE EDITOR-IN-CHIEF

Signal processing, MIMO and 5G business opportunities –
hear the latest in Infocommunications..... *Pál Varga* 1

PAPERS FROM OPEN CALL

The Processing Algorithm for Wideband Signals Propagating in Media
with Frequency Dispersion..... *Andrei A. Kalshchikov, Vitaliy V. Shtykov and Sergey M. Smolskiy* 2

Blind anti-collision methods for RFID system: a comparative analysis
..... *Chaofu Jing, Zhongqiang Luo, Yan Chen and Xingzhong Xiong* 8

Developing a Noise Awareness Rising Web Application within the “Protect
your Ears” Project..... *Dániel Szántó, Attila Zoltán Jenei, Miklós Gábor Tulics and Klára Vicsi* 17

Detection of 2x2 MIMO signals *János Ladvánszky* 24

Business opportunities and evaluation of non-public 5G cellular networks –
a survey *Gábor Soós, Dániel Ficzer, Tamás Seres, Sándor Veress and István Németh* 31

Modeling the near-field of extremely large aperture arrays in massive
MIMO systems *Botond Tamás Csathó, Bálint Péter Horváth and Péter Horváth* 39

CALL FOR PAPERS / PARTICIPATION

DRCN 2021 / 17th International Conference on Design of Reliable Communication Networks
IEEE ComSoc, Milan, Italy 47

WFloT2021 / 7th IEEE World Forum on the Internet of Things
IEEE World Forum, New Orleans, Louisiana, USA 49

ADDITIONAL

Guidelines for our Authors 48

Technically Co-Sponsored by



Editorial Board

Editor-in-Chief: PÁL VARGA, Budapest University of Technology and Economics (BME), Hungary

Associate Editor-in-Chief: ROLLAND VIDA, Budapest University of Technology and Economics (BME), Hungary

Associate Editor-in-Chief: LÁSZLÓ BACSÁRDI, Budapest University of Technology and Economics (BME), Hungary

- | | |
|---|---|
| JAVIER ARACIL
Universidad Autónoma de Madrid, Spain | MAJA MATIJASEVIC
University of Zagreb, Croatia |
| LUIGI ATZORI
University of Cagliari, Italy | VACLAV MATYAS
Masaryk University, Brno, Czech Republic |
| JÓZSEF BÍRÓ
Budapest University of Technology and Economics, Hungary | OSCAR MAYORA
FBK, Trento, Italy |
| STEFANO BREGNI
Politecnico di Milano, Italy | MIKLÓS MOLNÁR
University of Montpellier, France |
| VESNA CRNOJEVIĆ-BENGIN
University of Novi Sad, Serbia | SZILVIA NAGY
Széchenyi István University of Győr, Hungary |
| KÁROLY FARKAS
Budapest University of Technology and Economics, Hungary | PÉTER ODRY
VTS Subotica, Serbia |
| VIKTORIA FODOR
Royal Technical University, Stockholm | JAUDELICE DE OLIVEIRA
Drexel University, USA |
| EROL GELENBE
Imperial College London, UK | MICHAL PIORO
Warsaw University of Technology, Poland |
| ISTVÁN GÓDOR
Ericsson Hungary Ltd., Budapest, Hungary | ROBERTO SARACCO
Trento Rise, Italy |
| CHRISTIAN GÜTL
Graz University of Technology, Austria | GHEORGHE SEBESTYÉN
Technical University Cluj-Napoca, Romania |
| ANDRÁS HAJDU
University of Debrecen, Hungary | BURKHARD STILLER
University of Zürich, Switzerland |
| LAJOS HANZO
University of Southampton, UK | CSABA A. SZABÓ
Budapest University of Technology and Economics, Hungary |
| THOMAS HEISTRACHER
Salzburg University of Applied Sciences, Austria | GÉZA SZABÓ
Ericsson Hungary Ltd., Budapest, Hungary |
| ATTILA HILT
Nokia Networks, Budapest, Hungary | LÁSZLÓ ZSOLT SZABÓ
Sapientia University, Tirgu Mures, Romania |
| JUKKA HUHTAMÄKI
Tampere University of Technology, Finland | TAMÁS SZIRÁNYI
Institute for Computer Science and Control, Budapest, Hungary |
| SÁNDOR IMRE
Budapest University of Technology and Economics, Hungary | JÁNOS SZTRIK
University of Debrecen, Hungary |
| ANDRZEJ JAJSZCZYK
AGH University of Science and Technology, Krakow, Poland | DAMLA TURGUT
University of Central Florida, USA |
| FRANTISEK JAKAB
Technical University Kosice, Slovakia | ESZTER UDVARY
Budapest University of Technology and Economics, Hungary |
| GÁBOR JÁRÓ
Nokia Networks, Budapest, Hungary | SCOTT VALCOURT
University of New Hampshire, USA |
| KLIMO MARTIN
University of Zilina, Slovakia | JÓZSEF VARGA
Nokia Bell Labs, Budapest, Hungary |
| DUSAN KOCUR
Technical University Kosice, Slovakia | JINSONG WU
Bell Labs Shanghai, China |
| ANDREY KOUCHERYAVY
St. Petersburg State University of Telecommunications, Russia | KE XIONG
Beijing Jiaotong University, China |
| LEVENTE KOVÁCS
Óbuda University, Budapest, Hungary | GERGELY ZÁRUBA
University of Texas at Arlington, USA |

Indexing information

Infocommunications Journal is covered by Inspec, Compendex and Scopus.

Infocommunications Journal is also included in the Thomson Reuters – Web of Science™ Core Collection, Emerging Sources Citation Index (ESCI)

Infocommunications Journal

Technically co-sponsored by IEEE Communications Society and IEEE Hungary Section

Supporters

FERENC VÁGUJHELYI – president, Scientific Association for Infocommunications (HTE)

Editorial Office (Subscription and Advertisements):
Scientific Association for Infocommunications
H-1051 Budapest, Bajcsy-Zsilinszky str. 12, Room: 502
Phone: +36 1 353 1027
E-mail: info@hte.hu • Web: www.hte.hu

Articles can be sent also to the following address:
Budapest University of Technology and Economics
Department of Telecommunications and Media Informatics
Phone: +36 1 463 4189, Fax: +36 1 463 3108
E-mail: pvarga@tmit.bme.hu

Subscription rates for foreign subscribers: 4 issues 10.000 HUF + postage

Publisher: PÉTER NAGY

HU ISSN 2061-2079 • Layout: PLAZMA DS • Printed by: FOM Media

Signal processing, MIMO and 5G business opportunities – hear the latest in Infocommunications

Pal Varga

THE wide scope of Infocommunications Journal is presented in the current, 2020 autumn issue. Unlike the previous special issues this year, readers with wide range of interest find articles in various topics: from signal processing through RFID anti-collision method comparisons, and about an application for educating children on ear protection. As 5G keeps being the hot topic in applied Infocommunications, our journal provides room for disseminating the latest results in this area, repeatedly.

The following paragraphs provide brief overviews of these papers.

In their paper, Kalshchikov, Shtykov, and Smolskiy show a possibility to use the wideband chirp pulse signals in systems of ground penetrating radar sensing under conditions when the concept of the group delay time of the sensing pulses cannot be applied. The proposed signal processing method – that can also be spread to tasks related to the elastic wave propagation – allows the essential reduction of the influence of the frequency dispersion of medium properties upon an accuracy of the object position determination. There could be practical interest for the method when using wideband chirp pulse signals at the presence of medium dispersion. This paper appears within very sad circumstances, since one of the authors, Sergey M. Smolskiy has passed away before its publication.

In their study, Jing, Luo, Chen and Xiong provided a comparative analysis regarding blind anti-collision methods for RFID systems. While the RFID technology is becoming key in various Internet of Things scenarios, its actual development towards better performing equipment should be faster. Although the tags in RFID systems are more and more utilized, all they communicate in the same channel. The reader receives mixed signals, from which the reader cannot always separate the proper message. Such collisions are the main obstacles of RFID system scalability; against which various methods are available – and compared in this article.

Even though hearing is an important sense for humans, we tend to under-estimate effects of destructive stimuli our ears receive. Education on noise awareness is really important, so Szántó, Jenei, Tulics and Vicsi present their results of the "Protect our Ears" project. Playing with heir web application helps children to be more aware in protecting their hearing. Their study shows that children in the test group playing with the web application became more aware of the noise in their surrounding and mastered preventive behavior.

János Ladvánszky investigates synchronization and equalization of 2x2 MIMO signals in his article – making a step further than the related state-of-the-art patent of theirs. The Costas loops used for frequency synchronization fitted the problem very well, and as a result, the standing constellation diagrams appear fast in the output, and remain almost constant for the rest of the measurement interval. Since the input data were real measurements, the analyses here serve as experimental verification, as well.

In their survey paper, Soós, Ficzer, Seres, Veress and Németh describe the business opportunities for non-public 5G cellular networks and evaluate them. They approach the fundamental aspects of 5G's business potential from the aspects and requirements of the Industry 4.0 revolution. They present innovative, 5G-based industrial architectures – and their application benefits through the looking glasses of industrial production and logistics stakeholders, telecommunication equipment vendors, as well as network operators.

As massive MIMO is a key technology in modern cellular wireless communication systems, extremely large aperture arrays are planned to be used in 5G as well. Csathó, B. P. Horváth and P. Horváth present the modeling of the near-field for such extremely large aperture arrays. They compare one- and two-dimensional array models, different antenna element models and antenna geometries through various key design parameters in their model. Among other findings they reveal that by choosing spectral-efficiency as a design objective, the size of the aperture is a critical design parameter.

Enjoy the latest articles of the Infocommunications Journal.



Pal Varga received the M.Sc. and Ph.D. degrees from the Budapest University of Technology and Economics, Hungary, in 1997 and 2011, respectively. He is currently an Associate Professor at the Budapest University of Technology and Economics. Besides, he is also the Director at AITIA International Inc. Earlier, he was working for Ericsson, Hungary, and Tecnomen, Ireland. His main research interests include communication systems, network performance measurements, root cause analysis, fault localisation, traffic classification, end-to-end QoS and SLA issues, as well as hardware acceleration. Recently he has been actively engaged with research related to Cyber-Physical Systems and Industrial Internet of Things. He has been involved in various industrial as well as European research and development projects in these topics. Besides being a member of HTE, he is a member of both the IEEE ComSoc (Communication Society) and IEEE IES (Industrial Electronics Society) communities, and the Editor-in-Chief of the Infocommunications Journal.

The Processing Algorithm for Wideband Signals Propagating in Media with Frequency Dispersion

Andrei A. Kalshchikov, *Student Member IEEE*, Vitaly V. Shtykov and Sergey M. Smolskiy, *Member IEEE*¹

Abstract— The new processing algorithm for wideband signals, which are propagating in frequency dispersion media, is developed in the context of the ground penetrating radar technology. The mathematical substantiation of offered method is presented on the base of linear functional spaces. The method is described for calculation acceleration on the base of the recursive approach. Results of numerical modeling of this method are presented for electromagnetic waves propagating in frequency dispersion media at utilization of chirp pulse signals. The Debye model is used as the model of electrical medium properties. The frequency dispersion of losses in the medium is taken into consideration at modeling. Results of operation modeling of the ground penetrating radar are described. Results of this paper will be useful for the ground penetrating radar technology and the ultrasonic flaw detection.

Index Terms—phase velocity, frequency dispersion, phase correction, ground penetrating radar technology, ultrasonic flaw inspection.

I. INTRODUCTION

An increase of the radio systems noise-immunity and effectiveness takes the central place in the modern theory and engineering of information transmission. During the growth of the information transmission rate, we see the effect increase of dispersion characteristics of the communication channel. This increase is manifested in distortions of the transmitting signal shape. These distortions can make impossible to extract of transmitted information from the received signal.

The complex transfer function of the channel route with the length L [1] for the plain wave is

$$\tilde{K}(j\omega, L) = \exp[-j\uparrow(\omega)L], \quad (1)$$

where $\uparrow(\omega) = \beta(\omega) - j\alpha(\omega)$ is the complex propagation constant, $\beta(\omega)$ is the phase constant, $\alpha(\omega)$ is the damping constant.

Signal distortions after passage through the channel route are caused by disturbances of the amplitude-phase relations between its spectral components.

The phase constant $\beta(\omega)$ in (1) can be expanded into the power series around the frequency of the carrier oscillation ω_0 :

$$\beta(\omega) = \beta(\omega_0) + \frac{d\beta}{d\omega} \Omega + \frac{d^2\beta}{2d\omega^2} \Omega^2 + \dots \text{Rem}_n(\Omega).$$

where $\Omega = \omega - \omega_0$, $\text{Rem}_n(\Omega) \leq \frac{|\Omega|^n}{n!} \sup_{0 < \varepsilon < \Omega} \left| \frac{d^n h}{d\omega^n} \right|_{\varepsilon}$ is the series remainder.

For the case of the weak dispersion, we may be limited by the first term and can introduce the group velocity:

$$V_{gr}(\omega) = \frac{d\omega}{d\beta}.$$

For the channel route of the given length L , we can introduce the group delay time:

$$\tau_{gr} = \frac{d\beta}{d\omega} L.$$

With this very convenient approximation, the signal envelope (at bottom of fact, information) propagates through the channel route with the group velocity practically without distortions.

Using $\text{Rem}_n(\Omega)$, we can estimate the relative error of this approximation as follows:

$$\delta_\beta \approx \delta_\Omega \omega_0 \left| \frac{d^2\beta}{d\omega^2} \Big|_{\omega_0} \right| / \left| \frac{d\beta}{d\omega} \Big|_{\omega_0} \right|, \quad (2)$$

where δ_Ω is the relative frequency bandwidth of the signal spectrum.

However, this condition is necessary but not sufficient. The thing is that the real and imaginary parts of the substance permittivity are connected with each other by the Kramers-Kronig relations. This means that the dispersion of the phase velocity inevitably accompanies by the damping index $\alpha(\omega)$ dispersion. Therefore, for the relevancy of the group velocity approximation, the following equality is necessary:

$$\delta_\alpha = \delta_\Omega \frac{\omega_0}{\alpha(\omega_0)} \frac{d\alpha}{d\omega}. \quad (3)$$

With transfer to wideband and ultra-wideband signals, the error of the group velocity approximation becomes so much that its application becomes impossible at signal processing.

In traditional radar technology with strongly expressed frequency dispersion, we can meet not very often, for example, in tasks of electromagnetic wave propagation in an ionosphere [2], or in tasks of the radar ground penetrating sensing [3,4]. In the sonar technology and especially in the

¹ Andrei A. Kalshchikov is with Moscow Power Engineering Institute (National Research University), Russia (e-mail: KalschikovAA@gmail.com).

Vitaly V. Shtykov is with Moscow Power Engineering Institute (National Research University), Russia (e-mail: ShtykovVV@yandex.ru).

Sergey M. Smolskiy is with Moscow Power Engineering Institute (National Research University), Russia (e-mail: SmolskiySM@mail.ru).

ultrasonic flaw inspection, we can practically often meet with the frequency dispersion of the elastic wave velocity.

Firstly, the frequency dispersion leads to the shape distortion of the probing pulse, and secondly, leads to disturbance of the direct proportional connection between the delay time of the reflected signal and the distance to the sensing object [5]. In the radar ground penetrating technology, this complicates the deciphering of received data. The problem of the phase velocity dispersion influence is discussed in [6,7,8]. The necessity to develop the signal processing methods, which can decrease its distortions and increase the accuracy of objects' sensing remains very relevant. In this paper, we describe of the one of possible methods of signal processing at the presence of the frequency dispersion in the route of its propagation.

II. MATHEMATICAL SUBSTANTIATION OF THE OFFERED METHOD

If the phase constant $\beta(\omega)$ and the route length L are known, which is typical for the communication channel, the task of signal distortion correction can be solved. To decrease the influence of the frequency dispersion, different methods of the filter-corrector synthesis are actively developed both in time and frequency domains. For the transmission line without losses, such a filter, as a matter of fact, represents the phase corrector with the phase-frequency response of the following type:

$$\Phi_{cor}(\omega) = \beta(\omega)L.$$

The task can be also solved if the transmitted signal shape and $\eta(\omega)$ are given, while the route length L is unknown and is a subject to determination. In this case, the initial signal reconstruction is not required, and L (the sensing object position) can be determined using the cross-correlation function $\Psi(t, L, z)$ of the received signal $r(t, L)$ and the trial function – the signal model $s(t, z)$:

$$\Psi(t, L, z) = r(t, L) * s(t, z). \tag{4}$$

This situation is typical for manifold radar systems.

Considering (4) as an equation for reconstruction of the $r(t, L)$ function, we come to the known procedure of the deconvolution.

The function $\Psi(t, L, z)$ represents the surface above the plane $\langle t0z \rangle$. The determination of the L value is reduced to the search of the global maximum position of this surface: $\Psi_M(t_M, z_M = L)$. However, such the search procedure requires the large time expenses and the large volume of the processor memory, while the abscissa value t_M does not any interest for us. Therefore, we can try to accelerate this procedure by excluding the variable t from the equation (4).

III. INITIAL RELATIONSHIPS OF THE OFFERED ALGORITHM

In order to exclude time from the equation (4), we make use the generalized signal theory [8].

Let us form on the base of trial functions $s(t, z)$ the $M = \{s(t, z_1), s(t, z_2), s(t, z_3), \dots\}$ infinite-dimension linear set, which, in the general case, forms the linear, complex functional space [8,9]. In this space, we can form the scalar product of the signal and the trial function:

$$W(z) = \int_{-\infty}^{\infty} r(t, L) s^*(t, z) dt, \tag{5}$$

which, in essence, represents the mutual energy. According to the Cauchy–Schwarz inequality:

$$|W(z)|^2 \leq \|r\|^2 \cdot \|s\|^2,$$

where $\|r\|^2 = \left| \int_{-\infty}^{\infty} r(t, L) r^*(t, L) dt \right|$ and

$\|s\|^2 = \left| \int_{-\infty}^{\infty} s(t, z) s^*(t, z) dt \right|$ is the energy of the signal and the trial function, relatively.

The equality is fulfilled if:

$$s(t, L) \equiv r(t, z).$$

Thus, the variation of the functional (5) solves the problem of L determination.

If to make use the generalized Rayleigh's energy theorem [8], then the functional (5) can be transformed to the form:

$$W(z) = \int_{-\infty}^{\infty} R(\omega, L) S^*(\omega, z) d\omega, \tag{6}$$

where $R(\omega, L)$ and $S(\omega, z)$ are spectral densities of the signal and the trial function, relatively.

If $\eta(\omega)$ is known, and the shape of the transmitted signal – the probing pulse (PP) $y(t)$ and its spectral density $Y(\omega)$ – are known, the spectral density of the trial function is:

$$S(\omega, z) = Y(\omega) \exp[-j2\eta(\omega)z].$$

Substituting this in (6), we obtain:

$$W(z) = \int_{-\infty}^{\infty} R(\omega, L) Y^*(\omega) \exp[j2\eta(\omega)z] d\omega. \tag{7}$$

Thus, the procedure of the distance search to the object can be performed both in the space-time (6) and the frequency domains (7). In the first case, it is necessary to transform the trial function spectrum $S(\omega, z)$ into the pulse characteristic of the filter-corrector $h(t, z)$. In the second case, we need to transform the received signal $r(t, L)$ into the spectral function $R(\omega, L)$.

IV. THE SOFTWARE REALIZATION OF THE ALGORITHM

Functionals (6) and (7) do not contain time in the explicit form. Therefore, at digital implementation of the algorithm, the operation of L determination can be performed

The Processing Algorithm for Wideband Signals Propagating in Media with Frequency Dispersion

independently on the operation of other parts of the system, using stored in the separate memory buffer of the signal, which is received on the next stage of the radar operation.

Since the object position is unknown in advance and the receiver signal shape differs from PP, the search in the distance can be performed only on the signal sample with the duration not less than $T_D \leq 2D/V_{gr}$, where D and V_{gr} are the system operation distance and the group velocity on the central frequency, relatively.

The functional flow block-diagram is shown in Figure 1.

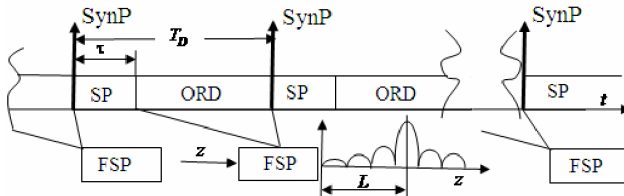


Figure 1. The functional flow block-diagram of the system: SynP is the synchronization pulse, SP is the radiation interval τ of the sensing pulse, ORD is the operation distance range, FSP is the flow of signal processing

The upper part of the diagram represents the flow of data recording, which are recorded into the memory buffer for the further parallel processing.

As the example, we examine the spectral method of the object position determination. The functional (6) in the discrete form has the form:

$$\mathcal{W}_n = \Delta\omega \sum_{m=0}^{M-1} \hat{R}_m \mathcal{S}_{m,n}^* \quad (8)$$

where $\hat{R}_m = \hat{R}(\omega_m)$, $\mathcal{S}_{m,n} = \mathcal{Y}(\omega_m) \exp(-j2\eta_m n \Delta z)$, $n = 0, N-1$. For discrete samples \mathcal{W}_n the recurrent relation acts:

$$\mathcal{W}_{n+1} = \Delta\omega \sum_{m=0}^{M-1} \mathcal{W}_n \exp(-j2\eta_m \Delta z), \quad (9)$$

which allows the acceleration of the functional values calculation.

The number of samples M and the discretization frequency $f_d = 1/\tau_d$ are determined as usual. As to the step in Δz , it is determined by the spatial spread of the SP autocorrelation function.

V. PRELIMINARY PREREQUISITES TO THE ALGORITHM MODELING

In the ground penetrating radar (GPR), two operating modes are used [3,4,10]: the pulse mode and the Continuous Wave GPR (CW-GPR) mode. Both in the first and in the second case, the ultra-wideband sensing pulses are used.

In the pulse GPR, these are radio pulses containing the pair or of periods of the carrier frequency. In CW-GPR, the signal with linear frequency modulation is used or the train of short pulses, which frequency varies in the wide limits by steps (the Step Frequency GPR - SF-GPR) [3,10,11].

As the illustration of the offered method, we perform the numerical modeling for the signal with the linear frequency modulation of the following type:

$$u(t) = U_m \exp[-(t/\tau)^2 \cos[2\pi f_0(t/\tau) - \pi B(t/\tau)^2]], \quad (10)$$

where U_m is the SP amplitude, τ is the pulse duration on the level of e^{-1} , f_0 is the frequency of the carrier oscillation, B the signal base.

The signal choice in the form of (10) is caused by the fact that its' spectral density is expressed through the elementary functions. This allows the presentation of the trial function in the form of the formula avoiding the utilization of the Fourier transform.

For the sake of more generalization achievement, we use further the normalized time $t = t/\tau$, the non-dimension frequency of the carrier oscillation $F_0 = f_0\tau$ and non-dimension co-ordinate $z = z/\lambda_0$, where $\lambda_0 = C/f_0$ is the wavelength in the vacuum, and C is the light speed.

To describe the electrical properties of the humid soil, we use models, which take into consideration the orientation polarization and the ionic conduction [3,6,7,12,13]. In conformity with tasks of the ground penetrating radar, parameters of such models are obtained as the result of the numerous experiments.

The orientation polarization is described by the Debye model:

$$\epsilon(\omega) = \epsilon_\infty + \frac{\epsilon_{st} - \epsilon_\infty}{1 + j\omega\tau_{rl}} = \epsilon_\infty + \frac{\epsilon_{st} - \epsilon_\infty}{1 + j2\pi FT_{rl}}, \quad (11)$$

where ϵ_∞ and ϵ_{st} is the relative permittivity at $\omega \rightarrow \infty$ and $\omega = 0$, relatively; τ_{rl} in the relaxation time of the orientation polarization, $T_{rl} = \tau_{rl}f_0$.

To illustrate the possibilities of the above-described method, we can be limited by the single-component medium model. For numerical modeling, we use parameters of the hypothetic medium presented in [13]. We take in (11):

$\epsilon_{st} = 8.1$, $\epsilon_\infty = 5.7$, $\tau_{rl} = 22$ ps. For the frequency f_0 about 100 MHz, T_{rl} has an order of 10^{-3} .

VI. NUMERICAL MODELING OF THE METHOD

The modeling software consists of two parts. The first one imitates the SP propagation in the route and operation of the homodyne receiver. The second part is the processing algorithm itself.

At signal modeling $f_0\tau = 128$, $B = 32$ ($\delta_\omega = 25\%$). In the medium model (11) we use $T_{rl} = 0.002$.

Results of signal modeling received from the distance $L = 64$ wavelengths are presented in Figure 2. The first pulse corresponds to SP propagation at the dispersion absence ($T_{rl} = 0$), and the second – to its presence. We will see that

the SP shape is essentially distorted owing to the frequency dispersion of the medium parameters (see Figure 2b).

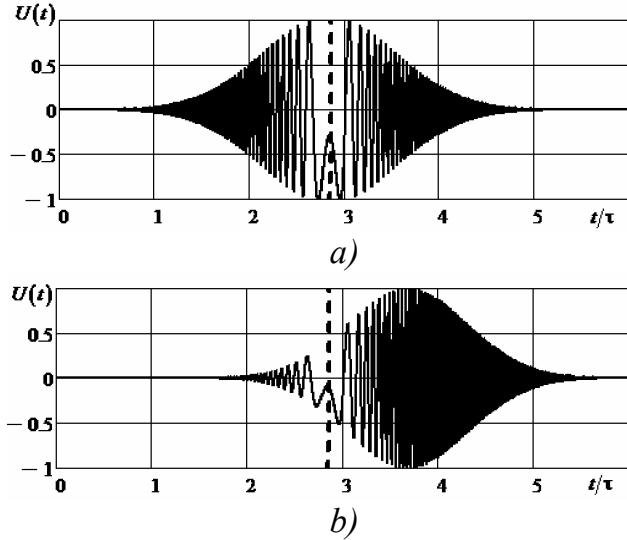


Figure 2. The signal in the receiver output at the absence (a) and at the presence (b) of the phase velocity dispersion, the dotted line corresponds to $t_{gr} = L/V_{gr}$

The delay of the first pulse is equal to $t_{gr} = L/V_{gr} = 2.846$. The group delay time of the second pulse does not practically differ from $t_{gr} = 2.846$. The error estimation in accordance with (2) gives $\delta_{\beta} \approx 3 \cdot 10^{-5}$. It would seem that the group velocity approximation may be fully used. However, the signal shape in Figure 2b essentially differs from SP.

Distortions are the result of the frequency dependence of the damping index. For SP of the (10) type in the region $t > t_{gr}$, the instantaneous frequency is less than f_0 and the wave is less while for $t < t_{gr}$ the situation is opposite. The error estimation in accordance with (3) gives $\delta_{\alpha} \approx 0.5$. Obviously that the group velocity approximation cannot be used for the used SP and the medium parameters.

Thus, in spite of the fact that the group velocity is known, the distance determination to the object in the time domain is impossible.

Figure 3 shows the result of the numerical modeling of the above-described method of the object detection in the medium with the frequency dispersion. The object is situated on the depth of 64 wavelength.

The plot of the mutual energy displaces directly in coordinates of the geometrical space. We see that the signal can be well compressed, which guarantees an accuracy of object position determination.

Modeling results of the stepwise operation mode for GPR are presented in Figures 4 and 5.

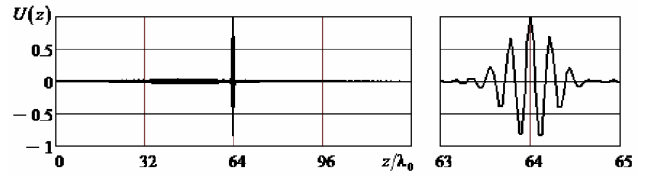


Figure 3. The modeling result of the method of distance determination to the object in the medium with the frequency dispersion

Figure 4 shows the totality of GPR routes at its displacements in the horizontal direction. The depth of the object bedding (the equivalent reflection point) is $z_{obj} = 24\lambda_0$. The peculiarity of Figure 4 consists in the fact that the algorithm described presents routes directly in co-ordinates depth-displacement.

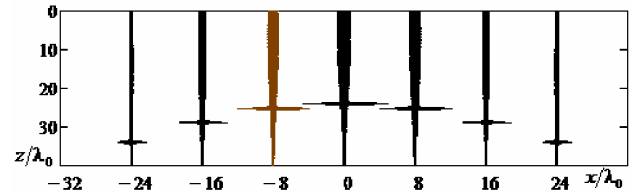


Figure 4. The set of GPR routes at its displacements along the horizontal axis

The result of the model signal processing in the form of the total image is presented in Figure 5.

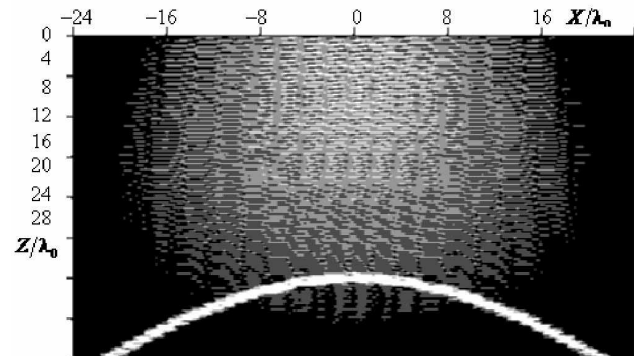


Figure 5. The graphical representation of modeling results.

As in Figure 4, the result presents directly in the geometrical space. The parabolic profile is clearly seen in the figure. Its peak corresponds to the object bedding depth.

VII. CONCLUSIONS

We have shown a possibility to use the wideband chirp pulse signals in systems of ground penetrating radar sensing under conditions when we cannot apply the conception of the group delay time of the sensing pulses.

The offered method of signal processing allows the essential reduction of the influence of the frequency dispersion of medium properties upon an accuracy of the object position determination. Since the one of the distinguished features is the presentation of signal processing results of the geo-radar directly in natural geometrical space instead of “time-

The Processing Algorithm for Wideband Signals Propagating in Media with Frequency Dispersion

horizontal displacement” space. The algorithm’s peculiarity consists also in the fact that such data presentation is performed by the single pulse. Hence, using the set of such pulses, we can perform the data accumulation. This will permit to increase the geo-radar noise immunity and to improve its energy characteristics. In the aggregate, all this accelerates the analysis process of received data.

The method verification is performed by the numerical modeling, and the stepwise operation mode of the geo-radar is checked by the imitation on PC. Obtained results demonstrate a reliability of the object position determination.

This method can be spread to tasks related to the elastic wave propagation.

Thus, we can assume that the offered signal processing method of the wideband chirp pulse signals at the presence of medium dispersion will attract practical interest.

REFERENCES

- [1] Günther Lehner. *Electromagnetic Field Theory for Engineers and Physicists*//Translated by Matt Horre, ISBN 978-3-540-76305-5, e-ISBN 978-3-540-76306-2, Springer Heidelberg, Dordrecht, London, New York. Springer-Verlag, Berlin, Heidelberg. 2010. doi: 10.1007/978-3-540-76306-2
- [2] P. M. Kintner, B. M. Ledvina. The ionosphere, radio navigation, and global navigation satellite systems. *Advances in Space Research*, №35, 2005.
- [3] *Ground Penetrating Radar Theory And Applications* // Edited By Harry M. Jol. Elsevier Science, First Edition. 2009.
- [4] *Problems of ground penetrating radar technology* (in Russian). Collective book / Under edition of A.Yu. Griniov. - Moscow: Radiotekhnika Publ., 2005. 416 p.: (Series “Radar Technology”)
- [5] A.P. Annan, Transmission Dispersion and GPR. *JEEG*, v.0, №2, January 1996, p. 125-136
- [6] Parametric study on processing GPR signals to get a dispersion curve X. Xiao, A.Ihamouten, G. Villain, X. Dérobert. 15th International Conference on Ground Penetrating Radar. GPR 2014, June 30 – July 4, 2014 Square Brussels Meeting Centre, Brussels, Belgium.
- [7] Detection and Target-Shape Recognition in Lossy and Dispersive Soil. Khalid M. Ibrahim1, Y. Khalid F. A. Hussein, and Abd-El-Hadi A. Amman Land-Buried Object Progress In Electromagnetics Research B, Vol. 57, 279-298, 2014
- [8] S. I. Baskakov, Signals and Circuits, Mir Publishers, Moscow, 1987.
- [9] *Mathematical Handbook For Scientists And Engineers Definitions, Theorems And Formulas*. 2nd edition. New York: McGraw-Hill, 1968.
- [10] *Application of Ground Penetrating Radar to Civil and Geotechnical Engineering*. Richard J. Yelf, *Electromagnetic Phenomena*, V.7, №1 (18), 2007
- [11] LFM ground penetrating radar with increased resolution capability (in Russian) A.S. Lopatchenko, I.Yu. Malevich, S.A. Savenko. Belorussia State University of Informatics and radio-electronics Publ. №3, 2015, 9. pp.43-48.
- [12] Chun An Tsai, Rebecca Ghent, Alexander Boivin, and Dylan Hickson, “Discrimination of dispersive materials from radar signals using Q*,” *Ground Penetrating Radar*, Volume 2, Issue 1, March 2019, pp. 26-50, doi: 10.26376/GPR2019EP1/
- [13] Frequency-dependent attenuation analysis of groundpenetrating radar data. John H. Bradford. *Geophysics*, vol. 72, №3 _may-june 2007; p. 7–16, 8 figs., 1 table. doi: 10.1190/1.2710183



Andrei A. KALSHCHIKOV, born in 1994 in Ufa-city (Russia). Graduated with honor in 2016 National Research University “Moscow Power Engineering Institute” in specialty “Radio Electronic Systems and Complexes”. From 2016 he is the PhDstudent of the Radio Engineering Fundamentals Department in NRU MPEI. He is engaged in development of compensation methods for signal distortions in transmission lines with the phase speed dispersion. He has several publications in Russian scientific journals. Worked in 2015 as a technician in R&D Institute of Radio Engineering, and from 2016 fulfils the job of the engineer in the Department of A-D converters and signal processing. Participated in R&D projects and testing of new radar stations. The current interests are fight with active noisy interferences, processing of moving targets, equalization of multi-channel systems, matched filtering, correction of signal propagating in media with the phase speed dispersion.



Vitaly V. SHTYKOV graduated from Radio Engineering Faculty of Moscow Power Engineering Institute (Technical University) in 1963. He had got Ph.D. (Techn.) in 1970. From 1963 he was a teacher of Department of Fundamentals of Radio Engineering of MPEI. Now he works as a full-professor of this department. He delivers various lecture courses in Theoretical Fundamentals of Radio Engineering, Radio Engineering Circuits and Signals, Electrodynamics. He prepared lecture courses in Advanced Physics, Radio Physics, Functional Electronics, Acoustic-Electronics, Quantum Electronics, Biophysics. He has more than 200 scientific and academic publications, 21 patents. Scientific results of V.V. Shtykov are connected with investigations of new physical principles of signal detection and processing. He examined problems of quantum electronics, nonlinear phenomena in the plasma of gas discharge and semiconductors, in ferrimagnetic media, and also in the field of acoustic electronics.



Sergey M. SMOLSKIY, born in 1946, Ph.D. in Engineering, Dr.Sc. in Engineering, full professor of Department of Radio Signals Formation and Processing of the National Research University “MPEI”. He was engaged in theoretical and practical problems of development of transmitting cascades of short-range radar. In 1993 defended the Doctor of Science thesis and now he works as a professor of Radio Signals Formation and Processing Dept. Academic experience - over forty years. The list of scientific works and inventions contains over three hundreds of scientific papers, 15 books, more than 100 technological reports on various conferences, including international. The active member of International Academy of Informatization, International Academy of Electrotechnical Sciences, International Academy of Sciences of Higher Educational Institutions. The active member of IEEE. The scientific work for the latter fifteen years is connected with conversion directions of short-range radar systems, radio measuring systems for fuel and energy complex, radio monitoring system etc.



In memory of
Sergey M. Smolskiy
1946 – 2020

Sergey M. Smolskiy

1946 – 2020

Sergey M. Smolskiy passed away on April 29 2020. He was a great professional with a rich creative, scientific, pedagogical and organizational biography, Honorary Academician of the Academy of Electrotechnical Sciences of the Russian Federation, Honorary Worker of Professional Education of the Russian Federation, Eminent Radio Engineer of the Russian Federation, Doctor of Technical Sciences, Emeritus Professor of the National Research University "Moscow Power Engineering Institute".

Sergey M. Smolskiy was born on January 2, 1946 in Moscow. In 1964 he entered the faculty of Radio Engineering of Moscow Power Engineering Institute which he graduated from in 1970 with a degree in Radio Physics. Already in his student years he became an R&D staff member of the department of radio transmitting devices and showed a propensity for scientific research and development. Under the guidance of V.M. Bogachev he achieved his first significant results. In 1970-1973 he pursued his postgraduate studies at MPEI with excellent academic performance.

After graduating and obtaining the degree of Candidate of Technical Sciences in 1974, he continued scientific work in the same department on theoretical and practical issues of radio transmitters, problems of the theory of frequency-modulated generators and autodyne. He was a responsible executor and scientific adviser of numerous research projects, including those carried out according to the decrees of the Government of the USSR.

Particular mention should be made of the last almost twenty-year period of Sergey M. Smolskiy's life. It was a period of his serious illness and at the same time a period of amazing creative activity.

Professor of the Department of Signal Formation and Processing since 2006 S.M. Smolskiy worked continuously until the last days of his life. He was the scientific director of a number of competitive projects of the Russian Foundation for Basic Research, Russian Scientific Foundation and the Ministry of Education and Science of the Russian Federation, he was a member of the Organizing Committee of a number of annual international scientific conferences and constantly interacted with colleagues from MPEI and other domestic and foreign universities and scientific organizations. During this period the number of scientific articles published by him doubled (more than 300), 15 original voluminous books were published in co-authorship, 11 of them were published in English in leading foreign scientific publishing houses. The latest book on quantum electronics and nonlinear optics, co-authored with Professor V.V. Shtikov, was released in early 2020.

In addition, Sergey M. Smolskiy translated from English into Russian and published 3 original books by foreign authors with a total volume of more than 1000 pages. At least 6 books translated by him into Russian with a total volume of about 2000 pages have not yet found their publishers, but are in use by colleagues.

The loss of Sergey M. Smolskiy is irreparable. The memory of a talented scientist, teacher, organizer and simply amazing, friendly, caring person will forever remain in our hearts.

Blind anti-collision methods for RFID system: a comparative analysis

Chaofu Jing, Zhongqiang Luo, Yan Chen, and Xingzhong Xiong

Abstract— Radio Frequency Identification (RFID) is one of the critical technologies of the Internet of Things (IoT). With the rapid development of IoT and the extensive use of RFID in our life, the pace of RFID development should be increased. However, the tags in an RFID system are more and more utilized, all of them communicate in the same channel. The RFID reader receives mixed signals, and the reader cannot get the correct message the tags send directly. This phenomenon is often called a collision, which is the main obstacle to the development of the RFID system. Traditionally, the algorithm to solve the collision problem is called the anti-collision algorithm, the widely used anti-collision algorithm is based on Time Division Multiple Access (TDMA) like ALOHA-based and Binary search-based anti-collision algorithm. The principle of the TDMA-based anti-collision algorithm is to narrow the response of tags to one in each query time. These anti-collision algorithms perform poorly when the number of tags is huge, thus, some researchers proposed the Blind Source Separation (BSS)-based anti-collision algorithm. The blind anti-collision algorithms perform better than the TDMA-based algorithms; it is meaningful to do some more research about this filed. This paper uses several BSS algorithms like FastICA, PowerICA, ICA_p, and SNR_MAX to separate the mixed signals in the RFID system and compare the performance of them. Simulation results and analysis demonstrate that the ICA_p algorithm has the best comprehensive performance among the mentioned algorithms. The FastICA algorithm is very unstable, and has a lower separation success rate, and the SNR_MAX algorithm has the worst performance among the algorithms applied in the RFID system. Some advice for future work will be put up in the end.

Index Terms—BSS, RFID, FastICA, ICA_P, PowerICA, SNR_Max.

Radio Frequency Identification (RFID) plays an important role in future IoT applications. It consists of three parts, computer, reader, and tags [1,2]. All of the tags communicate with the reader through the same wireless channel [3], once more than one tags in the scope of the reader, the backscattering signals will be mixed randomly, thus, the reader cannot recognize the message the tags transmitted directly. To solve this problem, the reader must use specific methods to avoid the collision, i.e., anti-collision algorithm [4,5,6].

This work was supported by National Natural Science Foundation of China (No. 61801319), the Opening Project of Key Laboratory of Higher Education of Sichuan Province for Enterprise Informationalization and Internet of Things (No. 2017WZJ01), Sichuan Outstanding Youth Fund Project (No. 2020JDJQ0061), the Education Agency Project of Sichuan Province (No.18ZB0419), and the Major Frontier Project of Science and Technology Plan of Sichuan Province (No. 2018JY0512).

RFID belongs to the sensor layer of IoT, various sensors connect to IoT through RFID [7,8]. As IoT is an important technology of future life, the RFID system is required to be faster and with high stability [9-12], which is a huge challenge. The anti-collision algorithm plays an important role of the RFID system, via robust anti-collision algorithms, the RFID system will perform better and match the IoT better.

The traditional anti-collision algorithms are ALOHA-based and Binary search-based anti-collision algorithms. Both of them are based on Time Division Multiple Access (TDMA). They are easy to apply, but the time cost of these algorithms is high and the tags in such a system may not be identified in some cases [13-15]. The rule of the TDMA-based anti-collision algorithms is narrowing the tag's response to one in each query time. The RFID system uses these anti-collision algorithms will query and response several times, in some low Signal Noise Ratio (SNR) channel, the tags may be lost because of the silent command of the reader [16]. The maximum throughput of the RFID system using the dynamic frame slotted Aloha (DFSA, one of the TDMA-based anti-collision algorithm) is only 42.6% [17], and the maximum throughput of the RFID system using the Binary-tree searching of regressive index anti-collision algorithm is lower than 50% [18]. To get better performance, some researchers proposed the anti-collision algorithms based on the FastICA algorithm [19,20]. The RFID systems use these algorithms received a better result. the throughput of these systems is up to 69% of the highest [21-26], but the performance is not equal to expectation, the system uses FastICA algorithm performance bad in a low SNR channel, and the tag may not be identified even in a high SNR channel [27].

This paper aiming to find the fast and stable blind algorithms which can separate the RFID system mixed-signal well. This paper cites some BSS methods like PowerICA, ICA_p, and SNR_MAX to the RFID system, and simulate in the computer via MATLAB. The performance of the algorithms can be represented by the Similarity between Source and Results (SSR) [22]. When the SSR is bigger than 0.92, we believe that separation is a success. The Success Rate (SR) can represent the performance in another form. We hypothesize the SNR of the channel, and the length of the tags can influence the performance of the anti-collision algorithms. So, we do the simulation in these two aspects.

Chaofu Jing, Zhongqiang Luo, Yan Chen and Xingzhong Xiong are with Artificial Intelligence Key Laboratory of Sichuan Province, Sichuan University of Science and Engineering, Yibin 644000, China(757949023@qq.com).

Zhongqiang Luo is also with Key Laboratory of Higher Education of Sichuan Province for Enterprise Informationalization and Internet of Things, Sichuan University of Science and Engineering, Yibin 644000, China (Corresponding author: zhongqiangluo@gmail.com)

The rest of the paper is structured as follows. In section 2, the model of the RFID system and collision in the RFID system will be constructed. The collision problem will be elaborated. In section 3, we will introduce the theory of FastICA, PowerICA, ICA_p, and SNR_MAX. In section 4, the simulation of these mentioned algorithms will be implemented. In section 5, the result of the simulation will be brought up and analyzed, and some advice for future anti-collision work will be suggested.

II. SYSTEM MODEL AND PROBLEM FORMULATION

The RFID system consists of three parts: the computer the reader and the tags. The reader sends the order and the energy through the Radio Frequency (RF) channel to the tags. The tags send back the data to the reader through the RF channel. Then the reader sends the data to the computer connected to it. The computer handles these signals from the reader. Figure 1 shows the traditional model of the RFID system. Generally, the RFID systems have no more than 8 antennas in one reader, and with hundreds or thousands of tags [4]. The reader is expected to identify hundreds of tags in a short time in real life, and this made the model becoming an under-determined model. However, the algorithms we used are both only matches a determined or over-determined model, so we need to divide the tags into several groups then separate the mixed signals of every group.

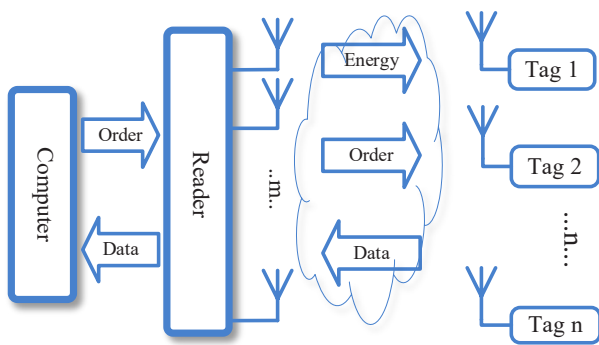


Fig. 1. RFID model

Assume that there are m reader antennas, the received signals are $\mathbf{X} = [\mathbf{x}_1, \mathbf{x}_2, \dots, \mathbf{x}_m]^T$, $\mathbf{x}_1, \mathbf{x}_2, \dots, \mathbf{x}_m$ is the received signal vector of each reader antenna. Suppose that each group has n tags, the unknown signals of the n tags are $\mathbf{S} = [\mathbf{s}_1, \mathbf{s}_2, \dots, \mathbf{s}_n]^T$, where $\mathbf{s}_1, \mathbf{s}_2, \dots, \mathbf{s}_n$ is the source signal vector of each tag. After the source signal \mathbf{S} transmits through the RF channel, the signals may be randomly mixed, and the received signals \mathbf{X} are far different from \mathbf{S} , we presume the mixing matrix is $\mathbf{M}^{m \times n}$. Then the relation between \mathbf{X} and \mathbf{S} is:

$$\mathbf{X} = \mathbf{MS} + \mathbf{n} \tag{1}$$

The received signals \mathbf{X} cannot be processed by the traditional reader, in other words, the collision has happened. The \mathbf{n} is the noise matrix, it is white Gaussian noise usually. We can see the model of collision from Figure 2.

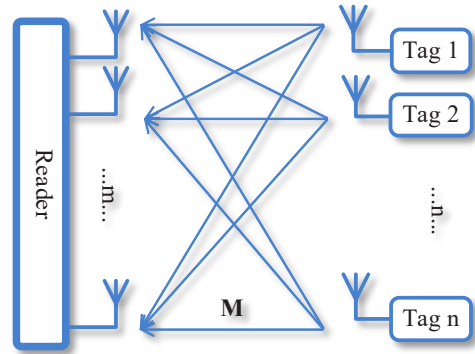


Fig. 2. Collision model

We can see from Figure 2, each antenna of the reader will receive the weighting sum of all tag's signal, as the RF channel is uncertain, we cannot know the weight of each tag's signal respectively, in other words, the \mathbf{M} in Figure 2 is unknown. So, the signals cannot be identified by the readers without an anti-collision algorithm. The traditional way to solve this problem is to avoid this mixing by identifying the tags one by one. It will increase the identification time and reduce the efficiency of the RFID system. Figure 3 shows the traditional anti-collision method.

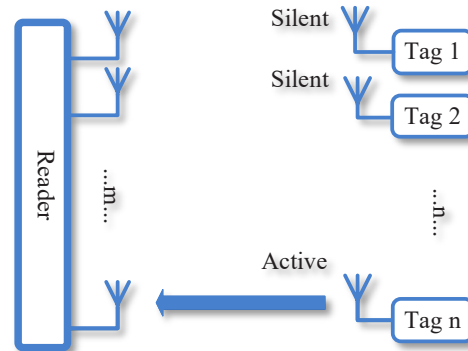


Fig. 3. Traditional anti-collision method

BSS is a data-driven signal processing method which posed in the 1980s [28,29]. It involves extracting and recovering the underlying source signals from multivariable statistical data. The source signal is unknown and either the mixing process is unknown in advance. There is only a small amount of prior knowledge such as statistical independence of source signal, the distribution of the source signal is at most one Gaussian distribution.

The source signal is the wave the tag backscattered we don't know before, and the mixed process in the wireless channel is unknown too. The source signal generated by the interior circuit of each tag, thus, it is statistically independent. The distribution of the source signal is non-Gaussian distribution. So, the mixed signal of the RFID system can be separated by the BSS methods.

Blind anti-collision methods for RFID system: a comparative analysis

The BSS algorithms can calculate a de-mixing matrix \mathbf{W} by the received signal \mathbf{X} , which can make the equation:

$$\mathbf{W}\mathbf{M} = \mathbf{I} \quad (2)$$

\mathbf{I} in equation (2) is an identity matrix. It is equal to the equation:

$$\mathbf{W} \approx \mathbf{M}^{-1} \quad (3)$$

Denote the signal we separated as \mathbf{Y} , then we get the equation:

$$\mathbf{Y} = \mathbf{W}\mathbf{X} = \mathbf{W}\mathbf{M}\mathbf{S} \approx \mathbf{I}\mathbf{S} = \mathbf{S} \quad (4)$$

Use the BSS algorithms to separate the mixed signal of RFID system. We can identify several tags in each time, it can save a lot of time and improve the efficiency of the RFID system significantly. We can see the new anti-collision method in Figure 4.

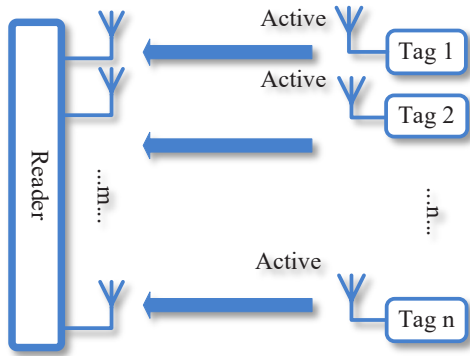


Fig. 4. BSS anti-collision method

III. BSS ALGORITHMS

BSS algorithms is a huge Data-driven signal processing algorithm family, include several algorithms such as Principle Component Analysis (PCA), Independent Component Analysis (ICA), Non-negative Matrix Factorization (NMF), Sparse Component Analysis (SCA) and so on [28]. The ICA algorithm is the presentation of BSS algorithms, in the next work, the traditional FastICA algorithm and the improved ICA_p and ICA_p algorithm will be introduced. The SNR-MAX algorithm is also included for its simplification to make a comparison.

A. ICA method

ICA is mainly used to solve the problem of BSS [29]. In cases where the source signal and mixing matrix are unknown. To make sure the ICA algorithm can separate the source signals from the mixed signals well, merely assuming that the source signals are statistically independent [27]. The ICA algorithm has an assumption that: (1) source signals are real random variables with zero means and are statistically independent of each other; (2) the number of source signals n should be less than or equal to the number of observed signals m ($n \leq m$). The mixing matrix \mathbf{M} is a $m \times n$ unknown matrix with full rank; (3) At most one source signal is allowed to satisfy the Gaussian distribution. The schematic block diagram of the ICA is depicted in Figure 5.

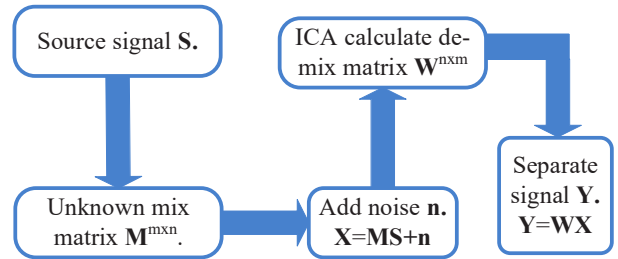


Fig. 5. Block diagram of ICA

The ICA method minimizes the statistical dependence between each component of the signal, highlights the essential structure of the source signal. One of the most popular ICA algorithms is the FastICA fixed-point algorithm [28], and the FastICA algorithm has a requirement that the data should be centered and pre-whitened. We can subtract the mean of the received signal to center the data.

$$\mathbf{X} = \mathbf{X} - \mathbf{E}(\mathbf{X}) \quad (5)$$

$\mathbf{E}(\cdot)$ is the operator to get the expectation. The whitening process [28] can be finished by the following steps: First, we calculate the eigenvalues: $\mathbf{E}=(e_1, e_2, \dots, e_m)$ and eigenvectors $\mathbf{D}=(d_1, d_2, \dots, d_m)$ of the received data, Then the whitening matrix can be calculated by:

$$\mathbf{T} = \mathbf{D}^{-1/2}\mathbf{E}^T \quad (6)$$

Then the whitened data:

$$\mathbf{Y}_1 = \mathbf{T}\mathbf{X} \quad (7)$$

Then the data can be separated successfully by the FastICA algorithm. The FastICA algorithm finds the de-mixing matrix \mathbf{W} by the iteration objective function:

$$J(\mathbf{y}) \approx \sum_{i=1}^p k_i \{ \mathbf{E}[G_i(\mathbf{y})] - \mathbf{E}[G_i(\mathbf{v})] \}^2 \quad (8)$$

Where k_i is a positive constant and \mathbf{v} is a random variable of the Gaussian with zero mean and unit variance. $G_i(\bullet)$ is a non-quadratic function, the select of G is different of the Gaussian distribution [28]. As the RFID signals are sub-Gaussian so the G can be chosen as follows:

$$G(\mathbf{u}) = \frac{1}{a_1} \log \cosh(a_1 \mathbf{u}), G'(\mathbf{u}) = \tanh(a_1 \mathbf{u}) \quad (9)$$

$$1 \leq a_1 \leq 2$$

Then maximizes the Lagrangian:

$$L(\mathbf{w}, \lambda) = \left| \mathbf{E}[G(\mathbf{w}^T \mathbf{R})] \right| - \frac{\lambda}{2} (\mathbf{w}^T \mathbf{w} - 1) \quad (10)$$

B. PowerICA method

The ICA algorithm has some drawbacks, such as: The fixed-point ICA algorithm can only do a serial computation. Some unnecessary assumptions in the iteration of the FastICA algorithm are exist. The classical derivation of the FastICA algorithm has difficulty in separating large sets of real data quickly and accurately. To solve the problems mentioned before, the PowerICA and the ICA_p algorithm have been proposed respectively.

Shahab Basiri [27] provided a novel power iteration algorithm for FastICA which is remarkably more stable when the sample size is not orders of magnitudes larger than the dimension. And the PowerICA algorithm can be run on parallel computing nodes. Basiri cut the oversimplified assumptions of the Lagrangian and the Jacobian matrix in the FastICA algorithm and put up with a new power iteration method for FastICA. The new PowerICA algorithm can converge in the case of the $n=m$, and drastically reduce the computational time by a run on parallel computing nodes. They change the Lagrangian to:

$$L(\mathbf{w}, \lambda) = \mathbb{E}[G(\mathbf{w}^T \mathbf{R})] - \frac{\lambda(\mathbf{w})}{2} (\mathbf{w}^T \mathbf{w} - 1) \quad (11)$$

Thus, the algorithm solving:

$$F(\mathbf{w}) = m(\mathbf{w}) - \lambda(\mathbf{w})\mathbf{w} = 0 \quad (12)$$

Iterates:

$$\mathbf{w} \leftarrow \frac{m(\mathbf{w}) - \beta(\mathbf{w})\mathbf{w}}{\|m(\mathbf{w}) - \beta(\mathbf{w})\mathbf{w}\|} \quad (13)$$

Until convergence. The $\beta(\mathbf{w})$ in (13) is a scalar multiplier defined as $\beta(\mathbf{w}) = \mathbb{E}[g'(\mathbf{w}^T \mathbf{x})] \in \mathbb{R}$.

C. ICA_p method

Pierre Ablin [30] introduced a Preconditioned ICA for the Real Data algorithm, which is a relative L-BFGS algorithm preconditioned with sparse Hessian approximations. They found that the Hessian approximations have a low cost per iteration but not accurate enough on real data. To solve this problem, the use of an optimization algorithm which ‘learns’ curvature from the past iterations of the solver, and accelerates it by preconditioning with Hessian approximations. They put the Hessian approximations as follows:

$$\begin{cases} \hat{h}_{jl} = \hat{\mathbb{E}}[\varphi'_i(\mathbf{y}_i) \mathbf{y}_j \mathbf{y}_l], \text{ for } 1 \leq i, j, l \leq N \\ \hat{h}_{ij} = \hat{\mathbb{E}}[\varphi'_i(\mathbf{y}_i) \mathbf{y}_j^2], \text{ for } 1 \leq i, j \leq N \\ \hat{h}_i = \hat{\mathbb{E}}[\varphi'_i(\mathbf{y}_i)], \text{ for } 1 \leq i \leq N \\ \delta_i^2 = \hat{\mathbb{E}}[\mathbf{y}_i^2], \text{ for } 1 \leq i \leq N \end{cases} \quad (14)$$

They denote the approximation by \tilde{H}^2 in the first step:

$$\tilde{H}_{ijkl}^2 = \delta_{il} \delta_{jk} + \delta_{ik} \delta_{jl} \hat{h}_{ij} \quad (15)$$

Then denoted \tilde{H}^1 , goes one step further and replaces \hat{h}_{ij} by

$$\begin{cases} \hat{h}_i \hat{\sigma}_j^2 \text{ for } i \neq j : \\ \tilde{H}_{ijkl}^1 = \delta_{il} \delta_{jk} + \delta_{ik} \delta_{jl} \hat{h}_i \hat{\sigma}_j^2 \\ \tilde{H}_{iii}^1 = 1 + \hat{h}_i \end{cases} \quad (16)$$

They designed an algorithm to precondition the data based on the Hessian approximation mentioned before.

D. SNR-Max method

ZHANG Xiao-bing [24] proposed a low computational complexity instantaneous linear mixture blind separation algorithm. They take care of the complexity of the traditional algorithms, eye on the character that SNR is maximal when statistically independent source signals are entirely separated. They expressed the source signals and noise to the generalized eigenvalue problem, and get de-mixing matrix without iteration. They use the difference between the source signal and the estimated signal: $\mathbf{e} = \mathbf{s} - \mathbf{y}$ as a noise signal. Then get the SNR function:

$$SNR = 10 \log \frac{\mathbf{s} \bullet \mathbf{s}^T}{\mathbf{e} \bullet \mathbf{e}^T} = 10 \log \frac{\mathbf{s} \bullet \mathbf{s}^T}{(\mathbf{s} - \mathbf{y}) \bullet (\mathbf{s} - \mathbf{y})^T} \quad (17)$$

But the source is unknown, so the use the moving average $\tilde{\mathbf{y}}$ of the signal to replace the source signal \mathbf{s} , so the SNR changes to:

$$SNR = 10 \log \frac{\mathbf{s} \bullet \mathbf{s}^T}{\mathbf{e} \bullet \mathbf{e}^T} = 10 \log \frac{\tilde{\mathbf{y}} \bullet \tilde{\mathbf{y}}^T}{(\tilde{\mathbf{y}} - \mathbf{y}) \bullet (\tilde{\mathbf{y}} - \mathbf{y})^T} \quad (18)$$

After some simplification, the final objective function is:

$$F(\mathbf{y}) = SNR = 10 \log \frac{\mathbf{y} \bullet \mathbf{y}^T}{(\tilde{\mathbf{y}} - \mathbf{y}) \bullet (\tilde{\mathbf{y}} - \mathbf{y})^T} \quad (19)$$

They use a gradient descent method to find the maximum value of the object function, the get the suitable de-mixing matrix \mathbf{w} .

IV. SIMULATION ANALYSIS AND DISCUSSION

We use computer software MATLAB to do the simulation. We set a RFID system with m reader antennas and n tags in each group, the data length of tags is k . Then the source signal noted as $\mathbf{S}^{n \times k}$, the received signal noted as $\mathbf{X}^{m \times k}$, the unknown mix process simulated by a randomly full rank matrix $\mathbf{M}^{m \times n}$. Then we multiply the \mathbf{M} by \mathbf{S} , as the equation: $\mathbf{X} = \mathbf{MS}$. Then the algorithms mentioned before will be used to estimate the de-mix matrix $\mathbf{W}^{n \times m}$, we denote the signal we separate by the algorithms as \mathbf{Y} . then: $\mathbf{Y} = \mathbf{WX}$. The block diagram of the simulation process is shown in Figure 6.

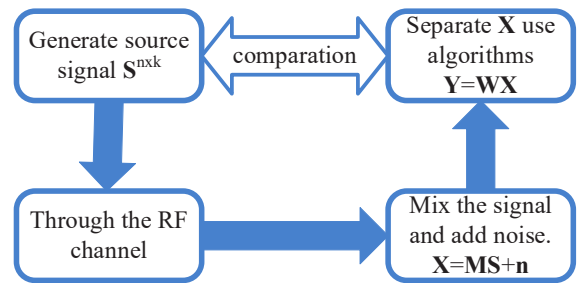


Fig. 6. Block diagram of the simulation process

This paper compares the result in SSR and SR change with the SNR. Secondly, compare the SSR and SR change with the data length of the tags.

Blind anti-collision methods for RFID system:
a comparative analysis

Aiming to get a better comparison, we set a RFID system with 5 reader antennas and 5 tags need to be separated each time. When compare the SSR and SR change with the SNR, we set the data length of the tags to 1000, the SNR change from 0 to 30, simulation results are shown in Figure 7 and Figure 8. When compare the SSR and SR change with the data length of the tags, we set SNR to 25, the data length of tags change from 500 to 5000 with a step of 500, the results are shown in Figure 9 and Figure 10. All of the data are an average of 3000 times.

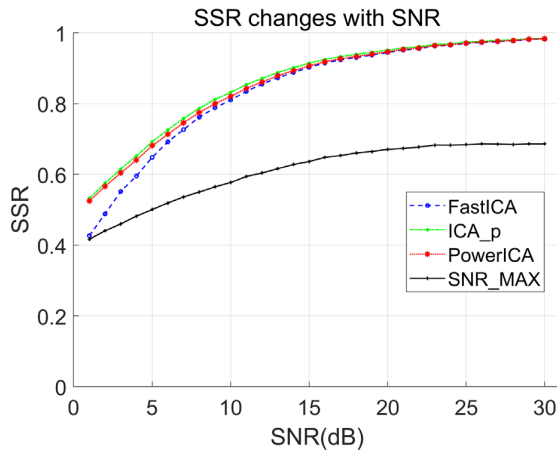


Fig. 7. SSR changes with SNR

In Figure 7, firstly, the trend of SSR changes with SNR is correct. Generally, when the channel's SNR is up to 20, the SSR is more than 0.92, it is a very good performance. When the channel's SNR is less than 20, the performance of the ICA_p algorithm is the best, and the PowerICA algorithm is as good as the ICA_p algorithm but just a little bit worth than the later, the FastICA algorithm has a low SSR, especially in the low SNR channel. Actually, the FastICA algorithm is not stable, the iteration of the FastICA algorithm may not convergence, we deleted the data not convergence then draw Figure 7 and Figure 8. The performance of the SNR_MAX is very poor no matter the condition of channel is good or bad, we believe the low computational complexity of the SNR_MAX algorithm may explain this result. In conclusion, the ICA_p has the best comprehensive performance. The PowerICA algorithm has almost the same performance with the ICA_p algorithm. FastICA performnot so good in a channel with low SNR, and it is not stable. The SNR_MAX algorithm can not meet the requirement of the RFID system.

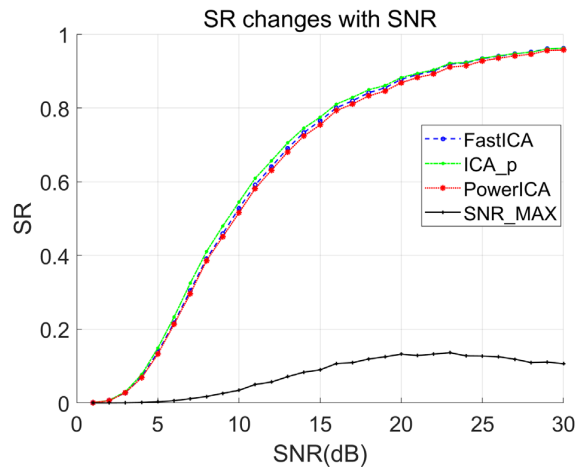


Fig. 8. SR changes with SNR

The paper also compared the SR changes with the channel's SNR, the result is shown in Figure 8. Usually, if the SSR is bigger than 0.92, we claim the separate is a success. In the curve, we found the FastICA, ICA_p, PowerICA algorithm have the related SR trend, but the ICA_p algorithm performance a little better. The SNR_MAX algorithm is hard to satisfy the system.

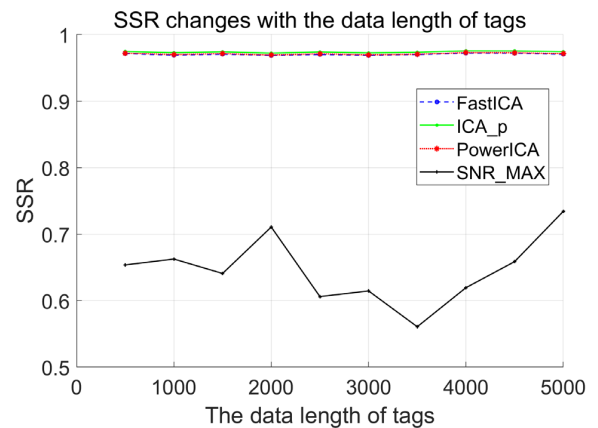


Fig. 9. SSR changes with the data length of tags

From Figure 7 and 8, we can find that the curve becomes smooth when the SNR of the channel is more than 25 and the performance of the algorithms are both very good, which means the SNR in this level make no much difference of the SSR. So, we set the SNR to 25, then compare the algorithms' performance in different data length of tags. Figure 9 shows the performance, it tells the trues that all of the algorithms do well when the length of the tags change from 500 to 5000. Because of the relation between the SSR and the SR, we believe that the success rate has the same trend as the correlation. Figure 10 verify the guess.

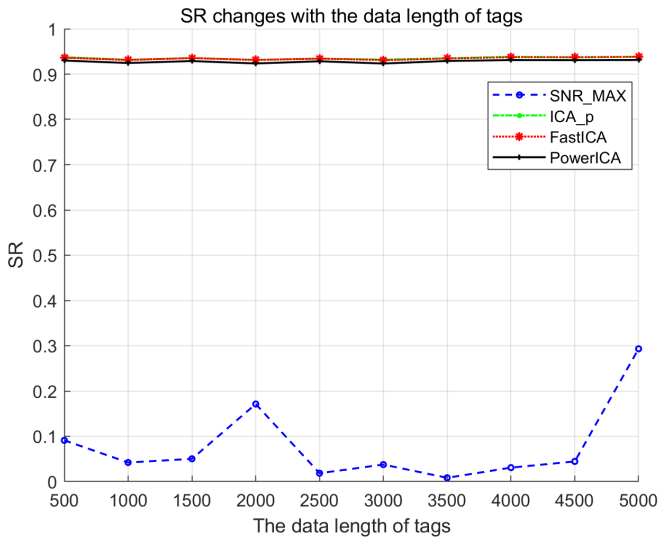


Fig. 10. SR changes with the data length of tags

As we said before, the FastICA algorithm is unstable, Figure 11 shows the FastICA algorithm default convergence time changes with the SNR, even when the SNR more than 20, the FastICA emerge the case of not convergence, but the PowerICA and the ICA_p will not occur such thing. The reason why this situation arises is that the algorithm oversimplified the Lagrangian and the Jacobian Matrix [26].

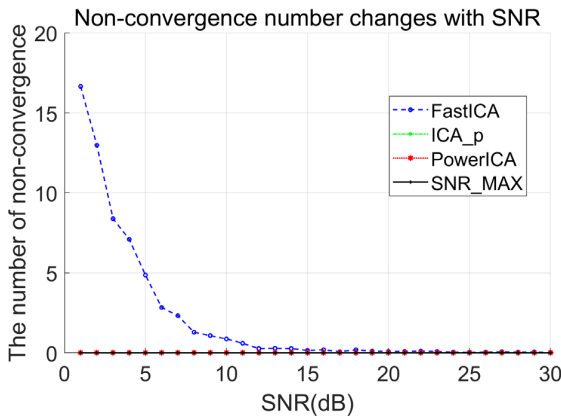


Fig. 11. The non-convergence time changes with SNR

By the way, we compared the time cost of the algorithms changes with the length of the tags, we can see it in Figure 12. The SNR_Max uses the least of time, and the Power needs the most of the time, the others between them. But the PowerICA can run in a parallel model, so it can perform better in parallel systems.

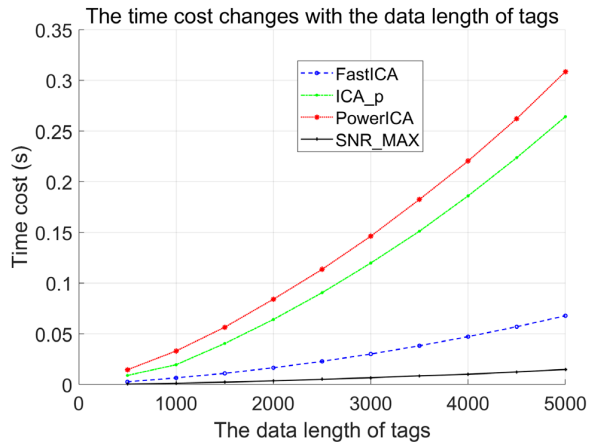


Fig. 12. the time cost changes with the length of tags

To show the BSS algorithm's separate performance visually, we put the source signal, the mixed-signal, and the algorithms separate the signal in Figure 13 to 18. Considering the comfort of view, we decline the number of tags to 3, and only draw the first 20 data of the signal.

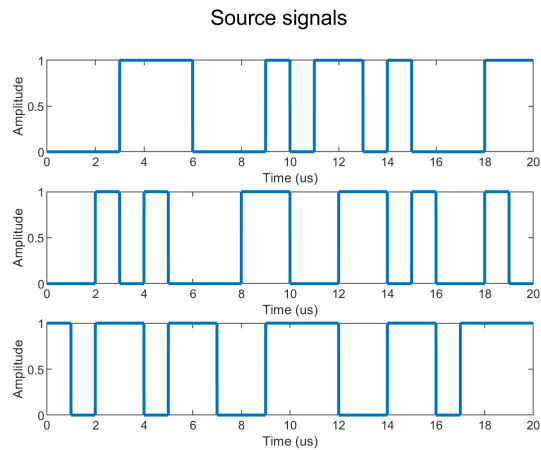


Fig. 13. The source signals

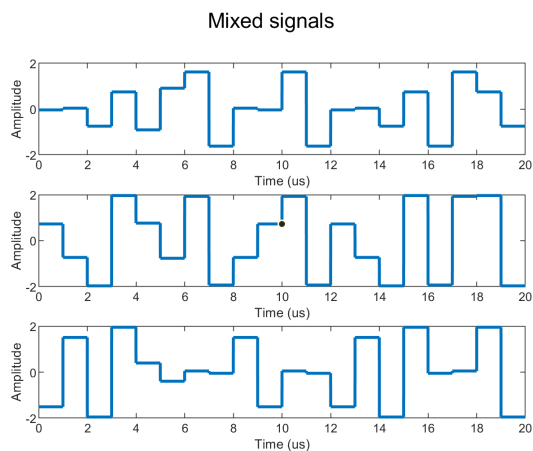


Fig. 14. The mixed signals

Blind anti-collision methods for RFID system:
a comparative analysis

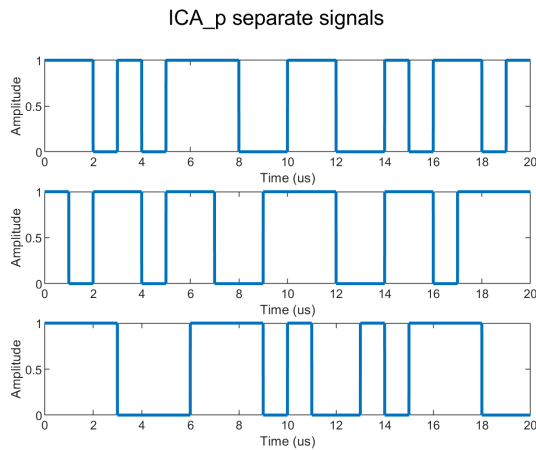


Fig. 15. The ICA_p separate signals

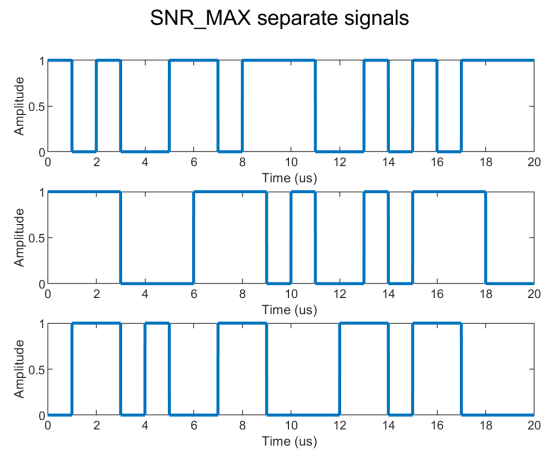


Fig. 18. The SNR-Max separate signal

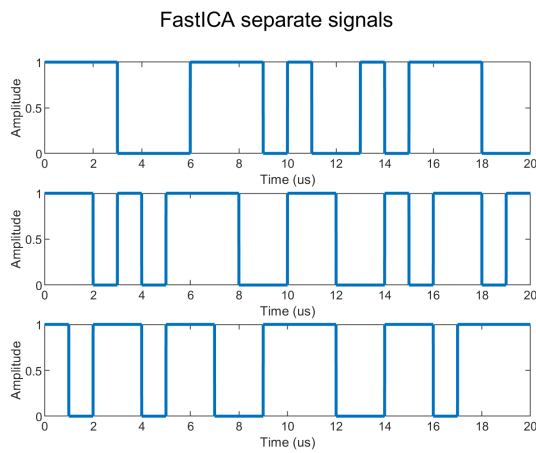


Fig. 16. The FastICA separate signals

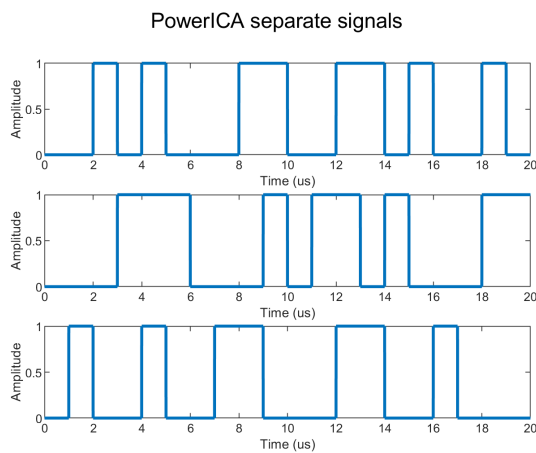


Fig. 17. The PowerICA separate signals

We can see from Figure 12 to Figure 18 that the BSS methods change the order and the polarity of the signal, and most of the signal be separated successfully. The first signal of source (Figure 13) corresponds to the third signal of ICA_p separate signals (Figure 15) with the opposite polarity, corresponds to the first signal of the FastICA separate signals (Figure 16) with the opposite polarity, corresponds to the second signals of PowerICA separate signals (Figure 17), however we cannot find the corresponding signal from the SNR_MAX separate signals. As the use of FM0 coding in RFID system, the polarity and the order change of the signals doing nothing for us to recognize the information the tags send.

We make a table to show the performance of the algorithms we used. Shown as Table 1.

TABLE I
ALGORITHMS PERFORMANCE

Algorithm	Accuracy	Stability	instantaneity
FastICA	Medium	Low	High
PowerICA	High	High	Medium
ICA_p	High	High	Medium
SNR_MAX	Low	medium	High

There are some useful simulation data to prove our conclusion. The data in Table 2 got in the channel which has a 25 SNR and the tags' length is 1000. We do the simulation 1000 times, then get the average data. As we can see the ICA_p algorithm has the highest correlation in this situation. From the low correlation and the mean success rate we can say that the ICA_p and the PowerICA algorithm are stable. From the time for one separation, we know the Fast ICA algorithm is the most real-time and with excellent performance.

TABLE II
SOME USEFUL DATA

Algorithm	Highest correlation	Low correlation	Mean successes rate	Time for one separate
FastICA	0.9952	0.8222	0.9680	0.0053s
PowerICA	0.9970	0.8662	0.9680	0.0176s
ICA_p	0.9999	0.8439	0.9680	0.0126s
SNR-Max	0.8055	0.5302	0.3440	0.0006s

RFID is located at the sensor layer of IoT, it has an important role of IoT. As IoT develops rapidly, the RFID system is required to be more effective and real-time in practical applications. The simulation of the paper shows that the FastICA algorithms perform well in real-time but has poor stability performance. The PowerICA and the ICA_p algorithms perform well in stability and accuracy, but need a little more time. And the SNR-Max algorithm is not suitable for the RFID system. In conclusion, we can design a system that uses ICA_p algorithm or PowerICA algorithm when the channel's SNR is low and use the FastICA algorithm to reduce the time when the channel's SNR is very high. The ICA_p algorithm has the best general performance.

This work confirms the feasibility of using BSS methods as anti-collision algorithms in RFID systems, verifies the good performance of BSS methods like ICA_p and PowerICA. However, our current work only takes care of over-determined or determined receiving model. The meaningful and practical underdetermined receiving model needs more attention from researchers. In future work, the underdetermined receiving model will be engaged for anti-collision in RFID application.

REFERENCES

[1] Want, and R. "An Introduction to RFID Technology." IEEE Pervasive Computing, vol. 5, no.1, pp. 25-33. Jan. 2006. doi: 10.1109/MPRV.2006.2.

[2] Azambuja, Marcelo & Marcon, César & Hessel, F.. (2008). Survey of Standardized ISO 18000-6 RFID Anti-collision Protocols. 468 - 473. doi: 10.1109/SENSORCOMM.2008.124.

[3] Quan CH., Hong WK., Kim HC. (2006) "Performance Analysis of Tag Anti-collision Algorithms for RFID Systems". In: Zhou X. et al. (eds) Emerging Directions in Embedded and Ubiquitous Computing. EUC 2006. Lecture Notes in Computer Science, vol 4097. Springer, Berlin, Heidelberg. doi: 10.1007/11807964_39

[4] Jia, Xiaolin, Q. Feng, and L. Yu. "Stability Analysis of an Efficient Anti-Collision Protocol for RFID Tag Identification." IEEE Transactions on Communications vol. 60, no. 8, pp.2285-2294.

[5] Dacuña, Javier & Melià-Seguí, Joan & Pous, Rafael. (2012). "Multi-tag spatial multiplexing in UHF RFID systems". IEICE Electronics Express. 2012 vol. 9, no. 21, pp.1701-1706. doi: 10.1587/elex.9.1701.

[6] Mota, Rafael & Batista, Daniel. (2013). A RFID QoS mechanism for IoT tracking applications. 2013 International Symposium on Wireless and Pervasive Computing, ISWPC 2013. 1-4. doi: 10.1109/ISWPC.2013.6707429.

[7] Zhang, Dacheng & Liu, Yu & Han, Kun & Liu, Aiyong & Liu, Lijing. (2012). The Application of RFID-Based on IOT in Logistics Management. doi: 10.1007/978-3-642-29455-6_97.

[8] Alsinglawi, Belal & Nguyen, Quang & Gunawardana, Upul & Simoff, Simeon & Maeder, Anthony & Elkhodr, Mahmoud & Alshehri, Mohammad. (2019). Passive RFID Localization in the Internet of Things. doi: 10.1007/978-3-319-99966-1_7.

[9] Kumar, Sachin, P. Tiwari, and M. Zymbler. "Internet of Things is a revolutionary approach for future technology enhancement: a review." Journal of Big Data 6.1(2019):1-21. doi: 10.1186/s40537-019-0268-2.

[10] Chen S, Xu H, Liu D, et al. "A Vision of IoT: Applications, Challenges, and Opportunities with China Perspective." IEEE Internet of Things Journal, vol. 1, no. 4, pp. 349-359. 2014. doi: 10.1109/jiot.2014.2337336.

[11] Khan, Sarfaraz . "Health care monitoring system in Internet of Things (IoT) by using RFID." IEEE's 6th International Conference on Industrial Technology and Management (ICITM 2017) IEEE, 2017. doi: 10.1109/ICITM.2017.7917920.

[12] Li Xue-qiao, JIA Xiao-ai, ZHAO Lei, XU Ben-fu. "Anti-collision Algorithm Based on Dynamic Searching of Regressive Index." Communications technology. Vol. 42, no. 06, pp. 118-120. 2009. doi: 10.3969/j.issn.1002-0802.2009.06.041.

[13] Xu Haifeng, Jiang Hui, "Research and Simulating on ALOHA Anti-collision Algorithm with Higher Efficiency in Real-time for RFID System." Computer and Digital Engineering, vol. 39, no. 05, pp.19-22+26. 2011.

[14] Z. Xiao-Hong, Liu-Yang Z. "Research on Passive RFID System Adaptive Frame Slot Anti-collision Algorithm." Acta Electronica Sinica. Vol. 044 no.009. pp. 2211-2218. 2016. doi: 10.3969/j.issn.0372-2112.2016.09.028.

[15] HAN Xianming NAN Jingchang, "Anti-Collision Algorithm for RFID Based on Regressive Index Binary-Tree Searching." Microelectronics, vol. 43, no. 05, pp. 708-712. 2013.

[16] M. Vedhekar, Sairam A S, Kumari A. "Binary countdown anti-collision protocol for RFID tag collision problem." 2016 International Conference on Accessibility to Digital World (ICADW). IEEE, 2016. doi: 10.1109/ICADW.2016.7942522.

[17] Jiang Xia, Bai Tiecheng Zheng Hongjiang, "Research on Binary Search Anti-collision Algorithm for RFID System." Journal of Tarim University, vol. 25, no. 04, pp. 30-35. 2013.

[18] MU Yuchao ZHANG Xiaohong, "Adaptive tree grouping and blind separation anti-collision algorithm for radio frequency identification system." Journal of Computer Applications, vol. 35, no. 01, pp. 19-22, 2015. doi: 10.1021/JM9005093.

[19] Nguyen C T, Hayashi K, Megumi Kaneko.... "Probabilistic Dynamic Framed Slotted ALOHA for RFID Tag Identification." Wireless Personal Communications, vol. 71, no. 4, pp. 2947-2963. 2013.

[20] LI Hua, JIA Zhi-ping, "UHF RFID anti-collision algorithm based on blind separation and dynamic bit-slot grouping." Journal on Communications, vol.33, no. 04, pp. 47-53. 2012.

[21] PENG Yong-hua HE Yi-gang, "Application of a New Type ICA Algorithm in RFID System." Computer Engineering, vol. 38, no. 19, pp. 25-29. 2012.

[22] L.I. Hua. W. Hong-jun and S. Zi-liang, "ICA-based UHF RFID Multi-tag Hybrid Data Blind Separation". in International conference on communication and electronics information. Haikou (CN). p. 52-56. 2013.

[23] Zhang Xiaohong Jin Yungang, "Research of Under-determined Blind Source Separation Anti-collision Algorithm Based on RFID Frame-slot." Journal of System Simulation, vol. 28, no. 05, pp. 1100-1108+1116. 2016.

[24] T. Chu, Zou S X, Ren W, et al. "DRICA design of multi-antenna RFID system based on ICA." International Workshop on Wireless Communication and Network (IWWCN2015). 2016. doi: 10.1142/9789814733663_0044

Blind anti-collision methods for RFID system: a comparative analysis

- [25] P. Yong-Hua, Yi-Gang H E. "Application of a New Type ICA Algorithm in RFID System." *Computer Engineering*, Vol. 38, no. 19, pp. 25-29 2012.
- [26] Basiri, S., E. Ollila and V. Koivunen, "Alternative Derivation of FastICA With Novel Power Iteration Algorithm." *IEEE Signal Processing Letters*, vol. 24, no. 9, pp. 1378-1382. 2017.
doi: 10.1109/lsp.2017.2732342.
- [27] Luo, Z., C. Li and L. Zhu, "A Comprehensive Survey on Blind Source Separation for Wireless Adaptive Processing: Principles, Perspectives, Challenges and New Research Directions." *IEEE Access*, vol. 6, no. 6, pp. 66685-66708. 2018. doi: 10.1109/ACCESS.2018.2879380.
- [28] X. Yu, D. Hu, J. Xu, "Blind Source Separation: Theory and Applications", Singapore: John Wiley & Sons, 2014.
- [29] Ablin, Pierre, Jean-François Cardoso, and A. Gramfort . "Accelerating Likelihood Optimization for ICA on Real Signals." *Latent Variable Analysis and Signal Separation*. 2018.
doi: 10.1007/978-3-319-93764-9_15.



Chaofu Jing received the B. S. degree in Electronic and Information Engineering from Sichuan University of Science and Engineering (SUSE) Zigong, China, in 2018. Now he is a postgraduate student in Automation & Information Engineering of SUSE. He will receive a M. S. degree in 2021. His research contain Blind Source Separation, Radio Frequency Identification, intelligent Signal Processing and Artificial Intelligence.



Zhongqiang Luo received the B.S. and M.S. degrees in communication engineering and pattern recognition and intelligent systems from Sichuan University of Science and Engineering, Zigong, China, in 2009 and 2012, respectively. He received the Ph.D. degree in communication and information systems from University of Electronic Science and Technology of China (UESTC), in 2016. Since 2017, he has been with the Sichuan University of Science and Engineering, where he is currently an associate professor. From

December 2018-December 2019, he was a visiting scholar with Department of Computer Science and Electrical Engineering in University of Maryland Baltimore County (UMBC). His research interests include machine learning, blind source separation, signal processing for wireless communication system and intelligent signal processing.



Chen Yan received the B.S degrees in communication engineering from Sichuan University of Science and Engineering, Zigong, China, in 2018. Since 2018, she has studying for a master's degree at Sichuan University of Science and Engineering, Yibin. Her research interests include blind source separation, signal processing for wireless communication system and intelligent signal processing.



Xingzhong Xiong received the B.S. degrees in communication engineering from Sichuan University of Science and Engineering, Zigong, China, in 1996. He received the M.S and Ph.D. degrees in communication and information system from University of Electronic Science and Technology of China (UESTC), in 2006 and 2009, respectively. In 2012, he completed a research assignment from the Postdoctoral Station of Electronic Science and Technology at the UESTC. He is currently a professor at the School of Automation and

Electronic Information, Sichuan University of Science and Engineering. His research interests include wireless and mobile communications technologies, intelligent signal processing, Internet of Things technologies, and very large-scale integration (VLSI) designs.

Developing a Noise Awareness Rising Web Application within the “Protect your Ears” Project

Dániel Szántó¹, Attila Zoltán Jenei², Miklós Gábor Tulics³ and Klára Vicsi⁴

Abstract — Noise from our environment is causing ever-greater problems such as hearing loss among the young. In many cases, children may be exposed to harmful noise even in the most common places such as schools and events. For this reason, we developed a web application in the frame of the “Protect your Ears” project that aims the teaching of noise awareness. Playing with this web application helps children to be more aware in protecting their hearing. The web application was subjected to a cohort study where a test and control group was separated at an elementary school. The test group was able to use the web application for two weeks during the teaching sessions, while the control group could not. For objective measurement, the pedagogue used questionnaires before and after the examination. Statistical analyses were performed on the values obtained from the questionnaires. At the beginning of the study, we showed that the control and test groups were not heterogeneous at 5% significance level using the Mann Whitney U test. As a result, there was a significant difference between the pre- and post-condition for the test group using the Wilcoxon test at the 5% significance level comparing to a control group. From this results, we can conclude that playing with the web application the children in the test group became more aware of the noise in their surrounding and mastered preventive behavior.

Index Terms — children hearing loss, noise awareness, web application, Wilcoxon paired test

I. INTRODUCTION

According to the World Health Organization (WHO) hearing loss affects millions of people around the world, and it is estimated to be the world's fourth leading disease [1]. Hearing protection is very important as hearing loss affects every area of an individual's life (workplace, social environment, home activities). By identifying the causes of hearing loss preventive behavior can be learned.

Generally, there are two types of causes of hearing loss: congenital (born with) and acquired. This latter category includes the noise pollution caused by environmental noise [3], [4].

According to WHO approximately 466 million people have hearing loss above 40 dB Hearing Level (referred to as HL) (30 dB HL in children), 7.3% of whom are under 15 years of age [2]. As reported as forecasts, this number could reach the value of 900 million by 2050. Reports also suggests that 60% of childhood hearing loss could be prevented with proper prevention and awareness.

In Europe, noise levels have been shown to rise, despite the fact that noise pollution is known to cause health problems [6], [7]. About 75 million people in urban environments are exposed to high levels of noise, of which 20 million are exposed to health hazards [8]. Sleep deprivation caused by environmental noise can occur, with ringing in the ears (tinnitus), increased stress, and various mental illnesses.

Research has shown that values between 70 and 90 dB (A) (A-weighted decibels) are not uncommon in schools. For example, a noise level test at a primary school in Kiel, Germany, showed that while in classroom work the noise level was 45-50 dB (A), during the break in the yard the noise level was 80 dB (A), before the teacher entered the classroom it increased to 90 dB (A) [9], [10]. At the same time, it has also been found that out-of-school noise can impair school performance. Not only does it interfere with communication and affect school performance, but it can also cause many health problems. Students complain of headaches and sleep problems due to the loud environment, but high noise levels can also be a cause of high blood pressure and circulatory problems [11], [12], [13], [14], [15].

All of this confirms that hearing loss begins to occur at an early age because of environmental factors. However, interventions are needed to prevent hearing loss.

Analyzing the 2014 European Population Health Survey (ELEF), the prevalence of hearing problems among the Hungarian population is 15% (~1415 people) in the surveyed population (9431 people in total) [16]. The proportion of people with severe hearing impairment is 3% (~283 people).

A WHO analysis, including Hungary, has shown that untreated hearing loss has a global cost of 750-790 billion American dollars (USD) per year worldwide [17].

^{2,3,4} Department of Telecommunication and Media Informatics, Budapest University of Technology and Economics, Hungary

¹email: danielszanto95@gmail.com ²email: jenei@tmit.bme.hu

³email: tulics@tmit.bme.hu ⁴email: vicsi@tmit.bme.hu

Developing a Noise Awareness Rising Web Application within the “Protect your Ears” Project

According to a Hungarian study published in 2017, the National Health Insurance Fund (NEAK - formerly known as OEP) spent 2.011 billion Hungarian forints (HUF) on treating patients with sensorineural and conductive hearing loss [18].

Children and young are at higher risk than adults are. The reason is that they are exposed to the same amount of noise, but their hearing is still intact, so their body is more sensitive. Juvenile hearing loss can affect a child's life, and therefore the importance of hearing protection should be recognized at a young age [19], [20].

In Section 2, we present research already done in rising or survey noise awareness. In Section 3 we describe the structure and the main ideas of the “Protect Your Ears” website, followed by the developed games that aim the teaching of noise preventive behavior. Then the methods of the statistical analysis are presented. Our results are shown in Section 4, followed by the discussion and the future direction in Section 5.

II. RELATED WORK

A questionnaire survey has been conducted on noise induced hearing loss, noise pollution and noise protection by Lee Donguk and his colleagues [21]. This questionnaire contained 22 questions in the three categories mentioned above. The questionnaire was completed by 150 people (aged 20-60). 17.3% of the respondents indicated noise as a serious source of danger, while 80% of the respondents did not know at all about noise induced hearing loss. This points out that lack of information / awareness can also be significant on the topic.

Based on a proposal from the General Hearing and Communication Center (CHC), a number of activities are being organized in many countries to encourage people to take action against noise [22]. In school education, teachers try to teach the right behavior in the face of everyday noise with the help of readings, lectures, posters and board games.

In Italy, the Acoustics Society of Italy (AIA) is responsible for holding International Noise Awareness Day every year. In the meantime, the emphasis is not only on education, but also on finding solutions to actual noise measurement and various noise-related problems.

In the early 2000s, as part of the Dangerous Decibels Project, the University of Northern Colorado developed a website that aims to educate students and develop positive behaviors to prevent hearing loss [23]. Several problems are highlighted, such as the fact that a North American child may suffer more noise at school than adults at an eight-hour workplace at the factory [24].

An American study has investigated the effectiveness of the Dangerous Decibels prevention program at students of 4 and 7 grades. The research showed that those who attended the preventive lecture had significantly improved their knowledge and behavior regarding the prevention of hearing loss [25].

In Jordan, an attempt was made to assess and raise noise awareness. 245 students (113 females, 132 males, age 21.5 years ±2.18) were involved from three different universities [26]. Subjects filled out a questionnaire about noise connected daily activities. 9.8% of the participants stated that they use

earplugs to protect themselves against noise. After receiving background material on the harmful effects of noise, as many as 56.3% said they would use earplugs in the future. This resulted in a significant difference with a two-tailed Chi-square test (paired $\chi^2 = 103.0$, $p < 0.01$).

Audio games (AGs) have been developed in the past for noise awareness research [27]. Within this project, a game has been created that contains noises that occur in everyday environments, namely domestic, urban and natural noises. The article did not perform a statistical analysis of the game's effectiveness in this area.

Based on the presented literature, it can be said that little scientific research deals with increasing noise awareness. To the best of our knowledge, there is no research (or statistical study) aimed at increasing children's noise awareness in a playful (web application) form. Of course, there are games designed to protect against noise (board games, computer games, online games), but a scientific study of their effectiveness is not available or is incomplete.

In this study, we aimed to raise children's awareness in the framework of the “Protect Your Ears” project by developing a web application.

The “Protect Your Ears” website was created on the initiative of the Acoustic Inter-Departmental Committee of the Hungarian Academy of Sciences. The aim of the Committee is to raise awareness of the hearing protection of the young generation, in the society's leading organizations and society. It is also important that the protection of children's hearing is currently not regulated in Hungary. The target group of the project is the Hungarian population. However, the basic idea can be transposed to other languages.

In the study, we developed online games for children on the project's website. These will help the child learn the basics of music, localizing and recognizing sound sources. One of these game modules specifically focuses on conscious noise protection and plays a role in developing preventive behavior.

We have created questionnaires for testing noise awareness before and after the use of the web application. We created a control and a test group at a school. The test group used the web application, while the control had not. We tested whether the web application helped the development of noise awareness in the test group compared to the control group with statistical tests.

III. DEMONSTRATION OF THE “PROTECT YOUR EARS” PROJECT

The main objective is to draw attention for the importance of protecting children's hearing, raise awareness, and deepen the knowledge of the subject that would prevent one from further acquired loss of hearing.

The created website (www.ovdafuled.hu) contains professional quality information that can be used as educational aids at conferences and schools. The website and its contents are available in Hungarian.

The project is represented through other media, such as radio or television interviews, or as a Facebook page.

The website is a custom-designed website, and its appearance and function can be fully customized to meet current needs. With the help of a web application we provided a tool to measure the sound pressure level, the metadata (environment type, Location, measured sound pressure level, distance from sound source, type of device used for measurement, etc.) of which is stored in a database. The sound pressure level measurement is for information only.

The visitors of the website can distinguish content for children, educators, and anyone who is interested in the topic. Teachers have access to lesson plans, presentations and notes to complement their school lectures. Those interested can be acquainted with basic concepts and mechanisms such as hearing mechanism and noise protection.

To increase children's awareness of environmental noises, a web-based application has been created to provide basic insight into sounds and hearing protection through playful animated tasks.

The development process involved gathering potential functions based on a literature study [28] [29], [30]: the following three aspects were of paramount importance in designing the application.

With easy to use aspect, the user may use the application without supervisor. For this, simplified elements were used. Interactive components have been minimized and text (and voice) guidance has been provided to help keep the game running smoothly.

Using the build-in help function in case getting stuck, the user can get help through the help function of the application to continue playing. In our case, we have placed a video below the game interface where the user plays the game. This will help if your child gets stuck in the game. In addition, there is a help button on the game interface that gives you more detailed information about the certain task.

User interface may draw the child's attention and gaze. In our case, this includes animated elements and sounds. For example, memory cards flip after click on it, keys become pressed on the piano, etc. Pleasant sounds and animations indicate when a child has successfully completed a task.

In addition to the literature, we also sought the views of educators dealing with children. Based on pedagogical opinion and practice the card and board games were successfully used in the educational institution (Dr. Török Béla Kindergarten and Primary School). In addition, the educators may apply audio and game programs that help the child to learn in a playful way. The educators highlighted the importance of emphasizing the function of the ear, the development of hearing loss and prevention ways for the classes.

According to the WHO Ear and Hearing Care Training Material, it is worthwhile to visually facilitate the transfer of knowledge by associating different sounds and noises with different subjects [31].

We compared the user needs with previous suggestions that we have sought from the most credible sources. The user usually looks for the essential interface of the screen, the functions that can be manipulated and keys which can the user move forward or backward.

On this basis, we made a visual hierarchy focusing on size, color, position, shape. For example, green color gives a pleasant impression, the red color something to avoid. Essentials are larger in size and usually centered on the screen. Creating the texts on the screen, we strove for simplicity and clarity.

During the development, the functions and algorithms were introduced into the application. We used HTML5, CSS and JavaScript web technologies.

The text of the tasks and instructions (i.e. the voice guidance) of the application was read by a person with a child-friendly voice, which was recorded with a clip-on condenser microphone. This took place at the Department of Telecommunications and Media Informatics of the Budapest University of Technology and Economics, in the Speech Acoustics Laboratory. This ensured studio-quality sound recording. FL Studio program was used to produce musical sounds, melodies and songs.

Videos (with mp4 extension) have been uploaded about the instructions to help the game experience to the "Protect Your Ears" YouTube channel.

Adobe Photoshop was used to create the graphics. All images and illustrations are free of charge and not protected by copyright.

For a harmonious color scheme, the Adobe Color Wheel tool was used, where you specified a base color to calculate what additional colors would match the theme of the game. Based on this, the main color is bright red, which has become the background color. The overall text color was white, and the highlighted, more prominent contents were given a yellowish-green color. If the highlighted content has a yellowish-green background, the text will be blue.

After the development, the testing phase was followed by the web application. Manual and automatic testing were done. Automatic testing was done using the JS testing framework. The developer did alpha testing, while independent university students did beta testing.

The children's interface created with this process included three games. The first game module is a hearing training, where the child can become familiar with sounds in a classroom and in a general room. He or she can localize its sources and recognize them by voice.

In the second game module, several difficulty levels can be distinguished. At the beginner level, the child can choose from 3 possible options for what sound was emitted. He or she can play an advanced memory game where the pairs should be found based on the sources and its sounds. On a difficult level, the child can categorize and sort hazardous and non-hazardous audio sources according to the dB scale.

In the third module, the player can also acquire basic music skills at several difficulty levels. Get started with getting to know the music sounds. The user can practice advanced song recognition by selecting from three options after listening the song. Finally, he or she can play an actual song on the virtual piano at the most difficult level.

The games can be found under the following link: <http://www.ovdafuled.hu/gyermek.php>.

Developing a Noise Awareness Rising Web Application within the “Protect your Ears” Project

A convenient feature is that the game volume can also be adjusted using the volume icon indicated in the lower left corner of the figure.

The game start screen shows the name of the game and a description of the task, which is read out loud automatically. If the user does not want this auto play to occur, this can be turned off.

For some tasks, the player can also get help, where he can find leading information on how to solve the task (HELP button) and also the uploaded videos can be a guidance.

At the end of the game, an animated greeting card rewards the player. This card is not only motivating, but also provides an opportunity to restart the game or select additional games. This is encouraging, as the child will have a sense of success and will probably want to try more games as well.

Of the three modules, the second one aims to raise awareness for hearing protection. It introduces the child to the noisy sounds in its environment. Herewith it makes the child aware that he or she should avoid it.

The effectiveness of the web application for raising awareness of hearing protection was investigated in Dr. Török Béla Kindergarten and Primary School with an experimental layout, which will be discussed in the next section. The study was conducted with the consent of parents and educators.

IV. STATISTICAL EXPERIMENTS

In the experiment, two groups were distinguished: the test group and the control group. In terms of hearing condition, both hearing impaired and normal hearing members were present in both groups.

The sample is not representative, as the sample is made by students of only one school, so no conclusions can be drawn for all children in Hungary, but as a local result.

The composition of the two groups is shown in Table 1.

TABLE 1
THE TEST AND CONTROL GROUP COMPOSITION
(UNIT: PERSON).

	H	HA	CI	TOTAL
TEST	5	3	2	10
CONTROL	4	4	2	10

Each group consisted of 10-10 children, 6 boys and 4 girls. In the test group, 5 had healthy (normal) hearing (H), 3 had hearing aids (HA) and 2 had cochlear implants (CI). In the control group, this distribution was 4-4-2. The average age of the test group was 10.2 years and the control group was 10.0 years.

The person conducting the survey is a surdopedagogue and speech therapist. During the pedagogical sessions, the educator has integrated the use of hearing application games for the test group in the curriculum. Based on this, the children used the software four days a week for an average of 15 minutes for two weeks.

A questionnaire was applied to assess children's noise awareness and preventive behavior. We designed the structure of the questionnaires in such a way that it would not be too complicated for the children, but at the same time provide enough information to get answers to the questions asked in the hypothesis.

Research focuses mainly on creating questionnaires on noise exposure for young adults and children [32], [33], but there is little research regarding noise awareness. For this reason, the questions of our questionnaire was based on the knowledge materials of the website working on the topic [23]. The compiled questions were also studied by experts, and then the questionnaire containing the three groups of questions was created.

In the first group of questions, sound sources could be identified that may have harm effect on hearing (“Task 1: Mark the ones listed that may be harmful to your ears.”). In the second group of questions, it had to be decided which of the listed objects / events had the highest noise level (“Task 2: Choose from the three objects which has the highest noise level.”). In the third group of questions, we collected situations that occur in everyday life where the child’s hearing may be impaired. We asked about the decisions made in these situations (“Task 3: When should you protect your ears (with earplugs, earmuffs, hearing aids)”).

The questionnaire examines general noise awareness, which were completed as follows: The surveyor reads out the questions and the child's answers are recorded on the printed test paper. Two questionnaires were made (A and B), which were the same on their structure and question types, differing only in the questions itself. Questionnaire A was completed by the children before the experiment, and B after the experiment. In both tests, points were obtained for correct answers, with a maximum of 17 points. On this basis, children's awareness was quantified.

Data was processed anonymously. Non-parametric statistical tests were used to examine these discrete values. The Mann-Whitney U test was used to examine the homogeneity of the two groups. In both groups, Wilcoxon paired test was used to examine the before and after condition.

Whole scores could be given for the questionnaires.

A. Mann-Whitney U Test

The Mann Whitney U test helps to compare the distribution of two independent sets. It has the advantage that it is applicable to a non-normally distributed dataset [34].

The null hypothesis of the test states that the two test sets originate from the same population. In other words, the two sets are homogeneous and have the same distribution. In our term

the null hypothesis is the following: There is no significant difference between control and test group performances.

Using the two-sided test, the alternative hypothesis can be formulated so that the test and control groups' performances differ from each other significantly. By accepting the alternative hypothesis, the null hypothesis is rejected.

Two-tailed statistical analysis was performed at 5% significance level.

B. Wilcoxon Paired Test

Related cohorts were tested using the Wilcoxon paired test. The distribution of the sample sets is assumed to be the same. This is used to test the values of the scores at pre and post condition [35].

Define the null hypothesis as there is no difference between the median values of the two sample sets. In this case, the sample sets are the pre- and post-performance on the given questionnaire. Because of this, the alternative hypothesis can be drawn up as there is a significant difference between the median values of the two sample sets.

Differences in pre- and post-performance (pre – A, post – B questionnaire) can be investigated separately for the control and the test groups with the paired Wilcoxon test.

Two-tailed statistical analysis was performed at 5% significance level.

V. RESULTS

Table 2 shows the scores of the two groups on the "A" and "B" questionnaires. We can see from the scores of questionnaires that the average of the points increases in both groups (except for one or two children). However, both types of questionnaire were designed with the same difficulty. This suggests that contact with the subject is capable of producing a small (non-significant) increase in noise awareness.

TABLE 2
SCORES OF QUESTIONNAIRE "A" AND "B".

Number of child	Control		Test	
	"A"	"B"	"A"	"B"
1	7	8	10	15
2	7	11	16	16
3	6	10	9	15
4	11	12	11	16
5	10	10	5	16
6	14	16	7	16
7	12	12	10	16
8	11	14	8	16
9	9	13	11	12
10	6	5	5	17

A. Mann-Whitney U Test Results

Testing the scores of the "A" questionnaires in the control and test groups, we found that they did not differ significantly (Mann-Whitney U test). In other words, the control and test groups are not heterogeneous at 5% significance level. (U value = 53.500, Z value = 0.265)

We also compared the score differences (after - before condition) of the two groups with a single test, because it could be more adequate for small groups (10 children). Table 3 shows the score differences.

TABLE 3
AFTER AND BEFORE QUESTIONNAIRES' SCORE DIFFERENCES FOR BOTH THE CONTROL AND TEST GROUPS PARTICIPANTS.

ID of participants	Control	Test
	B-A score diff.	B-A score diff.
1	1	5
2	4	0
3	4	6
4	1	5
5	0	12
6	2	10
7	0	7
8	3	8
9	4	6
10	-1	12

We found that they differ significantly (Mann-Whitney U test). In other words, after two weeks the control and test groups are not homogeneous at 5% significance level. (U value = 92.000, Z value = 3.175).

B. Wilcoxon Paired Test Results

Using the mean and standard error of the signatures of the test group, the value of t is 5.780. At 5% significance and 9 degrees of freedom, the critical t value is 2.260 [36]. Accordingly, we reject the null hypothesis and accept the alternative hypothesis for the test group. In other words, the noise awareness of the test group was significantly increased by the application (at 5% significance level).

In the control group, t is 2.249. Similarly, the critical t value is 2.262 [37] at 5% significance level. Based on this, we accept the null hypothesis. That is noise awareness did not change significantly in the control group.

VI. CONCLUSION

Literature research shows that noise awareness rising games/applications already exist. However, their scientific basis is still indigent. Although there are calls for noise-induced hearing loss on more and more platforms (for example International Noise Awareness Day).

In this study, we developed a web application within the "Protect Your Ears" project, that helps children increase their noise awareness and prevention methods in a playful form.

Different needs and implementation options were considered during the development process. Finally, three types of games were created for the website (www.ovdafuled.hu). Of these, one specifically served to raise noise awareness.

To test the completed application, we conducted a cohort study in Dr. Török Béla Kindergarten and Primary School. Accordingly, a test and control group was separated. The test group could use the application for two weeks, while the control group could not.

Through the questionnaires, we examined whether the web application significantly improves noise awareness in the test group or not. The homogeneity of initial setup was examined beforehand and resulted that the two study groups were sampled from the same population.

Wilcoxon and Mann-Whitney U (for score differences) tests showed a significant difference in the test group's performance in developing noise awareness. This was not observed in the control group. We have seen that familiarity with the subject that can increase noise awareness, but without using the web application the improvement was not significant.

So it can be said the use of developed games have helped to raise noise awareness. This highlights the importance of developing hearing protection games. This will allow the child to playfully learn about the ear protection and the importance of noise. While just mentioning information about the topic, noise awareness increase will be less effective.

Based on this study, we cannot draw conclusions - understandably - for the entire population. That is why it is necessary for validation, detailed professional review in order to form a more accurate opinion about its effectiveness. In doing so, it is worthwhile to increase the number of samples, to ensure representativeness, and to include other parameters that may affect the phenomenon (living environment, lifestyle, etc.). It is worth examining healthy as well as hearing-impaired children separately (ensuring homogeneity), and it may be interesting to assess a mixed arrangement from these groups in order to determine the correlation as accurately as possible. Instead of a possible questionnaire survey, it is worthwhile to examine awareness in other ways, as the collection of questionnaire data may not reflect the decisions made in real life. In this context, it would become possible to demonstrate whether the application is in fact able to raise awareness among children.

In the future, it may worth expanding the variety of the games or implementing a personalized recommendation (suggesting a suitable game in case of an age or problem option). Also, there is a need to examine this study with study groups of more participants.

Although this would require new, more comprehensive research, realizing this idea is likely to be more effective in raising awareness among children while having fun.

VII. ACKNOWLEDGMENT

The authors would like to thank Mónika Gyurkovics and her team from the Dr. Török Béla Kindergarten and Primary School for their help and guidance in creating the child interface and conducting the research. We would like to highlight Dávid Babiák's contribution towards creating the website. We would also like to thank Hala Muhanna for contributing with her voice to the application.

REFERENCES

- [1] World Health Organization. (2018). Addressing the rising prevalence of hearing loss. World Health Organization. <https://apps.who.int/iris/handle/10665/260336>. License: CC BY-NC-SA 3.0 IGO
- [2] World Health Organization, 'Deafness and hearing loss', 2019. [Online]. Available: <https://www.who.int/news-room/fact-sheets/detail/deafness-and-hearing-loss>. [Accessed: 30-Jan-2020].
- [3] American Speech-Language-Hearing Association (ASHA), 'Causes of Hearing Loss in Children'. [Online]. Available: <https://www.asha.org/public/hearing/Causes-of-Hearing-Loss-in-Children/>. [Accessed: 31-Jan-2020].
- [4] L. L. Cunningham and D. L. Tucci, 'Hearing Loss in Adults', *N. Engl. J. Med.*, vol. 377, no. 25, pp. 2465–2473, Dec. 2017, doi: 10.1056/NEJMra1616601.
- [5] S. F. Carroll YI, Eichwald J, 'Vital Signs: Noise-Induced Hearing Loss Among Adults - United States 2011-2012', 2017. doi: 10.15585/mmwr.mm6605e3
- [6] European Commission, 'Noise pollution in the EU'. [Online]. Available: https://ec.europa.eu/environment/basics/health-wellbeing/noise/index_en.htm. [Accessed: 25-Jan-2020].
- [7] European Environment Agency, 'Number of people exposed to average day-evening-night noise levels (Lden) ≥ 55 dB in Europe', 2019. [Online]. Available: https://www.eea.europa.eu/data-and-maps/daviz/number-of-people-exposed-to-8#tab-googlechartid_chart_21. [Accessed: 27-Jan-2020].
- [8] European Environmental Agency, 'Noise in Europe 2014', Luxembourg, 2014. doi: 10.2800/763331
- [9] L.-B. Johann-Wolfgang, E. Kerstin, and E. Angelika, *Lärm und Gesundheit. Köln (Noise and health), Bundeszentrale für gesundheitliche Aufklärung (BZgA), 2001. ISBN 3-933191-53X*
- [10] Téglás Zsolt Gábor, 'Iskolai zajártalmak', *Pedagogical Periodicals*, 2004. [Online]. Available: <https://folyoiratok.oh.gov.hu/tj-pedagogiai-szemle/iskolai-zajartalmak>. [Accessed: 22-Dec-2019].
- [11] K. Eysel-Gosepath, T. Daut, A. Pinger, W. Lehmacher, and T. Erren, 'Effects of noise in primary schools on health facets in German teachers', *Noise Heal.*, vol. 14, no. 58, pp. 129–134, May 2012,
- [12] B. Shield and J. Dockrell, 'The Effects of Noise on Children at School: A Review', *Build. Acoust.*, vol. 10, pp. 97–116, Jun. 2003, doi: 10.1260/135101003768965960.
- [13] B. Shield and J. Dockrell, 'The effects of environmental and classroom noise on the academic attainments of primary school children', *J. Acoust. Soc. Am.*, vol. 123, pp. 133–144, Feb. 2008, doi: 10.1121/1.2812596.
- [14] G. Evans and S. Lepore, 'Nonauditory Effects of Noise on Children: A Critical Review', *Child. Environ.*, vol. 10, pp. 31–51, Jan. 1993
- [15] S. Cohen, G. W. Evans, D. S. Krantz, and D. Stokols, 'Physiological, motivational, and cognitive effects of aircraft noise on children: Moving from the laboratory to the field', *Am. Psychol.*, vol. 35, no. 3, pp. 231–243, 1980, doi: 10.1037/0003-066X.35.3.231.
- [16] Központi Statisztikai Hivatal (KSH), 'A 2014-ben végrehajtott Európai lakossági egészségfelmérés eredményei', 2018. ISBN 978-963-235-508-5
- [17] World Health Organization, 'Global costs of unaddressed hearing loss and cost-effectiveness of interventions', 2017. ISBN 978-92-4-151204-6
- [18] T. Gázsó, A. Sebestyén, D. Endrei, and I. Boncz, 'PSS4 Health insurance burden of conductive and sensorineural hearing loss in Hungary: A nationwide, real world treatment cost of illness study', *Value Heal.*, vol. 22, pp. S363, May 2019, doi: 10.1016/j.jval.2019.04.1776.
- [19] L. C. Erickson and R. S. Newman, 'Influences of Background Noise on Infants and Children', *Curr. Dir. Psychol. Sci.*, vol. 26, no. 5, pp. 451–457, Oct. 2017, doi: 10.1177/0963721417709087.

[20] G. W. Evans, P. Lercher, M. Meis, H. Ising, and W. W. Kofler, 'Community noise exposure and stress in children', *J. Acoust. Soc. Am.*, vol. 109, no. 3, pp. 1023–1027, 2001, doi: 10.1121/1.1340642.

[21] Lee Donguk, Yu Jyachyung, Han Woojae, 'Evaluation and Analysis of Awareness in Noise-induced Hearing Loss Using Survey' *The Journal of the Acoustical Society of Korea*. 34. 274-281., 2015. doi: 10.7776/ASK.2015.34.4.274.

[22] Maricone Raffaele, Luzzi Sergio, Natale, Rossella, "Instruments, methods and activities for noise awareness", in the 22nd International Congress on Sound and Vibration, Florence, Italy, 2015.

[23] Dangerous Decibels, 'Dangerous Decibels'. [Online]. Available: <http://dangerousdecibels.org/>. [Accessed: 31-Jan-2020].

[24] WHO Programme for the Prevention of Deafness and Hearing Impairment. (1998). Prevention of noise-induced hearing loss: report of an informal consultation held at the World Health Organization, Geneva, on 28-30 October 1997. World Health Organization. <https://apps.who.int/iris/handle/10665/65390>.

[25] S. E. Griest, R. L. Folmer, and W. H. Martin, 'Effectiveness of "dangerous decibels," a school-based hearing loss prevention program', *Am. J. Audiol.*, vol. 16, no. 2, pp. 165–182, 2007, doi: 10.1044/1059-0889(2007)021.

[26] Alnuman Nasim, Ghnimat Talha, 'Awareness of Noise-Induced Hearing Loss and Use of Hearing Protection among Young Adults in Jordan' *International Journal of Environmental Research and Public Health*. 16. doi: 10.3390/ijerph16162961.

[27] E. Rovithis, A. Floros, A. Mniestris and N. Grigoriou, "Audio games as educational tools: Design principles and examples," 2014 IEEE Games Media Entertainment, Toronto, ON, 2014, pp. 1-8, doi: 10.1109/GEM.2014.7048083.

[28] S. Katie and N. Jakob, 'Children's UX: Usability Issues in Designing for Young People', Nielsen Norman Group, 2019. [Online]. Available: <https://www.nngroup.com/articles/childrens-websites-usability-issues/>. [Accessed: 01-Feb-2020].

[29] T. Nousiainen and M. Kankaanranta, 'Exploring Children's Requirements for Game-Based Learning Environments', *Adv. Human-Computer Interact.*, vol. 2008, pp. 1–7, 2008, doi: 10.1155/2008/284056.

[30] L. Darling-Hammond, L. Flook, C. Cook-Harvey, B. Barron, and D. Osher, 'Implications for educational practice of the science of learning and development', *Appl. Dev. Sci.*, vol. 0, no. 0, pp. 1–44, 2019, doi: 10.1080/10888691.2018.1537791.

[31] World Health Organization, 'Primary ear and hearing care training resource', *World Heal. Organ. Geneva*, pp. 1–90, 2006, doi: 10.1007/BF02887432.

[32] Johnson TA, Cooper S, Stamper GC, Chertoff M. 'Noise Exposure Questionnaire: A Tool for Quantifying Annual Noise Exposure', *J Am Acad Audiol*. 2017;28(1):14-35. doi: 10.3766/jaaa.15070

[33] Penafiel Emie, 'Developing a Questionnaire to Assess Noise Exposure in Children and Teens', Thesis, Department of Speech and Hearing Science Honors Theses, Ohio State University, Columbus, Ohio, United States, 2007.

[34] N. Nachar, 'The Mann-Whitney U: A Test for Assessing Whether Two Independent Samples Come from the Same Distribution', *Tutor. Quant. Methods Psychol.*, vol. 4, no. 1, pp. 13–20, 2008, doi: 10.20982/tqmp.04.1.p013.

[35] E. Whitley and J. Ball, 'Statistics review 6: Nonparametric methods', *Crit. Care*, vol. 6, no. 6, pp. 509–513, 2002, doi: 10.1186/cc1820.

[36] Ted Hessing, 'Z Scores (Z Value) & Z Table & Z Transformations', [sixsigmastudyguide.com](https://sixsigmastudyguide.com/z-scores-z-table-z-transformations/). [Online]. Available: <https://sixsigmastudyguide.com/z-scores-z-table-z-transformations/>. [Accessed: 02-Feb-2020].

[37] Six Sigma Material, 't-distribution (t-tests)', <https://www.six-sigma-material.com/t-distribution.html>. [Online]. Available: <https://www.six-sigma-material.com/t-distribution.html>. [Accessed: 03-Feb-2020].



Dániel Szántó was born in Gyöngyös, Hungary in 1995. He graduated from the Semmelweis University with Bachelor's Degree in Health Care Management (2018 - Hungary, Budapest). He also graduated from the Budapest University of Technology and Economics with Master's Degree in Biomedical Engineering (2020 - Hungary, Budapest).

Since March 2020, he has been software developer in Hatvan, Hungary. His diploma work focused on Developing a Noise Awareness Rising Web Application.

In 2017, he participated in Student Research Societies of Semmelweis University with the work of Mobile health application development. He won the National Higher Education Scholarship in 2017 and the Hungarian Republic Scholarship in 2016.



Attila Zoltán Jenei was born in Debrecen, Hungary in 1995. He is graduated at the Budapest University of Technology and Economics as Biomedical Engineer (Master's Degree, 2020). Since January 2020, he has been a research assistant in the Laboratory of Speech Acoustic, Department of Telecommunications and Media Informatics, Faculty of Electrical Engineering and Information Technology. His research and diploma work focuses on the speech-based diagnostic opportunities of depression, Parkinson's disease and

different voice disorder groups. In 2019, he participated in Student Research Societies of Budapest University of Technology and Economics with the work of Automatic speech-based detection of depression with 2D convolutional networks.



Miklos Gabriel Tulics was born in Baia Mare, Romania, on Aug. 15, 1988. He is currently a technical assistant and a Ph.D. candidate at the Laboratory of Speech Acoustics, Budapest University of Technology and Economics, focusing on automatic speech recognition, machine learning, pathological voice disorder recognition and noise awareness. He earned his Master's degree in Electrical Engineering in 2015. Tulics has been working for the Department of Telecommunications and Media Informatics, Budapest

University of Technology and Economics since 2013.



Klára Vicsi DSc Ph.D. is currently a lead research professor and was the Chief of the Laboratory of Speech Acoustics of the Department of Telecommunications and Media Informatics at Budapest University of Technology and Economics from 2002 until 2018. She earned her Master's degree at the Loránd Eötvös University of Sciences, Budapest in 1966-1971.

She earned her DSc degree at the Hungarian Academy of Sciences in 2005, her PhD degree at the Technical University of Budapest in 1992, and her Doctor's

degree at Loránd Eötvös University of Sciences in 1982. She has worked as a researcher and lecturer, participated in conferences and congresses in several countries such as Germany, California USA, Finland and Poland. She is responsible for the organization of many international conferences, workshops and summer schools. She holds project manager and participant member status in several international research projects such as: Contact person, of CLARIN, FLReNet, ELSNET. She is the leader of the Acoustical Complex Committee of the Hungarian Academy of Sciences, a Member of ISCA and a member of the scientific board of journals. She has more than 122 publications in peer-reviewed journals, 67 refereed conference proceedings and is the owner of three patents.

Detection of 2x2 MIMO signals

János Ladvánszky¹

Abstract— In this paper, we investigate synchronization and equalization of 2 x 2 MIMO signals. We make a step further than that is described in our patent. In the patent, 3 PLLs and a four-channel adaptive filter was needed. Here we decrease the number of PLLs to two and use an adaptive filter of only two channels. In addition to that, we shortly introduce the filter method and the FFT method as well, for synchronization. False detection cancellation is also mentioned. The so-called 1-bit technique has been compared to our method. After briefly introducing the ideas, detailed Matlab or AWR analyses follow. Input data are real measurements, so the analyses serve also as experimental verifications. We take a glimpse on higher order MIMO and higher order modulations as well.

Index Terms—MIMO, synchronization, equalization, false detection cancellation

I. INTRODUCTION

The 2 x 2 MIMO (Multiple Input Multiple Output) concept is shown in Fig. 1. The core of the idea is that 2-2 transmitter and receiver antennas can provide better system properties than two transmitter-receiver antenna pairs separately.

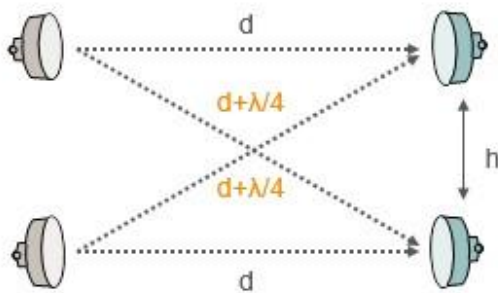


Fig. 1. The 2 x 2 MIMO concept. From d and the operation frequency, h is determined

For achieving this, a 90° difference in electrical length is needed between each transmitter antenna to the two receiver antennas.

Both receiver antennas receive two signals shifted in time. If the modulation is 4QAM, then based on the properties of the signal, the two transmitted information can be separated. For separation, estimated receiver frequencies should be known. Finding the exact receiver frequencies (synchronization) and the reconstruction of the constellation diagrams (channel equalization) can be realized by three PLLs and a four-channel adaptive filter [2].

¹ Formerly with Ericsson Hungary, Budapest, Hungary.
(e-mail: Ladvanszky55@t-online.hu)

In this paper, our more recent solution will be described that requires only two PLLs and a two-channel adaptive filter. The best overview about MIMO is found in [1]. In [2], our patent about MIMO is described. In [3], use of more than 4 antennas are investigated. Higher order modulations than 4QAM are discussed in [4]. DSc dissertation of the author, including a thesis about MIMO, is obtained in [5].

II. THE MODEL

The model of a 2 x 2 MIMO communication system is shown in Fig. 2.

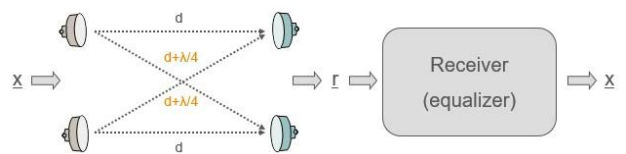


Fig. 2. Model of a 2 x 2 MIMO communication system. $\underline{x}, \underline{r}$ denotes the column matrices of transmitted and received signals, respectively

According to Fig. 2, an equalizer is applied for the receiver signal to reconstruct the transmitted signal.

$$\underline{r} = \begin{bmatrix} a & b \\ b & a \end{bmatrix} \underline{x} \quad (1)$$

Eq. (1) describes the antenna system. In ideal case,

$$a = 1 \quad (2)$$

$$b = e^{-j\pi/2} = -j \quad (3)$$

And the reconstruction:

$$\hat{\underline{x}} = \begin{bmatrix} a' & b' \\ b' & a' \end{bmatrix}^{-1} \underline{r} \quad (4)$$

Our goal is

$$|\hat{\underline{x}} - \underline{x}| = \min. \quad (5)$$

And the minimum in Eq. (5) is zero if

$$\underline{a}' = \underline{a} \quad (6)$$

$$\underline{b}' = \underline{b} \quad (7)$$

The problem is that Eq. (6,7) are not fulfilled in practice. The following secondary effects may occur:

- propagation loss,
- wind,
- mechanical tolerances,
- rain,
- aging,
- deviation of transmitter and receiver frequencies,
- time dependence of frequencies,
- noise, etc.

For that reason, both the frequency recovery and the equalizer should be adaptive. In the following, we discuss solutions for these problems.

III. EXAMPLE

Our work is based on a set of measured data in a file. The received signals on both antennas are measured and stored in a file. First, we try to reconstruct the frequencies. For a good start, the measurement set contains a pilot. Later, the pilot will be removed.

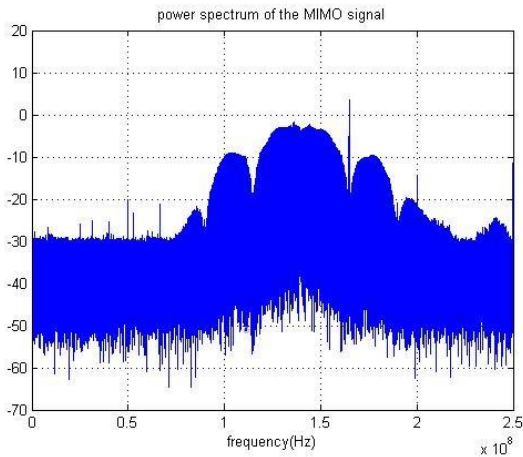


Fig. 3. FFT of the measured data with a pilot

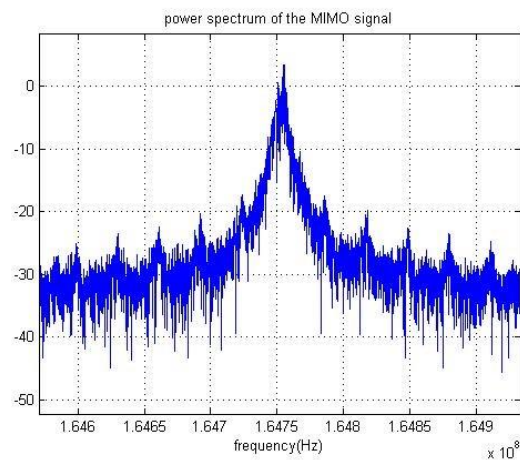


Fig. 4. The previous Figure, magnified

From Fig. 4, the pilot frequency is 164.75 MHz. But we observed that small deviations in frequency may cause a rotation of the received constellation diagram, and that may lead to false detection. For this reason, the frequencies should be determined with a high accuracy. That can be realized by a Costas loop. Matlab subsystems for the Costas loop will be described now.

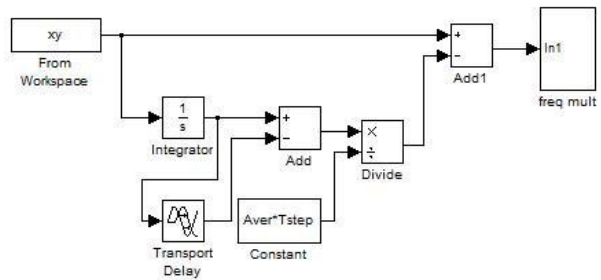


Fig. 5. The overall system

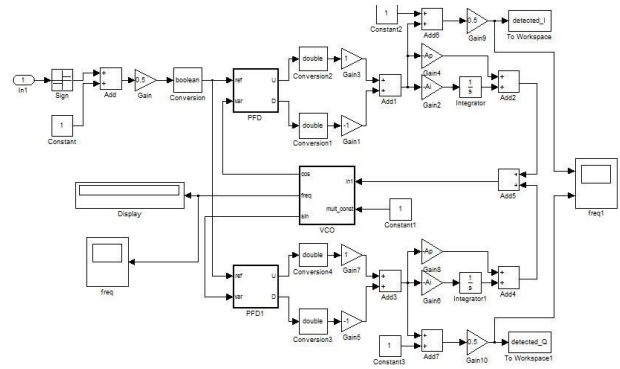


Fig. 6. The core: Costas loop. In Fig. 5, this is the block freq mult

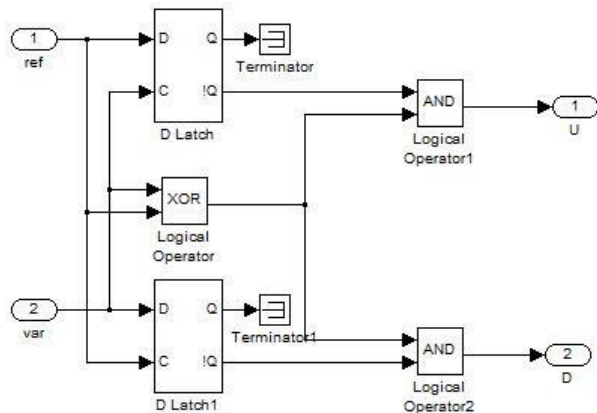


Fig. 7. The phase-frequency detector PFD in Fig. 6

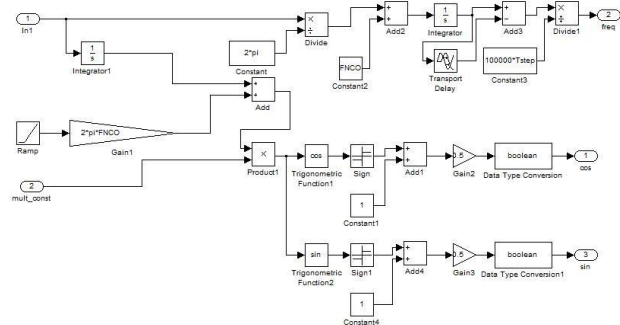


Fig. 8. The VCO in Fig. 6

Detection of 2x2 MIMO signals

First we show how the pilot frequency is found.

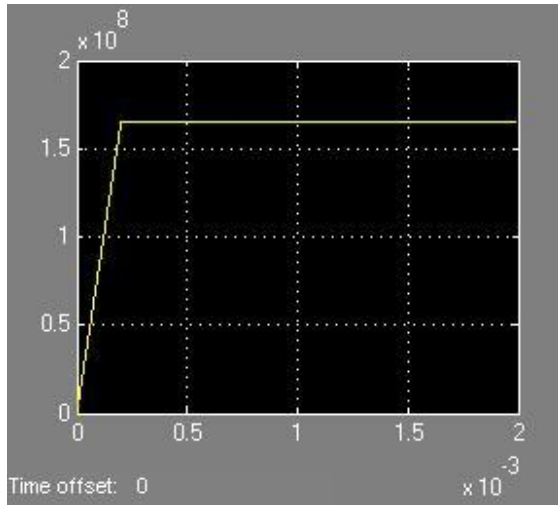


Fig. 9. Initial transient in instantaneous frequency

Settling time is about 0.2 msec. Now the detected I and Q signals are filtered.

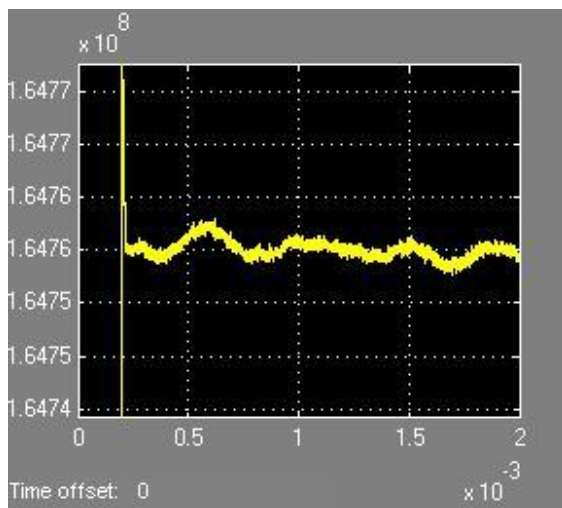


Fig. 10. The previous Figure, magnified. After settling, the frequency is kept within 1 kHz

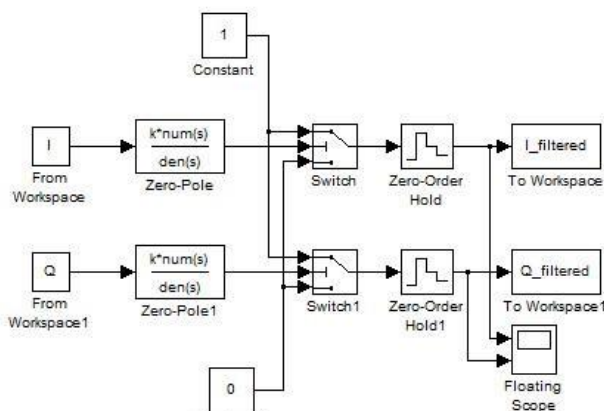


Fig. 11. Filtering system

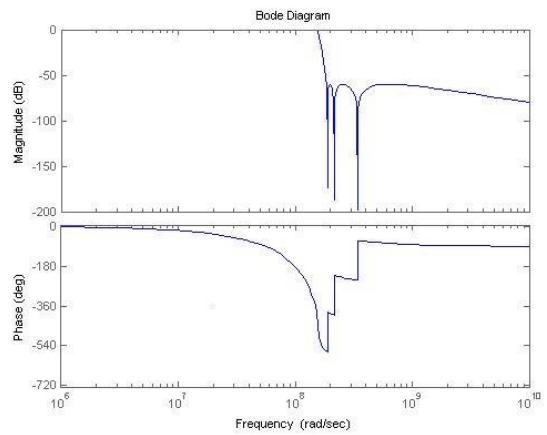


Fig. 12. Filter characteristics

As a conclusion of this example, a faster method is needed that is more accurate. Costas loop is too time-consuming.

Now we remove the pilot. The result is that the constellation diagram cannot be reconstructed in this way.

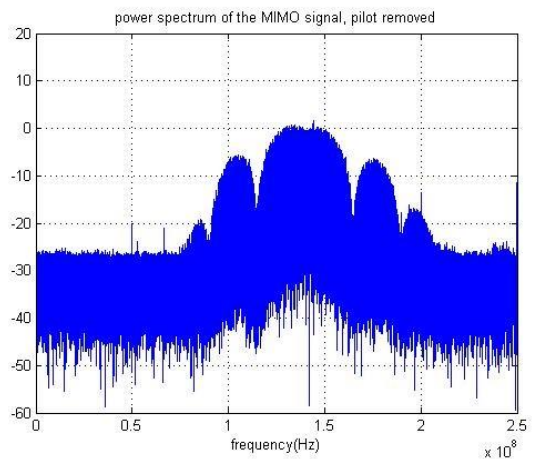


Fig. 13. FFT of the received signal without a pilot

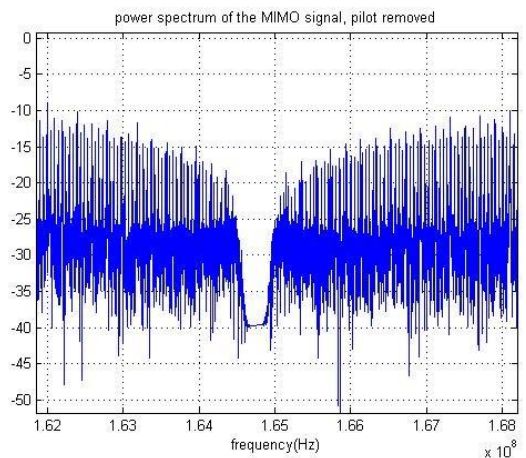


Fig. 14. The previous Figure, with increased frequency resolution

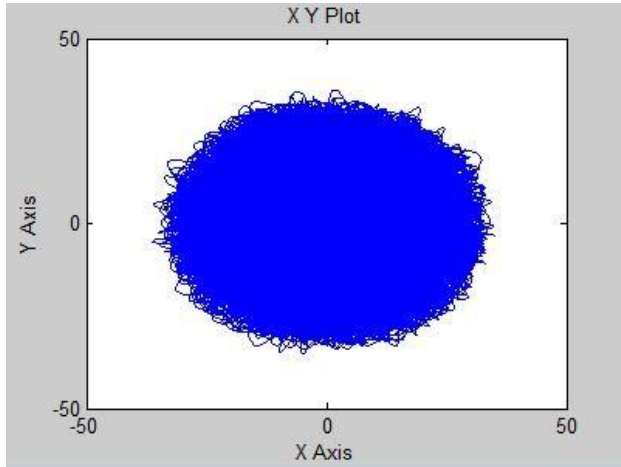


Fig. 15. The problem: The constellation diagram cannot be reconstructed in this way

IV. THE MCMA EQUALIZER AND PLLS

Basically, we have two problems. Deviation of the transmitted and received frequencies, and separation of the two transmitted signals at receiver side. Deviation is solved by PLLs, separation and signal equalization are solved by adaptive filters. Deviation can be modelled in the following way.

The baseband receiver signal $\underline{\hat{x}}$ for perfect separation, can be formulated as follows:

$$\begin{aligned} \underline{\hat{x}} &= \underline{A}^{-1} \underline{H}^{-1} \underline{B}^{-1} \underline{r} = \\ &= \begin{bmatrix} e^{-j\omega_1 t} & 0 \\ 0 & e^{-j\omega_2 t} \end{bmatrix} \begin{bmatrix} 1/2 & j/2 \\ j/2 & 1/2 \end{bmatrix} \begin{bmatrix} e^{-j\omega_3 t} & 0 \\ 0 & e^{-j\omega_4 t} \end{bmatrix} \underline{r} \end{aligned} \quad (8)$$

where ω_1, ω_2 are the two LO frequencies at transmitter side and ω_3, ω_4 are the two LO frequencies at receiver side. In ideal case, $\omega_1 = -\omega_3$ and $\omega_2 = -\omega_4$.

From our experiments we know that the equalizer can stop a slow rotation. For this reason, instead of Eq. (8), we may use

$$\begin{aligned} \underline{\hat{x}} &= \frac{1}{c} \underline{A}^{-1} \underline{H}^{-1} c \underline{B}^{-1} \underline{r} = \\ \begin{bmatrix} 1 & 0 \\ 0 & e^{-j(\omega_2 - \omega_1)t} \end{bmatrix} & \begin{bmatrix} 1/2 & j/2 \\ j/2 & 1/2 \end{bmatrix} \begin{bmatrix} e^{-j(\omega_3 + \omega_1)t} & 0 \\ 0 & e^{-j(\omega_4 + \omega_1)t} \end{bmatrix} \underline{r} \end{aligned} \quad (9)$$

where $c = e^{-j\omega_1 t}$. Consequently, three PLLs may solve the problem. One at the output of the equalizer with frequency $\omega_2 - \omega_1$, and two before the equalizer with frequencies $\omega_3 + \omega_1$ and $\omega_4 + \omega_1$.

According to our previous experience, the equalizer can compensate small frequency differences. It follows the three PLLs can be decreased to two. In ideal case, $\omega_3 = -\omega_1$, $\omega_2 = \omega_1$, and $\omega_4 = -\omega_2$. Thus, with two PLLs that are locked to the input carrier frequencies, the synchronization can be solved. Details are found on Fig. 16.

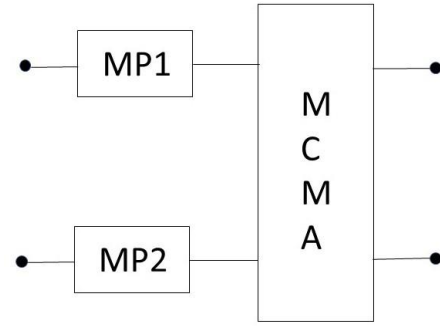


Fig. 16. Finding the proper LO frequencies at receiver side by use of two Costas loops. We use here our Costas loop version that is suggested for large noise [6]

The synchronizer consists of two Costas loops, and the VCO drive signal is formulated from both complex inputs. Realization of Fig. 16 in Matlab is presented in the next Figures that are found at the end of the paper. The detected I and Q signals are shown in Fig. 20.

Then the details of the equalizer follow. The equalizer is a four-channel adaptive filter. Inputs of the equalizer are the complex signals from the synchronizer as shown in Fig. 16.

The system diagram of the equalizer are also found at the end of the paper.

Now the I and Q signals at both channels must be reconstructed. We use the MCMA (Modified constant modulus algorithm) [1]. Its essence is the following. The equalized signal is, according to Eq. (8):

$$\hat{x}_1 = w_1 r_1 + w_2 r_2 \quad (10)$$

$$\hat{x}_2 = w_3 r_1 + w_4 r_2 \quad (11)$$

where w_i -s are the weight factors of the adaptive filter channels. Initial values are $w_{1,1} = w_{4,1} = \frac{1}{2}$, $w_{2,1} = w_{3,1} = \frac{1}{2}j$, according to Eq. (9). A possible choice would be $w_1 = w_4$ and $w_2 = w_3$. This would require an ideal placement of the antennas at vertices of a rectangle. But this rectangle may be distorted by several reasons resulting in hurting condition $w_2 = w_3$.

Change of the equalized signals is

$$\Delta \hat{x}_1 = \Delta w_1 r_1 + w_1 \Delta r_1 + \Delta w_2 r_2 + w_2 \Delta r_2 \quad (12)$$

$$\Delta \hat{x}_2 = \Delta w_3 r_1 + w_3 \Delta r_1 + \Delta w_4 r_2 + w_4 \Delta r_2 \quad (13)$$

where $\Delta w_{1,k} = w_{1,k} - w_{1,k-1}$ in the k th iteration, and similarly for the other weight factors. The signals in the next iteration are $\hat{x}_1 + \Delta \hat{x}_1$ and $\hat{x}_2 + \Delta \hat{x}_2$. The error signals are defined as

$$\varepsilon_1 = \{\hat{x}_{1,1}\}(|\hat{x}_{1,1}| - R_1) + j\{\hat{x}_{1,2}\}(|\hat{x}_{1,2}| - R_2) \quad (14)$$

$$\varepsilon_2 = \{\hat{x}_{2,1}\}(|\hat{x}_{2,1}| - R_1) + j\{\hat{x}_{2,2}\}(|\hat{x}_{2,2}| - R_2) \quad (15)$$

where the complex radius of the constellation diagram is $R = R_1 + jR_2 = |R|(1 + j)/\sqrt{2}$, braces denote signum, and $r_1 = \hat{x}_{1,1} + j\hat{x}_{1,2}$. The goal is $\varepsilon_1 = \min$. and $\varepsilon_2 = \min$.

Changes of the equalized signals are

$$\Delta\hat{x}_1 = -\mu_1\varepsilon_1 \quad (16)$$

$$\Delta\hat{x}_2 = -\mu_2\varepsilon_2 \quad (17)$$

where Δ denotes the change during the last sampling period. From Eq. (12, 13) changes of the weight factors during the last sampling period are

$$\begin{bmatrix} \Delta w_1 \\ \Delta w_2 \end{bmatrix} = [r_1 \quad r_2]^+ (\Delta\hat{x}_1 - w_1\Delta r_1 - w_2\Delta r_2) \quad (18)$$

$$\begin{bmatrix} \Delta w_3 \\ \Delta w_4 \end{bmatrix} = [r_1 \quad r_2]^+ (\Delta\hat{x}_2 - w_3\Delta r_1 - w_4\Delta r_2) \quad (19)$$

in the k th iteration, where $+$ denotes Moore-Penrose generalized inverse. Here we exploit the fact that the generalized inverse gives the minimum norm solution of an under-determined system [10].

The algorithm starts with w_1, w_2, w_3, w_4, r_1 and r_2 . Then Eq. (10, 11, 14-19) are executed. Then w -s and r -s are delayed. Similarly, for the other channel. The given algorithm significantly differs from known algorithms [1]. Robustness of the algorithm has been observed during all runs.

V. RELATED QUESTIONS

Here we summarize some other important ideas related to 2 x 2 MIMO detection.

Filter method

Essence of the filter method is that instead of a PLL, a filter is applied for synchronization. Advantage with respect to the previous Chapter is, that the random changes on LO frequencies are much smaller, and locking problems are eliminated. Hardware requirements are of the same amount.

FFT method

The filter function can be realized by applying FFT of the input signal. FFT is computation consuming, so it is a hard decision how often the FFT is made. Advantages are the same as for the filter method.

False detection cancellation

False detection occurs when the received constellation diagram suddenly rotates by 90°. Originally, we made a great effort on false detection cancellation. However, in our previous publication [8], we pointed out that the most efficient solution of this problem is application of differential coding. Thus, we omit here the list of other methods for false detection cancellation.

The 1-bit method [9]

The main difference between this and our method is that in this method, the signal after synchronization is digitized. This is a limiting case, in the literature few bits A/D conversion can also be found. The author's opinion is that the possible advantage of decreasing the noise effects is virtual, because it remains at the random variation of zero crossings. Moreover, strong learning algorithms may be needed for equalization that are time consuming.

More than 4 antennas

In case of more than 4 antennas, differences in distances between a transmitter antenna and neighboring receiver antennas cannot be kept constant. Even synchronization is more difficult, because there are many transmitter frequencies that can be different all. Equalization is to invert the matrix describing the relation between separate transmitter and receiver signals. But these are possible [3], however, the extra advantage of more than 4 antennas decrease.

Higher order modulation

Essentially arbitrary order (power of 2) can be used [4]. In our opinion, its significance is not too high because for higher order modulation, noise sensitivity rapidly increases, and it is a better solution to apply lower order modulation at higher speed.

VI. CONCLUSIONS

The synchronization by two Costas loops and the equalization using an adaptive filter have been detailed. The algorithms are robust. The system can follow the random variations of any kind that are included in the measured data. We call the attention to the fact that for synchronization we used our best version of Costas loop, but without differential coding, and for equalization, we corrected the errors found in the literature. As a result, the standing constellation diagrams appear soon at the output, and remain almost constant for the rest of the measurement interval. Other Hungarian efforts concerning MIMO technique are found in [11]. A possible use of MIMO is presented in [12].

In answering to the reviewer openly, this is not a summary paper. Material in Section 4 is brand new, especially Eq. (18,19). As its previous version is patented [2], it is used worldwide.

ACKNOWLEDGMENTS

This work was started at the microwave center of Ericsson in Gothenburg, Sweden in 2010 and continued at Ericsson Hungary, Budapest. The good research atmosphere at both places should be acknowledged.

The whole work in Gothenburg was performed with Dr. G. Kovács, my younger colleague at Ericsson. He was an excellent partner in every phase of the work. Special thanks for the first in-house review of this paper. Mrs. Anna Rhodin was our host in Gothenburg. She obtained the measurement data we used in our experiments. With her, three of us became the authors of our patent in this work. From management side, we were supported by Mr. V. Beskid, Dr. Á. Vámos and Dr. P. Verebély, and finally by Dr. B. Kovács.

REFERENCES

- [1] Ingason, T., Haonan, L.: "Line-of-Sight MIMO for Microwave Links", MSc Thesis, Chalmers University of Technology, Göteborg, Sweden, July 2009
- [2] Ladvánszky, J., Rhodin, A., Kovács, G.: "Synchronization and equalization of 2x2 LoS MIMO communication channels", invention disclosure, Ericsson Hungary, 2010, P32542
- [3] Han, D., Lee, C., Park, H., Kahng, S.: "Antenna Design for 4-by-4 MIMO Communication", 2016 International Conference on Signal Processing and Communication (ICSC)
- [4] Jacobsson, S., Durisi, G., Coldrey, M., Goldstein, T., Studer, C.: "Nonlinear 1-Bit Precoding for Massive MU-MIMO with Higher-Order Modulation", 2016 50th Asilomar Conference on Signals, Systems and Computers, 6-9 Nov. 2016, Pacific Grove, CA, USA
- [5] Ladvánszky, J.: "Integrated optical communication systems", DSc dissertation, Hungarian Academy of Sciences
- [6] Ladvánszky, J., Kovács, B.: "Methods and apparatus for signal demodulation", Ericsson patent, PCT/SE2018/050198, 2018
- [7] Kuznetsov, N. V., Blagov, M. V., Kudryashova, E. V., Ladvánszky, J., Yuldashev, M. V., Yuldashev, R. V.: "Non-linear analysis of a modified QPSK Costas loop", Elsevier, IFAC-PapersOnLine Volume 52, Issue 16, 2019, Pages 31-35
- [8] Ladvánszky, J.: "A Costas loop with Differential Coding", International Journal of Contemporary Research and Review ISSN 0976 – 4852, October, 2017/Volume 08/Issue 10
- [9] Mo, J., Schniter, P., and Heath JR., R. W.: "Channel Estimation in Broadband Millimeter Wave MIMO Systems with Few-Bit ADCs", ArXiv: 6 Dec. 2017
- [10] Boyd, S.: "Least-norm solutions of undetermined equations", lecture, EE263 Autumn 2007-08, <https://see.stanford.edu/materials/lsoidsee263/08-min-norm.pdf>
- [11] Fodor, G., Pap, L., Telek M.: "Recent Advances in Acquiring Channel State Information in Cellular MIMO Systems", Infocomm. Journal, 3/2019
- [12] Hilt, A.: "Microwave Hop-Length and Availability Targets for the 5G Mobile Backhaul", IEEE 42nd Telecommunications and Signal Processing Conference, TSP'2019, Budapest, Hungary, 1-3 July 2019. doi: 10.1109/TSP.2019.8768870



János Ladvánszky was born in Budapest, Hungary in 1955. He received his M.Sc. from the Budapest University of Technology and Economics in 1978. He received the Ph.D. from the Hungarian Academy of Sciences in 1988. He is now just before the defense of his D.Sc. dissertation at the Hungarian Academy of Sciences. His research interests include circuits and systems theory, with microwave and optical applications, and more recently, quantum communications. He is the World Champion in writing

scientific papers in 2018, in electrical engineering. He is an evaluator for the circuits and systems analysis program AWR, and available at LinkedIn, ResearchGate and Facebook.

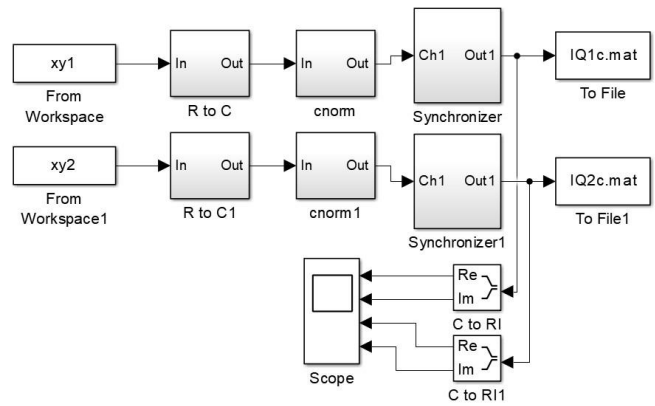


Fig. 17. The synchronization system in Matlab

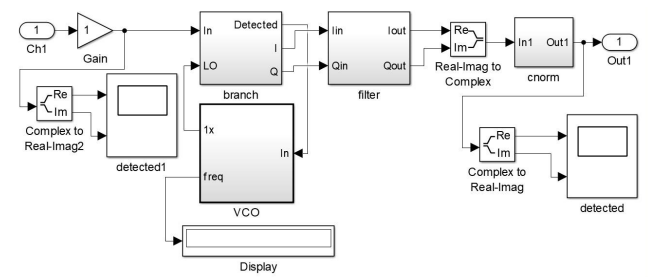


Fig. 18. The Synchronizer in Fig. 17

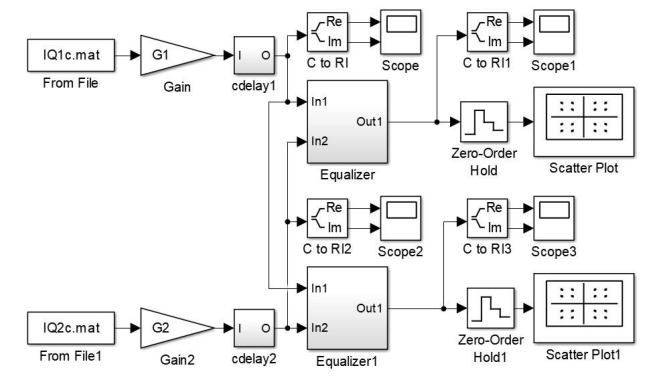


Fig. 19. The equalizer system diagram in Matlab. Input files containing data after synchronization, are IQ1c.mat and IQ2c.mat. Outputs are scatter plots of the equalized constellation diagrams

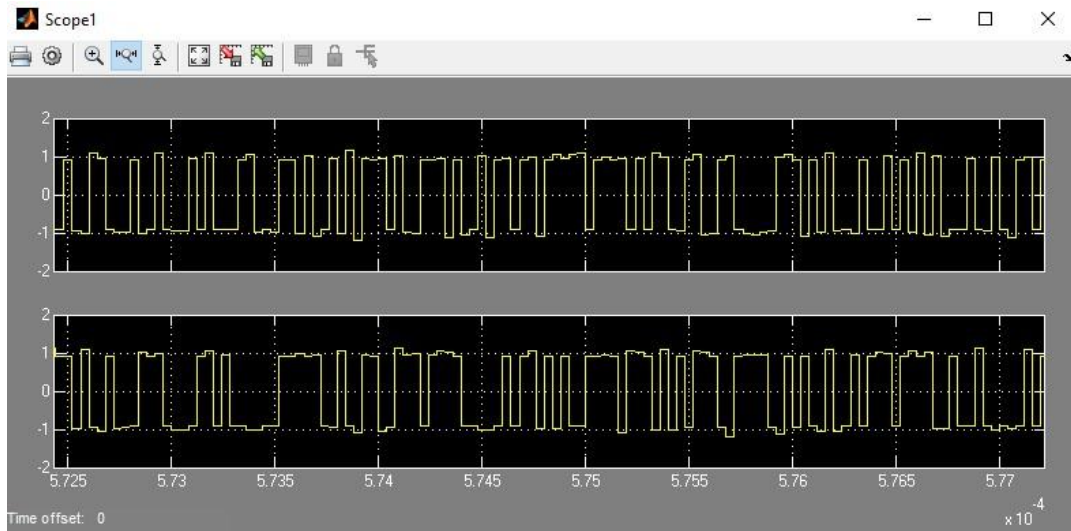


Fig. 20. Output I and Q signals in Fig. 19, Scope 1, with high time resolution

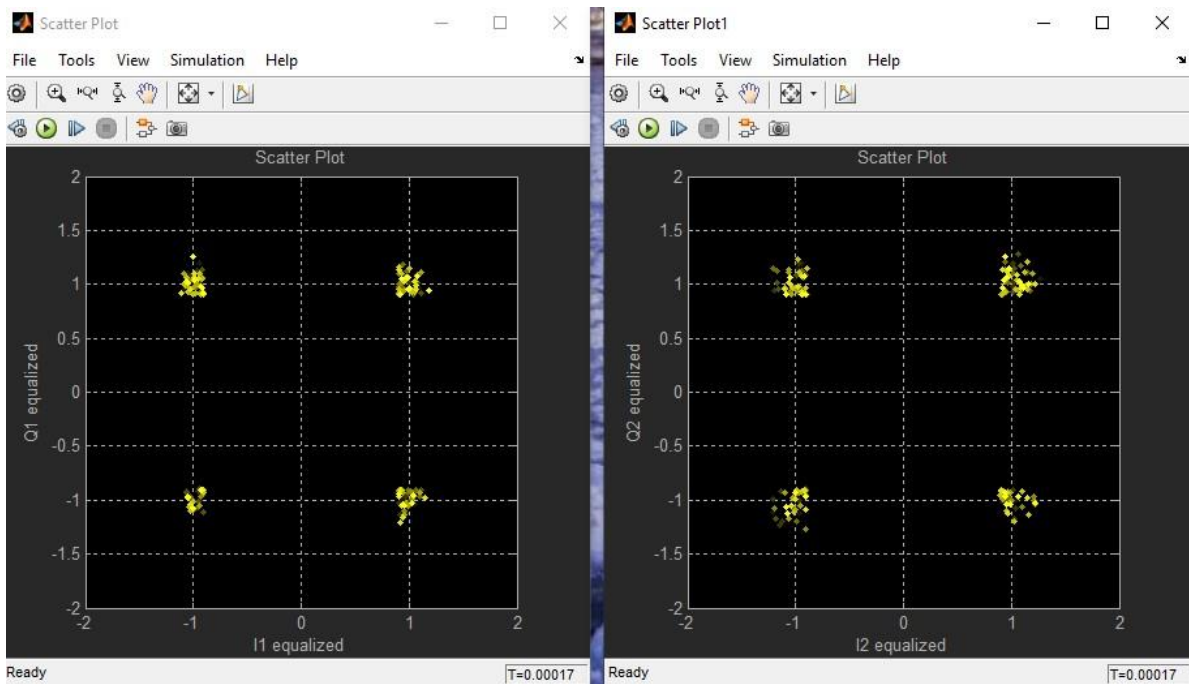


Fig. 21. Output scatter plots in Fig. 19. At the lower right corner of each scatter plot, it can be observed that these constellation diagrams were reconstructed at the very beginning of the simulation time

Business opportunities and evaluation of non-public 5G cellular networks – a survey

Gábor Soós¹, Dániel Ficzer², Tamás Seres³, Sándor Veres⁴ and István Németh⁵

Abstract— The family of cellular mobile telecommunications standards – including 5G – is mostly defined by the 3GPP standardizing organization. While these are well known in detail by researchers and engineers, but in the business world, people are unfamiliar with the concepts and the content of these documents. It is essential to define and designate how 5G is different from existing wired and wireless technologies, what are the main business benefits, and what are the key potential areas according to the new technology achievements. In our work, we present some fundamental aspects of the 5G business potential, where the key motives lay regarding the Industry 4.0 revolution and the innovation of 5G industrial architectures, including vendors, industrial players, and network operators.

Index Terms—5G, Industry 4.0, Private cellular network, Business development, Industrial use-cases

I. INTRODUCTION

The arrival and development of Industry 4.0 represent a revival similar to previous industrial revolutions in history. The revolution in Industry 1.0 was using complex machines to make work easier and faster instead of manual efforts [1]. The primary inventions of the first industrial revolution of 1784 were steam and chain-driven equipment, such as the weaving machine. The second industrial revolution took place in the 1870s when mass production first appeared — developing techniques for mass production and enabler functions such as assembly on a conveyor belt. The third industrial revolution dates back to 1969 when microelectronics brought a new phase of technology. Based on the program code, a robot/machine could perform several operations and work steps, replacing repeated/complex manual work. The fourth industrial revolution is underway, with production lines and robots becoming more intelligent. We are able to create robots that download and use the program, which means that the same production line can adapt to an industrial need very quickly. As a high-level example, at one minute, the workstation produces a Type A car, and in the other one, it can create a Type B car. To accomplish this, all equipment needs to be involved during the reconfiguration of the manufacturing process and must be connected as cyber-physical systems.

It is relatively easy to determine how much overall revenue can be gained from residential users on current

mobile networks. This will not increase significantly in the future, as network operators have almost reached the limit of potential human users, and the population is declining in many countries. In most of the developed countries, more than 90% of the citizens have a mobile phone [2], but using only one or two Subscriber Identity Module (SIM) cards, as the customer does not need more subscriptions. While there are devices in a general household that can use up to 10 or 100 SIM cards, this number can be much higher in industrial use-cases. Mobile Network Operators (MNO) cannot expect significantly more revenue from traditional customers. On the other hand, industrial use-cases could mean a much larger market than before, which is almost completely untapped yet. Thus, the main target user base of 5G is not people but industrial devices, making industrial Campus Networks or as 3GPP defines Non-Public Networks (NPN) [3] one of the flagships of 5G. MNOs and vendors invest in this promise. Besides, they can still stay in the traditional mobile business, but a new market can be created with industrial Campus Networks, similarly to what happened 20 years ago with General Packet Radio Service (GPRS).

Industrial Campus networks [4] have a lot of potential and many directions for development, but the widespread adoption of these solutions is still in its infancy.

The main contribution of the current work is that we present various factors that should be considered to define the business model and pricing of future industrial mobile networks. Moreover, we present some technical parameters to help design, scale, and implement these networks from a service point of view. The paper is organized as follows: Section II summarizes the related work, discussing the potential revenue effects of 5G and the new 5G Non-Public Networks. Section III describes the industrial players' motivations. Section IV presents the key factors of industrial Campus Networks' pricing aspects and customer needs, including network scaling factors, pricing parameters, frequency trading and different types of Campus networks. Section V identifies the business opportunities of customers, discusses the technological risks and backup solutions. Section VI concludes the paper.

II. RELATED WORK

5G's new use-cases [5] are generating tension currently for service providers, device manufacturers, and the industry in general. It is clear that 2G-3G [6] and 4G networks are designed primarily for people in terms of use-cases. Of course, a significant number of machines are connected to

^{1,3,4}T-Systems Magyarország Zrt, Budapest, Hungary

²Budapest University of Technology and Economics, Budapest, Hungary

⁵Magyar Telekom, Budapest, Hungary

E-mail: ^{1,2}{soos, ficzere}@tmit.bme.hu; ³seres.tamas.i@gmail.com;

⁴veres.sandor@t-systems.hu; ⁵nemeth.istvan@telekom.hu

Business opportunities and evaluation of non-public 5G cellular networks – a survey

these networks as end-devices, as well. The almost untapped resources to be provided by 5G are likely to be utilized by machines [7]. Therefore, it is worth separating services based on customer types, as users can be humans or machines [8]. In interpersonal communication, biorhythm has to be one of the important aspects of the network design. Human users' data consumption is related to their biorhythm, which defines the concept of busy-hour on traditional mobile networks. In contrast, machine communication is based on predefined scheduled programs, and the behavior is more determinable [9]. Human data consumption is more stochastic by nature. The current interpretation of busy-hour will probably disappear in the near future or at least significantly alter due to the nature of machine type communication [10]. This should have an impact on both network and service design. 5G network slicing is designed to handle efficiently these kind of network traffic profiles [11]. Networks should be designed [12], scaled, and tuned differently for humans and differently for machine-communication types of services. Machine type of use-cases can include not only the simplest household appliances or vehicles but also complex industrial robots [13]. Hard real-time connectivity – when a sensor-to-machine latency is less than 1 ms – will be utilized by several use-cases, however mostly by non-human applications [14]. With 5G, we will be able to achieve a real-time production monitoring [15], knowing the current state of equipment we are ordering, or the time when it is expected to be manufactured, with proper access rights from anywhere around the globe. It also facilitates the development of real-time business and the advancement of services where precision has immense business importance. All in all, this means that the economy as a whole will benefit from the spread of 5G [16].

To understand the exact economic effects, we have to examine which parts of the industry are affected and to what extent [17] [18] [19], [20]. According to a study published by Ericsson, it is estimated that the 5G-enabled industry digitization revenue for Information Communications Technology (ICT) players will reach \$ 1.3 trillion in 2026 [21]. When examining the most prominent domains, energy and utilities account for 19%, industrial production is there for 18%, and it is worth highlighting the automotive industry, which accounts for 8% [21]. In terms of industrial networks, naturally, the factories are the main stakeholders. The short term industrial impact of 5G and Internet of Things (IoT) [22] is expected to be around 619 billion USD. Of course, this includes other high-impact domains utilizing 5G, such as connected cities and vehicles.

The 5G standards [23] and architectures provide an opportunity to build highly flexible private industrial networks [24]. Some services can run on a small portion of network elements. Therefore, we can utilize merely a small percentage of network resources to provide elementary service needs. This allows for designing services and implementations based on individual customer needs. With the interoperability of standards and interfaces [25], systems will be able to co-operate and provide a high-quality

experience. 3GPP [3] will develop various solutions for the Non-Public Network [5], providing more options in terms of industrial network architecture. The most facile option is to install all the Core and Radio Access Network (RAN) elements required for service in the industrial area completely separated from any public mobile network (standalone isolated NPN – see Figure 1) [5]. The independence between this NPN and a public mobile network manifests in the use of a unique network identifier, the assignment of private spectrum to the NPN, and the full deployment of a 5G system (including RAN and Control Network) within the logical perimeter of the factory. There are several hybrid solutions where some Core elements are on-site adjacent to the dedicated RAN or shared RAN while others are located at the service provider (Public Network Integrated NPN – see Figure 2). The deployment of a public and private network in a Hybrid NPN solution can vary depending on the considered use-case and customer requirements.

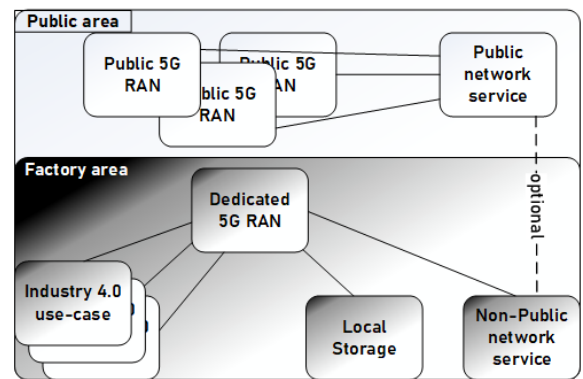


Fig. 1. Deployment as dedicated network

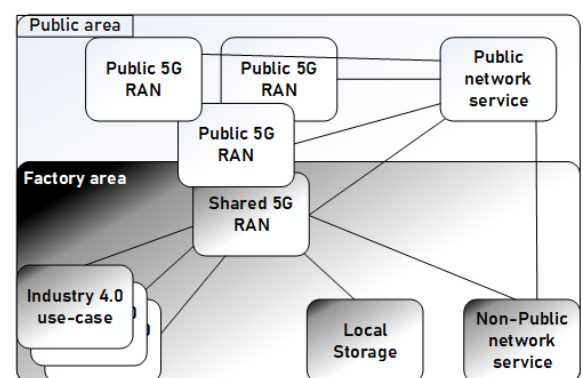


Fig. 2. Deployment with shared RAN and control plane

III. UNDERSTANDING INDUSTRIAL PLAYERS' NETWORK NEEDS

It is crucial to identify the target groups involved in telecommunications. New technology can be successful if all the target groups are motivated for the new service, product,

or technology. New investments are function-oriented: as long as there is no advanced function that the user needs – even if a new technology emerges –, they will not buy new assets, nor will vendors and operators invest in it. The idea of industrial Campus Networks and 5G itself appeared years ago, but now we have reached the point where each group has the motivation and the technical background to implement these types of networks cost-effectively. Taking advantage of these changes, there will be much more communication and feedback between participants in Industry 4.0.

In the case of industrial Campus Networks, we can identify the groups of contributors.

The first stakeholders are the Vendors – suppliers who manufacture the devices directly to the factory or for the MNOs. Examples include Ericsson, Cisco, Nokia, Huawei and so on. They need continuous technological innovations because otherwise, they would not have enough revenue from operation only. Their goal is constant innovation and constant generational change. For them, 5G becomes a “matter of existence”. In the case of vendors, the issue of greenfield or replacement investment also arises. In the case of a greenfield investment, a new industrial competitor jumps into the development of the latest technology much more efficiently because this is the only way for them. Start-ups would not be able to compete with the prominent vendors in the existing markets anyway. It is easier for a new competitor to start investing in new technology as they do not have any existing infrastructure or network from which they would expect any Return of Investment (ROI). On the other hand, existing prominent vendors find it harder to invest in new technologies too early because they do not want to cannibalize their existing solutions. However, over time, they will have to, as potential competitors’ pressure continues to grow. If they do not start investing in new technologies and succeed, they will definitely lose their market position in the future.

The second significant group is the Telecommunication Service Providers (TSP) or MNOs. With the rise of 2G, telco companies had not yet reached the customer limit; there was still a great potential user market that had not been exploited. With 3G, they were still able to grow in terms of revenue, due to the spread of the internet, and the spread of multimedia content. However, the market for 4G has not evolved and grown. Despite that, operators were forced to invest in it to avoid the reduction of their market share. However, they could not significantly increase their user base. It was just a matter of protecting existing markets and retaining revenue at 4G. For MNOs, sales may be stagnant at the moment, but the margin is melting, which results in downsizing and austerity – thus, they definitely need to find a new market. The greenfield and replacement investment phenomena mentioned at the vendors are also notable here.

Finally, in the case of industrial customers, there is a competitive situation. Industrial players can only produce cost-effectively and efficiently if they find a long term network solution that satisfies their needs.

IV. FACTORS INFLUENCING THE PRICING AND DESIGNING INDUSTRIAL CAMPUS NETWORKS

A. Network scaling

Telco equipment suppliers are interested in creating a kind of oligopoly market for the MNOs. They often use a flexible interpretation of standards and apply proprietary solutions and protocols. Operators can design and build a network infrastructure more efficiently with a single-supplier solution, where spare parts management, troubleshooting and backup logistics are also much simpler. However, at the same time, vendors can abuse their monopoly position, which can result in price inflexibility and dependence. A multi-vendor environment makes operators less dependent, forces suppliers to compete on price, but in most cases raises interoperability issues and requires a more well-trained team of professionals. As a consequence, a continually increasing product portfolio will be available to the enterprise sector, where they can use separate, private mobile network solutions. Separation may also cover the exclusive use of the radio transmission medium or – similarly to edge-computing – the Core network can be located at the industrial site [26]. The benefits can come from the availability of dedicated resources such as pre-determined bandwidth, reduced latency, higher availability, and complete isolation of sensitive information even from the Telco operator.

Of course, such complex solutions cannot be designed, deployed, and operated without MNO’s nearly 30 years of experience. The introduction of new features, implementation of software upgrades, possible troubleshooting, or capacity expansion cannot be solved without the know-how of MNOs. NPN or Campus Network solution is offered to business customers with higher service level requirements than what is possible on the public access cellular network service. As the operator cannot provide personalized service quality on public mobile data networks, there is no guaranteed bandwidth and availability. With NPN solutions, dedicated radio resources, customizable availability, and bandwidth can be provided to business customers for specific user groups at a given geographical location, according to the required services. The operator offers a solution that is separated from the regular Public network service according to the particular business needs using dedicated and redundant network elements to ensure the highest possible availability. It is only possible to access the customer’s own internal Local Area Network (LAN) or even access the customer’s private cloud-based data centers either via an Internet Virtual Private Network (VPN) or via leased line.

In response to different customer needs, several different NPN solutions can be defined, primarily in terms of the order of magnitude of the required customer terminal equipment and bandwidth. Besides, different architectures determine availability, the degree of on-site redundancy, the number of connection points between the operator and the customer, the number of hardware components that must be installed at the customer’s site, and influence the technical solution and so on.

B. Pricing parameters for 5G NPNs

The pricing strategy of a given solution can be influenced by the parameters of the included devices, services, and different operator tasks. Such factors are as follows:

- Traffic-based pricing – based on the amount of data included;
- Creation of a closed and secure system (VPN) and only the subscriptions fixed in the contract can access the service;
- Different IP address assignment methods;
- Various authentication solutions;
- Central green number for handling error reports;
- Service charges at endpoints (SIM cards).

The service shall include the continuous operation, provision, installation, maintenance, and, if necessary, repair of the equipment and related components. After a certain period of time, it is possible to pay the monthly fee by the customer. Pricing is based on the total investment cost (Asset Cost and Construction Cost) plus annual upgrade fee, maintenance fee, data center costs, business and overhead costs, and margin.

Table I summarizes – from the perspective of MNOs – what the main Capital expenditure (CAPEX) items are during the investment. The Table presents the RAN, Cellular Core, and IP transport parts following Figure 1 and 2. In the case of RAN, the most important aspect is the size of the physical area. The fact that the covered area is a hall or an entire part of the city or an outdoor multi-km motorway test track section can influence several technical parameters. The first and maybe the most critical parameter is the used frequency, which can be considered the MNO capability and must be paid for on behalf of the national regulatory organization. The density and the number of transmitter towers and antennas will be greatly influenced by the required user number, data rate per user, and overall data consumption.

The Cellular Core part is influenced by the number of connected eNBs and gNBs, but an equally important factor is the number of connected users at the same time. In the case of machines, it can be assumed that most of them will be connected continuously, while humans will have peak and unused periods due to their biorhythm. Thus, in the case of machines, the focus should be on traffic service to be served in a continuous and uniform quality instead of occasional peak loads. In addition, as we showed in Section II, the architecture can specify which Core elements should be placed redundantly to the macro network.

The IP transport part seems easy at first, as “only” data transmission is required here; however, physical size and architectural solutions can have serious Capex consequences. It is challenging from the transmission technology’s point of view when the architecture consists of long-distance installed radio transceivers (eNBs/gNBs), and different core network functions in different locations.

TABLE I
KEY PARAMETERS FOR DIMENSIONING CAPEX OF INDUSTRIAL CELLULAR TECHNOLOGIES

Radio Access Network	Cellular Core	IP - Transport
Physical size of network, Freq. band, max. data throughput/(user area), max. subscriber number/(square meter or area)	# of eNB or gNB, # of customer, total data throughput, architecture	# of customer, architecture, total data throughput

C. The key players in the frequency trading of NPNs

In the case of mobile network services, it is essential to decide who provides the service medium, at what price, and what commitments are needed from the user. In terms of frequency management, 3GPP [27] defines three stakeholders that have played a crucial role in the market since the advent of mobile networks: the state, service providers, and customers. The state is the owner, and also the regulator of the reusable frequency bands. MNOs purchase (trade) frequencies from the state over the long term and create suitable services for the customers based on standards. While the customers/users use the service for typically as a form of voice calls or data services developed by the MNOs.

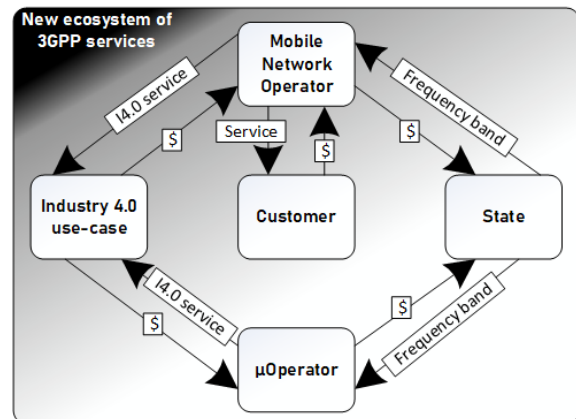


Fig. 3. New ecosystem on MNO market

We suppose there will be five players in the new Industry 4.0-MNO ecosystem. The relationships between them are shown in Figure 3. Traditionally the MNO pays money to the state in exchange for the frequency. On the other hand, they are contractually obliged to launch certain territorial coverage, population coverage or integrate several new base stations using the dedicated frequency bands. In the service providers’ prices, the cost of the frequency will play a role as a distributed expenditure cost. In return, the MNO receives dedicated frequency bands from the state for a fixed period, where the usable frequency band is guaranteed, and the transmitter’s power is typically regulated. Still, there is only a recommendation for the 3GPP standard to be used, MNO decides which technology to use on the frequencies. However, in recent years, companies requiring private/industrial mobile networks have emerged as third party frequency owners, also called micro Operators (μO).

μ O receive a long-term dedicated frequency band from the state, but for a limited area. This way, new types of customers who take advantage of their use-cases will be able to connect directly to the μ Os, eliminating the MNOs from the process. As this is an unknown area for all key players, the regulatory state has not defined any other frequency usage criteria. μ Os are experienced typically in generating new ideas and Industry 4.0 use-cases for MNOs. This new type of operation/connection is also unique for the μ Os and for the Industry 4.0 use-case customers. They have neither 3GPP-based network development nor operational experience. The operation of a 3GPP based cellular network can be a challenging task. Therefore MNOs cannot be eliminated entirely from the Industry 4.0 ecosystem. Even if the μ O can provide dedicated frequency and some off-the-shelf NPN solution to the customer, MNOs still have the advantage that they can offer much more flexible NPN solutions customized to the customer unique needs. μ Os opportunities will be limited by the manufacturer of their off-the-shelf NPN solution. Furthermore, in some countries, μ Os cannot buy frequency directly nor from the MNO as national authorities can limit frequency purchase and usage conditions. For instance, in Hungary, these kinds of μ O activities are not possible with the current regulation environment; only the big MNOs can buy frequencies. To increase complexity, the network-slicing feature that emerges with the development and integration of 5G standards will allow the MNOs to sell a time or frequency slice to a μ O in the network, or vice versa, to offer a slice used by a μ O to the MNOs. This will allow further transactions between each other and can threaten the existing relations among the MNO market.

V. BUSINESS DEVELOPEMENT FOR 5G

A. Defining the potential customers and network types

In Table II, different types of networks are presented, differentiated by architectural and Service Level Agreement (SLA) features. The four different types of network solutions are not created arbitrarily; they are determined based on the customer needs, our system integrator observations, and TSP experience. However, to understand each type of network and service feature, we still need to specify a few concepts, as the significant part of our target audience has more of the business approach. In explaining these concepts, we try to provide simple comprehensibility and an interpretation that is relevant in the present situation, rather than an entirely correct and standardized technological explanation.

Firstly SLA agreement is required, which is a commitment between a service provider and a client. Particular aspects of the service – Quality of Service (QoS), availability, responsibilities – are agreed between the TSP and the service user. The QoS is the description or measurement of the overall performance of a service or network. Perhaps one of the most crucial QoS features is that certain types of network traffic can be prioritized over other network traffic types. On public networks, voice traffic is treated that way. This feature will be vital in industrial cases, where industrial

partners want to prioritize the network traffic of certain types of machines over the others. Still, there are several additional QoS parameters, such as delay, coverage, bandwidth, etc. Another critical concept is network availability, which defines the amount of time period – in percentage – when the network is fully operational. It is a crucial parameter for industrial scenarios. By network control, we mean resource management and customization, network separation from the public network, network security management, and dependency on the public network, and the TSP.

The four network types can be interpreted quickly based on the previously overviewed concepts. In the Type I network, the network still completely depends on the TSP and the public network. There are very limited customization options, but a private Access Point Name (APN) can be provided to the customer. A private APN can be used to create a logically independent network for the client's devices and users. In this case, unique authentication mechanisms and arbitrary firewall rules can be applied. A typical scenario is the private network of banks, where only authenticated users can connect to the network, such as bank employees, ATMs, store terminals.

Network Type II provides a dedicated radio resource in the form of radio repeaters in addition to the logical network separation. This can be useful in cases where the particular customer does not need a special QoS or high data rate, but the radio conditions are not satisfying in the given geographical area.

Network Type III provides some dedicated RAN and Core services, which means the network still depends on the public network, but it offers a high level of control and QoS customization. It can be suitable for private office networks. The main advantage here is the RAN and Core separation from the public network, thus the network parameters can be fully customizable, and a different SLA can be designed.

Finally, network Type IV is entirely independent of the public network. It is able to operate without any problems in case of failure or degradation of certain public network services. It offers full QoS customization and complete control of the network services. For industrial applications and factory sites, such networks will be deployed where very low latency, high bandwidth, dedicated resources will be crucial. A minor disadvantage is that there is no standard agreed-upon 5G stand-alone NPN according to 3GPP yet, and even the solutions of large mobile network vendors are not uniform.

The presented four options are similar to the NPN deployment scenarios of [5], primarily Type II and IV, but it is not equivalent to these cases. [5] examines the topic from the MNO point of view where the NPN RAN can be shared with the public network RAN or the whole network completely isolated. However, there are use-cases where complete network isolation is not possible or would be too expensive, but in contrast, simple RAN sharing would not provide the QoS requirements of the customer. Therefore, as we suggest, there are several use-cases where extended RAN solution would be the optimal choice, which means additional radio equipment e.g., Radio Dot, or Distributed Antenna System besides the public network's RAN. Our

TABLE II
CAMPUS NETWORK MAIN TYPES OF SOLUTIONS

Network architecture	Potential customer use cases	Main features	Limitations
Type I	Requiring advanced user management and logically separated network with possible closed network connection	Private APN No QoS customization Very limited control	Completely dependent on public network SLA can be similar to the public network's SLA
Type II	Sites with poor radio coverage, or special use-cases requiring more bandwidth, redundancy or less latency	Extended RAN Partial QoS customization Limited control	Some resources as on public network except the advanced radio coverage but it can not be considered as dedicated resources
Type III	Advanced user management and advanced radio coverage	Dedicated RAN + Shared Core services High QoS customization High level of control	Still depends on public network Extra resources and features can be used on the dedicated radio interface
Type IV	Industrial use-cases with strict SLA requirements low-latency, high availability	Stand-alone network, Dedicated RAN + Core services Full QoS customization Full control	Standardization is still in progress

network differentiation does not specify all options. Individual cases may vary according to individual customer needs, as they can be expanded with certain services or even simplified. An additional aspect of network design can be the degree of redundancy, which is typically determined by the particular SLA. Similar features are network monitoring and support by the TSP, which also affects the network design and implementation. Currently, there are no real guarantees for the network services in contractual form for public networks. In the case of corporate networks, there are more strict guarantees and penalties, but mostly it only covers data consumption. In the future, this will change drastically for Campus Networks, where additional parameters, such as latency, throughput, jitter, and other key features will be included in SLAs.

B. Infrastructural investment

The range of potential customers can be divided into three groups from an infrastructure point of view, which significantly determines the possible development guidelines.

In the case of a greenfield investment, the industrial customer has not yet implemented the production processes. They have the opportunity to adapt them to meet the expectations of the desired industrial network. Unfortunately, in some cases, the industrial customer is unwilling to adapt its production workflows to the needs of the industrial network or is more expensive to redesign the workflows rather than the telecommunication network. In most cases, the TSP has to design the network according to their concepts and workflow. If there is no other way, and the TSP can not implement the appropriate telecommunication network for the workflow, then the industrial customer is willing to adapt. Still, the role of adaptation is usually the task of the TSP.

Another essential feature of greenfield investments is that all assets are bought at the same time. At that time – at the beginning of the investment – the industrial players react differently to the expenses of the telecommunication network. It is much easier for companies to spend more

Capex than later when services are already in operation, and the infrastructure is ready. The telecommunication network is a relatively small expenditure, in contrast to other elements of industrial investment. When the installation is already done and the network is not fulfilling the requirements, the rebuild of the network or the replacement of certain elements could lead to a substantial expenditure compared to the initial situation. It can significantly affect the ROI, one of the most fundamental performance measures (also Key Performance Indicator) of an investment.

When there is some existing network solutions already built, most of the time, the industrial player does not want to replace their network infrastructure, as the costs of construction are high and have not yet returned. Therefore, the customer is more inclined to complementary solutions than to replace the entire network. This is a significant difference between TSPs and green-field investments. Thus, it is necessary to adapt to the needs of the existing network architecture and equipment. In general, these additional installments represent a significantly more substantial investment than if the same telecommunications network were to be implemented as a green-field investment. The TSP can not offer and install the optimal, cheapest, and most efficient implementation due to the existing network dependencies. Furthermore, it is not possible to finish these network installations quickly, as in many cases, production processes can not be interrupted at any time. There will be predefined time windows for these kinds of tasks.

Finally, there are cases where the industrial player has an existing network solution, but it is obsolete and needs to be replaced. So it can now be considered as an almost green-field investment in terms of the telecommunications network. But it differs from a green-field investment as it can be considered what might be worth keeping and using from the previous network infrastructure.

C. Business and technological risks

When planning a new investment, in addition to revenue, it is worth paying attention to the risks that threaten income.

These can be natural disasters or unforeseen events such as war, rebellion, or the fall of governments or pandemics. These events are usually associated with a risk when a network or service failure is not caused by the TSP nor by the equipment. In such cases, the TSP can not influence the events, and they are also a passive endurer. It is necessary to consider the dependencies of a new service and network, and those activities that can make the industrial network vulnerable.

1) *Service failure or degradation*: As none of the networks operate without errors and service degradation, it is worth considering the various external and internal risks when determining the price of the service during business negotiation and planning. The given service must be examined from the following aspects:

- What is the size of the system and what type of services it provides. Further, the expected damage in case of failure must be examined;
- What type of alternative solutions can be provided in case of failures? Is it enough to offer some modest-quality solution, a fully redundant option, or nothing at all?

From these two concepts above, it is possible to calculate the amount of damage in the event of a certain period of network failure.

2) *The importance of redundancy and backup solutions*: The cost of built-in backup systems is always extremely high, and hopefully, it will never be in use. Also, the clear return of its investment is quite unlikely. On the other hand, installing a backup system is still recommended in the case of critical services. If human life depends directly on the system, it is absolutely obligatory to design a backup system, to minimize the possible damage. However, this raises several additional questions, which are sometimes philosophical:

- What happens if the machine loses communication with the server? Does it have a default program/state to return to? Or does it execute the last instruction?
- How does the machine/executable program notice the incorrect instruction? Simple counter, logic, or security algorithms can be used, but how do we detect an instruction that the controller issues incorrectly? There may be an instruction that the controller knows about and will be harmful to either a human or to another unit.
- If a robot does not receive instructions for a given time, how to react? Does the executing robot need a self-defense function, i.e., do you notice that it executes the same command indefinitely and has gone into an infinite loop? Does the robot need a self-stop or self-defense function then?
- Should a machine have an emergency mode where self-defense limits can be overridden? Will the executing device know whether the execution of the operation will significantly reduce its own life cycle, or even in reaching its operating limit, should the machine execute this instruction?

These questions are quite crucial as in the first phase of Industry 4.0 mixed environment will be typical. It means that

machines and the human workforce will be operating in the same industrial area, where machines can not threaten human life in any circumstances. Another simple example is automated driving, which includes road accident liability as one of the most fundamental aspects of technological integration.

ACKNOWLEDGEMENTS

This work has been performed in the framework of the H2020 project 5G-SMART co-funded by the EU. The authors would like to acknowledge the contributions of their colleagues. The consortium is not liable for any use that may be made of any of the information contained therein.

VI. CONCLUSION

In this paper, after a brief historical overview, we summarized existing studies on the business effects of 5G. In addition to the short technology analysis, our focus has shifted mainly to changes in Industry 4.0 business opportunities. We identified the major players involved in Industry 4.0 and presented their function and possible future role in Section III. An important finding is that, with the arrival of 5G, μ Operator and industrial manufacturers will also have a crucial role in the mobile network ecosystem. On the other hand, MNO will enter the industry as an operator expanding their market. We highlighted the advantages and drawbacks of a green-field investment in terms of business development and presented what factors and parameters need to be considered during the pricing of Campus Networks, including the key players of trading frequencies for NPN. Four different types of network solutions are distinguished, focusing on the key features, potential customer use-cases, and limitations of these networks. The main contribution of Section IV is not an architectural definition of the different NPN deployments, rather, we are highlighting these network options, limitations and motivations; moreover, the paper presents some typical use-cases for every scenario. Finally, we analyzed the business and technological risks of industrial 5G networks, presented research questions and concepts, and mentioned some ethical issues.

This paper analyzed the state of 5G NPN, primarily the business opportunities and key players was presented, while from the technical side only high-level evaluation was performed. In the future, we prefer to make further examinations in both domains. From a business point of view, MNOs and μ Os benefits would be examined, including the business motivations of cloud solutions, frequency allocation issues, network slicing potentials and energy-efficient networks. Furthermore, it would be interesting to describe how these new features change the network architecture of MNOs, highlighting the main effects on the Core and Radio elements from the business- and also the technical-side.

REFERENCES

- [1] A.G. Özüdođru, E. Ergün, D. Ammari, Students, and A. Görener, "How industry 4.0 changes business: A commercial perspective," vol. 4, pp. 84–95, July 2018.

Business opportunities and evaluation of non-public 5G cellular networks – a survey

[2] S. O’Dea, Statista. (2020) Smartphone ownership rate by country 2018 . [Online]. Available: <https://www.statista.com/statistics/748053/worldwide-top-countries-smartphone-users/>

[3] 3GPP TS 23.501. (2020-09) System architecture for the 5G System (5GS).

[4] Commscope. The smart campus. [Online]. Available: <https://www.commscope.com/solutions/enterprise-networks/smart-campus/>

[5] 5G-ACIA. (2019) 5G Non-Public Networks for Industrial Scenarios. (accessed: 17.08.2020). [Online]. Available: <https://www.5g-acia.org/publications/5g-non-public-networks-for-industrial-scenarios-white-paper/>

[6] 3GPP TS 21.101. (2008-12) Technical Specifications and Technical Reports for a UTRAN-based 3GPP system.

[7] D. Kozma, P. Varga, and C. Hegedűs, “Supply chain management and logistics 4.0 - a study on arrowhead framework integration,” Mar. 2019, pp. 12–16.

[8] D. Kozma, G. Soos, D. Ficzer, and P. Varga, “Communication challenges and solutions between heterogeneous industrial iot systems,” 10 2019.

[9] A. Kalør, R. Guillaume, J. Nielsen, A. Mueller, and P. Popovski, “Network slicing for ultra-reliable low latency communication in industry 4.0 scenarios,” Aug. 2017.

[10] G. Soos, F. Janky, and P. Varga, “Distinguishing 5g iot use-cases through analyzing signaling traffic characteristics,” 07 2019.

[11] NOKIA. (2020) Dynamic end-to-end network slicing for 5G, Addressing 5G requirements for diverse services, use cases, and business models. (accessed: 28.09.2020). [Online]. Available: <https://gsacom.com/paper/dynamic-end-end-network-slicing-5g/>

[12] P. Varga, J. Peto, A. Frankó, D. Balla, D. Haja, F. Janky, G. Soos, D. Ficzer, M. Maliosz, and L. Toka, “5G support for Industrial IoT Applications – Challenges, Solutions, and Research gaps,” *Sensors*, vol. 20, p. 828, Feb. 2020.

[13] S. Rácz, G. Szabó, and J. Pető, “Performance evaluation of closed-loop industrial applications over imperfect networks,” *Infocommunications Journal*, vol. XI, pp. 32–38, Aug. 2019.

[14] J. Varga, A. Hilt, J. Bíró, C. Rotter, and G. Jaro, “Reducing operational costs of ultra-reliable low latency services in 5g,” *Infocommunications Journal*, vol. X, pp. 37–45, Dec. 2018.

[15] D. Kozma and P. Varga, “Traffic analysis methods for the evolved packet core,” May 2016.

[16] Lindsay James, Technology Record. (2019) How Industry 4.0 is accelerating business. (accessed: 17.08.2020). [Online]. Available: <https://www.technologyrecord.com/Article/how-industry-40-is-accelerating-business-88964>

[17] Ericsson, “Internet of Things forecast,” Ericsson, Tech. Rep., 2020.

[18] ——. Future Mobile Data Usage and Traffic Growth. (accessed: 10.08.2019). [Online]. Available: <https://www.ericsson.com/en/mobility-report/future-mobile-data-usage-and-traffic-growth>

[19] M. Wollschlaeger, T. Sauter, and J. Jasperneite, “The future of industrial communication: Automation networks in the era of the internet of things and industry 4.0,” *IEEE Industrial Electronics Magazine*, vol. 11, no. 1, pp. 17–27, 2017.

[20] NOKIA. (2020) Nokia White Paper: Deploying 5G Networks, A framework for successful 5G network deployments and moving from 5G NR NSA to SA. (accessed: 28.09.2020). [Online]. Available: http://content.rcrwireless.com/nokia_deploying_5G_wp/

[21] Silvana Apicella. (2018) 5G Business Potential from Industry Digitalization. (accessed: 17.08.2020). [Online]. Available: <https://www.itu.int/en/ITU-D/Regional-Presence/Europe/Documents/Events/2018/5GHungary/S4%20Sylvana%20Apicella%205G%20Business%20Potential%20from%20Industry%20Digitalization%20Rev.A%20External.pdf>

[22] Silvana Apicella –Southern Europe Network Evolution Lead, Ericsson. (2018) Business Potential from Industry Digitalization. (accessed: 07.05.2020). [Online]. Available: <https://www.itu.int/en/ITU-D/Regional-Presence/Europe/Documents/Events/2018/5GHungary/S4%20Sylvana%20Apicella%205G%20Business%20Potential%20from%20Industry%20Digitalization%20Rev.A%20External.pdf>

[23] P. Rost, C. Mannweiler, D. S. Michalopoulos, C. Sartori, V. Sciancalepore, N. Sastry, O. Holland, S. Tayade, B. Han, D. Bega, D. Aziz, and H. Bakker, “Network Slicing to Enable Scalability and Flexibility in 5G Mobile Networks,” *IEEE Communications Magazine*, vol. 55, no. 5, pp. 72–79, May 2017.

[24] C. Simon, M. Máté, M. Maliosz, and N. Bella, “Ethernet with time sensitive networking tools for industrial networks,” *Infocommunications Journal*, vol. IX, pp. 6–14, Jun. 2017.

[25] P. Varga, D. Kozma, and C. Hegedűs, “Data-Driven Workflow Execution in Service Oriented IoT Architectures,” Sept. 2018.

[26] M. Szabó, D. Haja, and M. Szalay, “Cost-efficient resource allocation method for heterogeneous cloud environments,” *Infocommunications Journal*, vol. 10, pp. 15–21, Mar. 2018.

[27] 3GPP. (2020) The Mobile Broadband Standard. (accessed: 17.08.2020). [Online]. Available: <https://www.3gpp.org/>



Gábor Soós received the M.Sc. degrees in Electrical Engineering from Budapest University of Technology and Economics, in 2008. He joined T-Systems Corp. in 2007 and has been involved in radio network modelling as well as implementation for reliable advanced radio communication technologies. Currently, as a PhD student, he is also responsible for Magyar Telekom Cellular Core network development, and investigation of advanced process technology. Current interests are technology development of advanced mobile networks and testing for high reliable private Cellular core systems.



Dániel Ficzer is a MSc student at Budapest University of Technology and Economics. He works as a cellular packet Core engineer at Magyar Telekom. He is involved in several academic and industrial projects at BME SmartCom Lab. Despite his young age, he has already contributed to several conference and journal papers. His research interest covers private mobile networks, advanced cellular Core solutions and 5G industrial integration.



Tamás Seres received his BSc in Telecommunication and Electrical Engineering from the Faculty of Electrical Engineering at Kálmán Kandó Technical College in 1995, then his MBA in Marketing in the program by the Faculty of Business and Economics at the University of Pécs and by the Business School of Middlesex University in 2007. He is a consultant with a history of working in telecommunication. He is highly skilled in 5G and Campus Technology, IoT, Industry 4.0, Business Development, and Business Planning. Currently – among others – he is working for H1 Systems as a business developer and strategist focusing on Edge Cloud.



Sándor Veress was graduated as an electric engineer at the Digital Control Engineering faculty in 1993. He gained 20 years of professional experience in the telco/IT sector. Later he was responsible for the elaboration of the company’s electronic bill solution and the integration of partners into the tool. Under his leadership Magyar Telekom implemented its online collaboration system on its own SaaS platform. Subsequently he was responsible for T-Systems’ innovation projects, as an Innovation and business development expert.



István Németh is an experienced mobile packet core network integrator at Magyar Telekom Plc. He is highly skilled in implementing, integrating, testing, and troubleshooting mobile core network elements. His main research interests cover the area of packet core virtualization and private mobile network packet core development for LTE and 5G.

Modeling the near-field of extremely large aperture arrays in massive MIMO systems

Botond Tamás Csathó, Bálint Péter Horváth and Péter Horváth

Abstract—Massive multiple-input multiple-output (MIMO) is a key technology in modern cellular wireless communication systems to attain a very high system throughput in a dynamic multi-user environment. Massive MIMO relies on deploying base stations equipped with a large number of antenna elements. One possible way to deploy base stations equipped with hundreds or thousands of antennas is creating extremely large aperture arrays. In this paper, we investigate channel modeling aspects of massive MIMO systems with large aperture arrays, in which many users are located in the near-field of the aperture. One- and two-dimensional antenna geometries, different propagation models, and antenna element patterns are compared in terms of inter-user correlation, condition number of the multi-user channel matrix, and spectral efficiency to identify key design parameters and essential modeling assumptions. As our analysis reveals by choosing spectral-efficiency as a design objective, the size of the aperture is the critical design parameter.

Index Terms—massive MIMO, extremely large aperture arrays, near-field, channel modeling

I. INTRODUCTION

Massive multiple-input multiple-output (MIMO) is a state of the art physical layer technology, which is of key importance in modern wireless communication, moreover, an ingredient of 5G. In a massive MIMO system, the base station serves the mobile stations (MS) in the same time-frequency resource, while users are separated in the spatial domain. The core concept of massive MIMO is to have at least an order of magnitude higher number of antennas at the base station than the number of simultaneously transmitting mobile station antennas [1]. A mobile station can have an arbitrary number of antennas, although the number of antennas is limited due to the physical constraints of a handheld device. The large number of antennas at the BS will result in a significant number of different channels between an MS and the BS, which brings the benefits of the technology. It has been shown in [2], that by utilizing more antennas, the spectral efficiency (SE) will always increase. Therefore, the development of base stations with hundreds or thousands of antennas is expected. Interestingly, the increasing SE holds even with measured channel state information (CSI), linear precoding, and decoding [1].

The work of Björnson [3] considers extremely large aperture arrays (ELAA) [4] as a promising concept of massive MIMO. ELAA is one way of increasing the number of antennas, thus increasing the spectral efficiency. An essential property of the large aperture that its radiating near-field can stretch multiple kilometers. Therefore, some users are located in a region where the radiated electromagnetic (EM) waves cannot be

approximated by plane-waves as in the far-field. Consequently, classical lobe-based channel models do not hold. Investigation of practical channel models, as well as the acquisition of the channel features in a particular deployment scenario are of current research interest [3].

There are existing works about the properties of large apertures, for example [5], [6] and [7]. Nevertheless, the authors in these papers focus on one-dimensional antenna arrays, with antenna element spacing less than two wavelengths. Although these assumptions are common in the literature, if an ELAA system will be built, it is likely to be two-dimensional. Furthermore, if considering frequencies higher than 1 GHz, the spacing between the antenna elements can easily be orders of magnitude larger than the wavelength. As a demonstrative example, one can consider an office block, where antenna elements are affixed to the windows of the building, resulting in inter-element spacing in the order of a few meters. In [5] and [6], line of sight (LoS) propagation is assumed. On the contrary, in a realistic scenario, there is at least one significant reflection from the ground, as it is assumed in [7].

Our work will focus on the effect of modeling accuracy in the near-field of an ELAA. One- and two-dimensional arrays will be compared, and the effect of ground reflection will also be taken into account. Inter-element spacing is considered to be an order of magnitude larger than the wavelength. Consequently, mutual coupling between antenna elements can be neglected. Furthermore, different models of each antenna element and different array geometries will be compared. The metrics of the analysis are the inter-user correlation (IUC), condition number (CN) of the multi-user channel matrix, and spectral efficiency. The first goal is to analyze the effect of modeling accuracy of a realistic ELAA scenario. Furthermore, we aim to identify fundamental parameters that significantly influence the performance of such a system.

Let us summarize the mathematical notations. Vectors, matrices, their transpose, conjugate, conjugate transpose and inverse are denoted as \mathbf{a} , \mathbf{A} , \cdot^T , \cdot^* , \cdot^H and \cdot^{-1} respectively. Absolute value and the second norm are denoted by $|\cdot|$ and $\|\cdot\|$. \mathbf{I}_b represents the $b \times b$ identity matrix. $[\mathbf{A}]_{k,j}$ denotes the entry of the k^{th} row, and the j^{th} column of matrix \mathbf{A} .

The rest of the paper is organized as follows. In Section II, the difference between near- and far-field will be described in details. Afterward, further properties of ELAA are summarized in Section III. Then, the used model is introduced in Section IV. Subsequently, the results are presented in Section V. Finally, the conclusion is given in Section VI.

The authors are with the Budapest University of Technology and Economics Department of Broadband Infocommunications and Electromagnetic Theory. Email: bcsatho@evt.bme.hu, horvath.balint@hvt.bme.hu, hp@hvt.bme.hu

DOI: 10.36244/ICJ.2020.3.6

Modeling the near-field of extremely large aperture arrays in massive MIMO systems

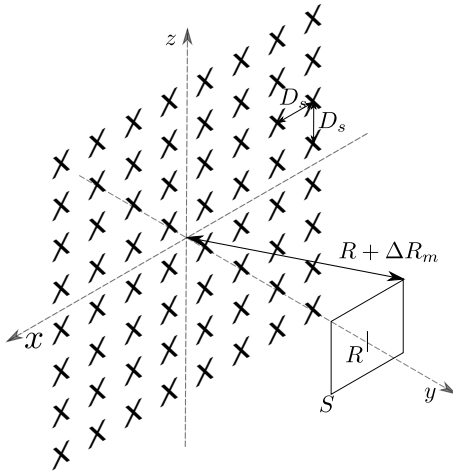


Figure 1. Scenario of 8 antenna element in the $x - z$ plane, $D_s = 1$ m. The EM field is evaluated on the S plane for different R .

II. COMPARISON OF THE NEAR- AND FAR-FIELD

Since our investigation principally assumes a radiating near-field scenario, first let us point out the difference between radiating near-field and far-field. A well-defined boundary does not exist between the two regions, whereas there are distinct differences among them. For the sake of completeness, three different field regions can be identified surrounding an antenna: reactive near-field, radiating near-field (Fresnel region, also referred to as near-field), and far-field (Fraunhofer region) [8]. In the following parts, these regions will be discussed in detail.

For the sake of simplicity, the widely used criteria for each region are summarized first:

- reactive near-field: $0 \leq R < 0.62\sqrt{D^3/\lambda}$,
- radiating near-field (Fresnel region or simply near-field in the following): $0.62\sqrt{D^3/\lambda} \leq R < R_F = 2D^2/\lambda$,
- far-field (Fraunhofer region): $R_F \leq R < \infty$,

where R is the distance from the surface of the antenna, D is the largest dimension of the aperture and λ is the wavelength.

The closest one to the antenna is the reactive near-field, which is defined as "that portion of the near-field region immediately surrounding the antenna wherein the reactive field predominates" [8].

If D is large compared to the wavelength, the Fresnel zone exists; otherwise, it does not. According to a definition in this region, "radiating field predominates, and the angular field distribution is dependent upon the distance from the antenna" [8]. Therefore, in the radiating near-field, spherical waves are utilized to describe the radiated electromagnetic field. In practical terms, even a small change in position might result in a significant change in the electromagnetic field.

In the far-field, "the field mainly has transverse component, and the angular field distribution is independent of the distance (R) from the antenna" [8]. In the Fraunhofer region plane-waves are utilized as a local approximation of the propagating field. Consequently, the EM field must not vary significantly on a surface element of a plane perpendicular to R in the far-field. A rule of thumb for the size of this surface element is

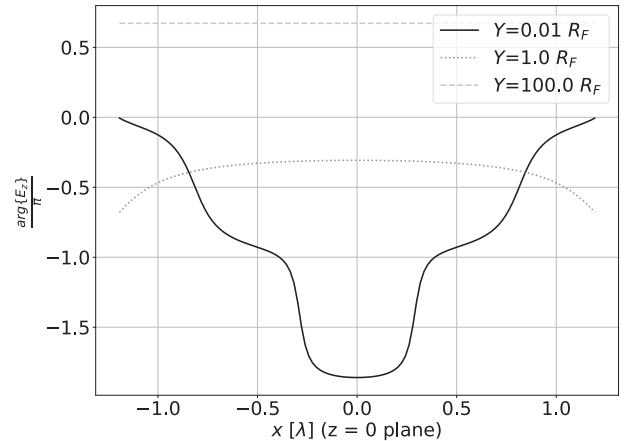


Figure 2. Illustrating the change in $\arg\{E_z\}$. In the near-field ($Y = 0.01R_F$), there is an abrupt change in the phase and $\arg\{E_z\} \in [-\pi, \pi]$. In the transition zone ($Y = R_F$), there is rather continuous change in the phase and $\arg\{E_z\} \in [-0.918\pi, -0.307\pi]$. In the far-field ($Y = 100R_F$), the change in phase can be neglected compared to the change in the transition zone.

$\Delta R_m \ll \lambda$. Where ΔR_m is the largest difference from R in the distance from the antenna along with the surface element.

As an illustration, consider a scenario depicted in Figure 1. In this scenario, there are 8×8 antenna elements deployed on the $x - z$ plane in the nodes of an equidistant mesh, the spacing between the antenna elements is denoted by D_s , which is chosen to be 1 m. The size of the near-field is denoted in Table I. Half-wavelength dipoles (also referred to as dipoles) model each antenna element, for which electromagnetic field is known in closed form [8]. Free-space parameters have been used for the numerical evaluation, the phasor of the excitation of each dipole is $I_0 = 1$ A, with the frequency $f = 2$ GHz. For visualizing the difference between near-field and far-field, the complex amplitude of the z component of the electric field (E_z) is evaluated for a finite surface (S). At the distance $R = R_F$ the largest difference from R in the distance along S is $\Delta R_m = 0.001\lambda$. Since $|E_z|$ evaluated on S does not vary significantly as R increases, it is beneficial to focus on the phase of E_z denoted as $\arg\{E_z\}$. Figure 2 depicts the phase for different Y coordinates of the S plane for a cross-section. Under near-field conditions ($Y \ll R_F$), there is an abrupt change in $\arg\{E_z\}$, which indicates that the S plane is in the Fresnel region. In the transition region ($Y = R_F$), there is a small and smooth change in the phase. Lastly, in the far-field, it is of key importance that in the far-field the phase almost constant, which falls in line with our expectation.

As has been shown, there are differences between the radiating near-field and far-field of an aperture. If we are considering large antenna apertures, R_F can easily be in the order of kilometers. Therefore users are located in the radiating near-field, which is a novel scenario compared to conventional MIMO systems.

III. EXTREMELY LARGE APERTURE ARRAYS

A conventional method to increase the number of antennas is to develop compact arrays that, for example, can be installed

Table I
NUMERICAL EXAMPLES OF THE SIZE OF THE FRESNEL ZONE.

λ	$N_{row} \times N_{col}$	D_s	R_F
0.15 m	8×8	1 m	1307 m
0.05 m	20×20	3 m	259.92 km
0.1 m	20×20	0.1 m	144.4 m
0.1 m	20×20	1 m	14.44 km
0.1 m	20×20	3 m	129.96 km

on a rooftop. Such a massive MIMO array has become available on the market in recent years [9]. As going more massive, weight, and the wind load of the array are going to act as limiting factors. Extremely large aperture arrays are promising candidates to overcome these limitations. In such a scenario, the antenna elements are spread over a large area, fixed to existing physical structures, such as windows of a building. Thus, the aperture size of the antenna array is increased significantly.

Furthermore, ELAAs are beneficial from other aspects as well. If an antenna array has more than one main lobes, spatial aliasing appears. These main lobes, which appear because of spatial undersampling, are called grating lobes. Spatial undersampling happens if the antennas are more than a half wavelength apart. Despite introducing grating lobes, increasing the distance between the antenna elements further than half wavelength will result in better performance, as this has been shown by simulations [6], [5] and validated by measurements [10]. There are two main underlying effects behind the growing performance: finer spatial resolution and larger aperture near-field.

Spatial resolution is the measure of user separation capabilities. It depicts how closely placed users can be distinguished based on their channels. Interestingly, the spatial resolution depends on the size of the aperture, not the number of antennas [11]. As a demonstrative example, let us consider an equidistant antenna row. If the number of antennas gets doubled while the length of the array stays the same, the resulting spatial resolution would be identical. Spatial resolution is proportional to the width of the main lobe. Although the width of the main lobe is measured based on the far-field radiation pattern, it is also relevant in the near-field. Since as the size of the aperture increases, the width of the main lobe decreases, and users placed closer to each other can be differentiated.

The other main effect is that the radiating near-field of the aperture expands rapidly along with the size of the aperture. As can be concluded from a numerical example presented in Table I, in an ELAA scenario, the majority of the users fall into the radiating near-field. In the Fresnel region, there can be abrupt changes in both the amplitude and phase of the electromagnetic field. Constructive interferences in distinct points in space characterize the structure of the EM field. Near-field effects will make user separation easier, this will result in better conditioned wireless channels, as it will be pointed in Section V-B. For example, users can be separated based on

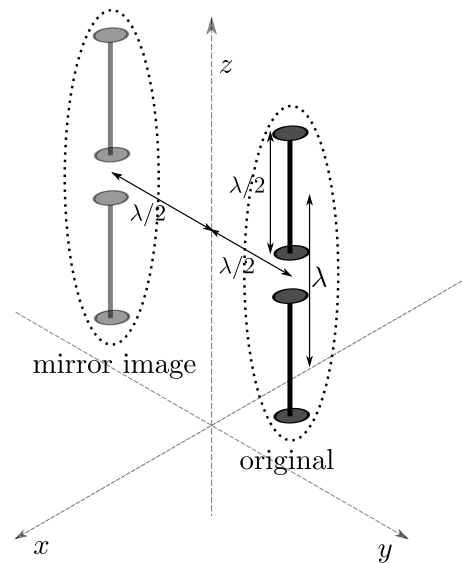


Figure 3. Constructing a simple directional antenna element from half-wavelength dipoles.

their channels, even if they are behind each other.

IV. MODEL DESCRIPTION

In this paper, we are focusing on a single cell of a cellular network. The cell consists of an M -antenna base station and K single-antenna mobile stations. In such a scenario, there is a radio channel between each BS and MS antenna. Flat fading channels are assumed, i.e., the channel gains are described by a single complex number [12]. Consequently, $\mathbf{h}_k \in \mathbb{C}^M, k = 0, 1, \dots, K - 1$ describes the channel of one terminal. By utilizing the channel vectors, the multi-user channel matrix can be built as

$$\mathbf{H} = [\mathbf{h}_0, \mathbf{h}_1, \dots, \mathbf{h}_{K-1}] \in \mathbb{C}^{M \times K}. \quad (1)$$

Based on the models introduced in Section IV-A, IV-B and IV-C, the multi-user channel matrix corresponding to a particular scenario can be calculated. A well-accepted convention that the dimension of \mathbf{H} is the number of receive antennas times the number of transmit antennas. Thus the above constructed \mathbf{H} can also be referred to as the uplink (UL) channel matrix, whereas \mathbf{H}^T is the downlink (DL) channel matrix. \mathbf{H} is of crucial importance in the following parts. The multi-user channel matrix will be simulated in realistic scenarios and with different approximations.

A. Propagation models

Three different propagation models will be compared. The first is a spherical-wave model, as in [5] and [7]

$$h_{m,k} = \frac{1}{r_{m,k}} e^{-j\beta r_{m,k}} \in \mathbb{C}, \quad (2)$$

where $r_{m,k}$ is the distance between the m^{th} MS and k^{th} BS antenna and $\beta = \frac{2\pi}{\lambda}$ is the wave number. The channel vector is constructed as

$$\mathbf{h}_k = [h_{0,k}, h_{1,k}, h_{2,k}, \dots, h_{M-1,k}]^T \in \mathbb{C}^M. \quad (3)$$

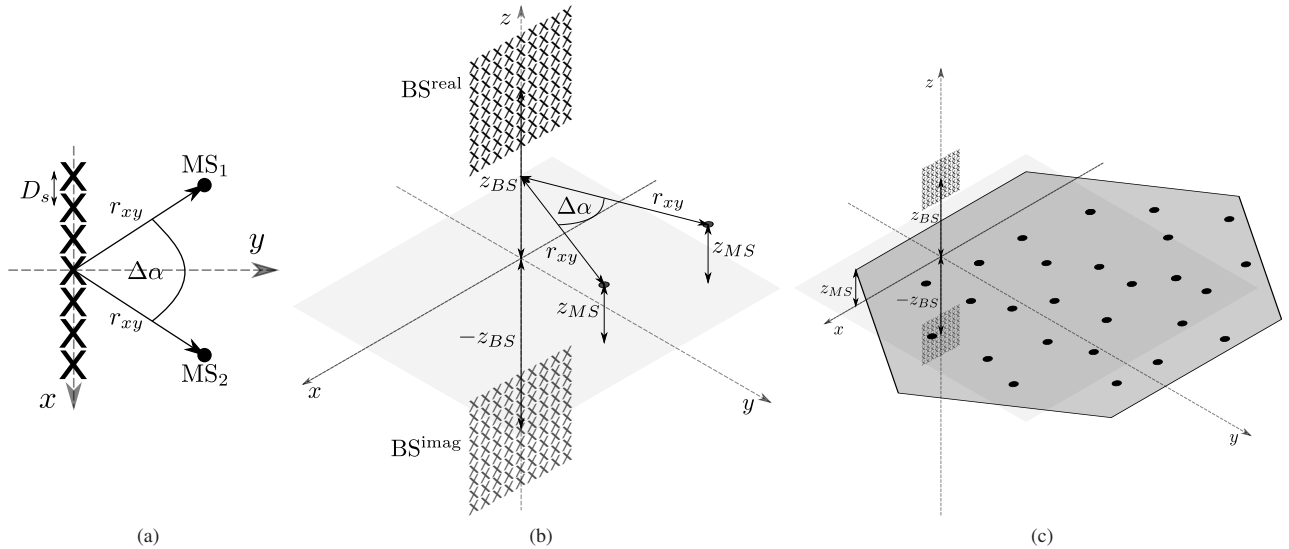


Figure 4. Different model scenarios. (a) depicts the one-dimensional case, whereas in (b), the two-dimensional case was drawn, with the mirror image antenna array utilized to model perfect reflection. In (c), uniformly distributed users are presented in a hexagonal cell.

Second, each antenna element is modeled by a half-wavelength dipole. At a given point in space, the field components of every dipole can be evaluated [8]. We assume that the dipoles are pointing toward the z axis, just as the antennas of the terminals. Therefore, the received signal is proportional to the z component of the electric field. As a result, the channel can be modeled as

$$h_{m,k} = \frac{E_z^m(\vec{r}_k)}{I_0^m}, \quad (4)$$

where $E_z^m \in \mathbb{C}$ is a phasor which represents the z component of the electric field created by the m^{th} BS antenna, \vec{r}_k is the position of the k^{th} terminal. $I_0^m \in \mathbb{C}$ is a phasor – with the same frequency as E_z^m – representing the excitation of the m^{th} BS antenna. Let $I_0^m = 1$ A for arbitrary m . Again, the channel vector is constructed as (3).

Third, as the most realistic model, simple directional antenna elements were employed. A straightforward way to achieve directivity is to use two half-wavelength dipoles and a perfect reflector behind them. Both dipoles should point toward the z axis. In spite of the fact that the distance between them is in the order of magnitude of wavelength, coupling effects will be neglected. This assumption will be supported by results that will be presented in Section V-B. The perfect reflector must be placed $\frac{\lambda}{2}$ from the dipoles to obtain the directivity. Subsequently, with an electrostatic analogy, the perfect reflector's effect can be modeled in terms of mirror image dipoles. Therefore, the resulting EM field will be identical if two other dipoles are placed behind the original ones at the distance of λ . As a result, each antenna is modeled by four half-wavelength dipoles. Since, the electromagnetic field of the dipoles are known analytically, \mathbf{h} can be obtained similarly to (4) and (3) [8].

After the above-described models, a natural question might follow whether these models include the polarization of electromagnetic waves. The spherical-wave model neglects this ef-

fect. However, if the field of the antenna elements is evaluated analytically, the polarization is also included. However, this only holds if the EM field is evaluated analytically. Therefore, from the evaluated electromagnetic field, a more accurate channel model can be derived.

B. One- and two-dimensional arrays

Two different model assumptions will be compared. The first approach is when only a one-dimensional array is considered. Thus, the mobile stations and the base station are in the same plane, as in Figure 4a.

In the second, novel approach, the antenna array is two dimensional, located in the $x - z$ plane, while users are in the $x - y$ plane. Mobile stations are assumed to be at a height of z_{MS} above the ground. Furthermore, if we neglect the reflection from other buildings and obstacles, there is at least one significant reflection from the ground. Let us consider a perfect reflection. Thus, the utilization of a mirror image antenna array will result in an identical electromagnetic, as we did to obtain a directional pattern. Therefore, the channel model must be modified as follow

$$h_{m,k} = h_{m,k}^{real} + h_{m,k}^{imag}, \quad (5)$$

where $h_{m,k}^{real}$ corresponds to the channel between the m^{th} antenna of the MS and k^{th} antenna of the real BS, whereas $h_{m,k}^{imag}$ represents the channel between the m^{th} antenna of the MS and k^{th} antenna of the mirror image BS. Figure 4b depicts this above described assumption. Modeling the ground reflection by means of a mirror image antenna array also includes the effect of polarization change, since boundary conditions are fulfilled on the ground.

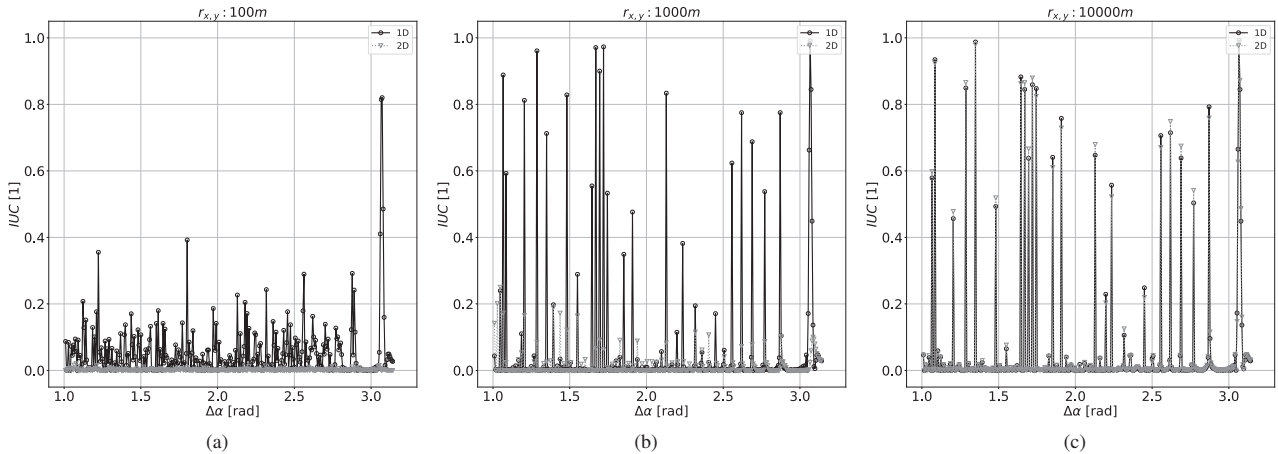


Figure 5. Comparing one- and two-dimensional models in terms of $IUC(\Delta\alpha)$.

C. Array geometry

Three different two-dimensional array geometries will be considered. The first one is an equidistant array, with parameters $N_{row} \times N_{col}$ and D_s .

Secondly, if we add random displacement to the x and z coordinates of each element of the equidistant case, a randomized array will be obtained. The displacements in both x and z directions are characterized by a normal distribution with standard deviation σ_{D_s} .

Lastly, we consider a scenario where the antenna elements are placed on a logarithmic spiral pattern. An analogy from acoustics inspired this scenario, where sensors are occasionally located on a spiral. The parameters of the spiral array are the distance of the closest and the farthest antenna element from the center of the array, the number of turns in the spiral and the number of antennas, denoted by R_{min} , R_{max} , N_{turn} and M , respectively. In polar coordinates (r, ϕ) , the equation of the logarithmic spiral is $r = R_{min}e^{k\phi}$, where k is a constant parameter, which calculated from R_{max} and N_{turn} . The antennas are positioned along with the pattern of the spiral, equal distance apart.

V. SIMULATION RESULTS AND DISCUSSION

A simulation framework has been developed in Python based on the models in Section IV. The metrics of the analysis will be introduced before the presentation of the results. Let us note here that a narrowband analysis is presented in this paper. However, the presented models hold in a wide frequency band. Investigating the behavior of the system for wideband signal excitation is left for further studies.

A. Comparing one- and two-dimensional array models

In order to compare the approaches mentioned in Section IV-B, the inter-user correlation will be evaluated between two users. The IUC is calculated as the inner product of the channel vectors of the two users

$$IUC = \frac{|\mathbf{h}_1^H \mathbf{h}_2|^2}{\|\mathbf{h}_1\|^2 \|\mathbf{h}_2\|^2}. \tag{6}$$

This quantity is a standard measure of the correlation of MIMO channels. The two users are located at the same distance from the BS (denoted by r_{xy}), and the angle between them (denoted by $\Delta\alpha$) is varied, see Figure 4a. As it is expected from (6), $IUC \in [0, 1]$. Higher IUC indicates stronger interference between users. Therefore, lower IUC is desired, thus the inter-user interference is smaller, which results in higher spectral efficiency. Besides, the appearance of grating lobes ($D_s \geq \lambda/2$) or side lobes will introduce inter-user correlation peaks.

A one-dimensional equidistant array with 20 antennas is simulated for the first modeling approach, only with the assumption of LoS propagation. For analyzing the second approach, a 20×20 equidistant array is utilized, and the ground reflection is accounted as well. In both cases spherical-wave propagation model is employed, D_s is 3 m and $f = 6$ GHz. In the two-dimensional model, the center of the antenna array is at a height of $z_{MS} = 40$ m above ground and the terminals are located at a height of $z_{MS} = 1.5$ m above the ground. In such a scenario, the size of the near-field is $R_F \approx 260$ km, as shown in Table I. The two users were located at the distances $r_{xy} = \{100\text{ m}, 1\text{ km}, 10\text{ km}\}$. The results of the IUC analyses are shown in Figure 5. The employed antenna spacing ($D_s = 3$ m) gave rise to multiple peaks in the $IUC(\Delta\alpha)$ graphs. As has been mentioned, this is due to the appearance of grating and side lobes. Closer to the array, the peaks correspond to smaller values, since the near-field effects mitigate the effect of grating lobes. As going farther from the array, peaks are becoming higher. Taking the reflection and real physical dimension into account results in lower IUC. Therefore if the simulation of a near-field scenario is required, the two-dimensional model is more accurate. Consequently, in the following simulations, the two-dimensional model will be utilized. On the contrary, the results of the two models converge to the same graph as the distance from the array increases, which is in line with our expectation. Thus, for far-field analysis, the simple model can be accurate enough.

Modeling the near-field of extremely large aperture arrays in massive MIMO systems

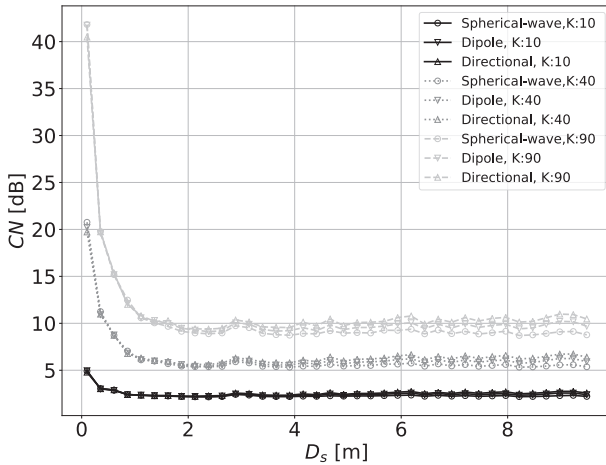


Figure 6. Condition number along with the element spacing of equidistant arrays for comparing propagation models.

B. Comparison of antenna element models

As has been described in Section IV-A, three different modeling approaches is considered: spherical-wave model, half-wavelength dipole, and a simple directional antenna element. The comparison is made in terms of the condition number of the multi-user channel matrix. The varying parameter is the spacing between the antenna elements (D_s). An equidistant antenna array with 20×20 elements is simulated, $f = 3$ GHz, $z_{MS} = 40$ m and the users are located in a hexagonal cell right in front of the array, at a height of $z_{MS} = 1.5$ m above ground, as depicted in Figure 4c. The cell radius is 250 m, and the users were uniformly distributed within the cell.

If the distance of the users from the BS differ significantly, power control will be required to provide the same service quality in the cell. There are multiple power control strategies [13]. In the following, an ideal power control technique will be used, thus the power of the received signal is identical for every user. Similarly to Normalization 1 in [14]

$$\mathbf{H}^{\text{norm}} = \left[\frac{\mathbf{h}_0}{\|\mathbf{h}_0\|}, \frac{\mathbf{h}_1}{\|\mathbf{h}_1\|}, \dots, \frac{\mathbf{h}_{K-1}}{\|\mathbf{h}_{K-1}\|} \right] \in \mathbb{C}^{M \times K}. \quad (7)$$

s (7) sets the channel of each user to the same norm. The condition number is evaluated based on \mathbf{H}^{norm} and defined as [5]

$$\text{CN}^{\text{dB}} = 20 \log_{10} \left(\frac{\sigma_g}{\sigma_s} \right), \quad (8)$$

where σ_g and σ_s are the largest and smallest singular values of the normalized multi-user channel matrix (\mathbf{H}^{norm}). The condition number strongly related to the orthogonality of the columns of the channel matrix. The evaluation of the inverse of (\mathbf{H}) is required for many massive MIMO transmission schemes. Positively, condition number also indicates the stability of the inversion [5]. In practical terms lower condition number indicates easier inversion and less correlated columns, for example, $\text{CN}^{\text{dB}} = 0$ for an identity matrix, since its inverse is trivial and its columns are orthogonal.

The condition number has been evaluated in 1000 different realizations, with varying MS positions as described above.

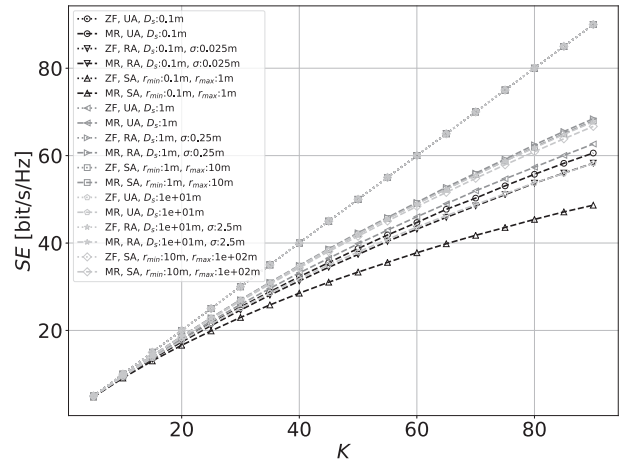


Figure 7. Cumulative spectral efficiency along with the number of users for different array geometries and precoding strategies. Dotted curves used for ZF precoding and dashed for MR, identical array settings are denoted with the same markers. The abbreviations EA, RA, SA stand for equidistant, randomized and spiral array, respectively.

In Figure 6 the average CN is plotted along D_s . The first observation is that the condition number shows a decreasing tendency as D_s increases, independent of the used antenna model or the number of users. Therefore, increasing the size of the aperture is beneficial, as mentioned in Section III. Interesting observation, that in the first part ($D_s \in [\lambda, \approx 10\lambda]$) of the investigated D_s range, the condition number decreases rapidly. In the second part ($D_s \in [\approx 10\lambda, \approx 100\lambda]$), it becomes approximately constant, it even increases a little, for particular antenna models. Consequently, based on the scenario, an element spacing range can be specified, where the system can provide a well-conditioned channel.

One might question the periodic peaks in the $\text{CN}(D_s)$ curves. This occurs because of the contribution of two effects. First, the reduction of the width of the main lobe and the correlation between the users are decreasing functions of D_s , whereas, grating lobes appear at discrete D_s values, thus introducing peaks [5].

A relatively straightforward observation, that service quality will degrade if more users are transmitting simultaneously. Since for more terminals the mean of the $\text{CN}^{\text{dB}}(D_s)$ curves are clearly larger.

Finally, there is no significant difference between the used models in terms of condition number. Therefore, using the spherical-wave model is enough to acquire channel features. Besides, by using a more accurate model, a slightly higher condition number is obtained, which indicates that an upper boundary of the system performance will result from the spherical-wave model. Based on these results, including the polarization of the electromagnetic waves seems to have minor effects.

C. Comparing different array geometries

In Section IV-C two different array geometries have been defined. In the following, these two will be compared in

terms of spectral efficiency. SE also gives an insight into the performance of the extremely large aperture array. The evaluation of the inter-user correlation and the condition number of the multi-user channel matrix are the same for uplink and downlink systems. On the contrary, spectral efficiency must be evaluated based on the direction of the data transmission. In the simulation, a downlink scenario is considered. In this case the received signal vector $\mathbf{y} \in \mathbb{C}^K$ is given by

$$\mathbf{y} = \mathbf{H}^T \mathbf{W} \mathbf{P} \mathbf{x} + \mathbf{w}, \quad (9)$$

where $\mathbf{W} \in \mathbb{C}^{M \times K}$ is the precoding matrix, $\mathbf{P} \in \mathbb{C}^{K \times K}$ is a diagonal matrix capturing the effects of the power control, $\mathbf{x} \in \mathbb{C}^K$ is the transmit signal vector and $\mathbf{w} \in \mathbb{C}^K$ represents the additive white Gaussian noise, $\mathbf{w} \sim \mathcal{CN}(0, \sigma_{DL}^2 \mathbf{I}_K)$. For the transmit signal vector $\mathbb{E}\{\mathbf{x}\mathbf{x}^H\} = \mathbf{I}_K$ holds. Each column $\mathbf{w}_k \in \mathbb{C}^M$ of \mathbf{W} corresponds to the coefficients which are used to precode the data x_k dedicated to the k^{th} MS.

Similarly to (7), the power control can be expressed by a diagonal matrix, constructed as

$$\mathbf{P} = \text{diag} \left[\frac{\rho_0}{\|\mathbf{h}_0\|}, \frac{\rho_1}{\|\mathbf{h}_1\|}, \dots, \frac{\rho_{K-1}}{\|\mathbf{h}_{K-1}\|} \right] \in \mathbb{C}^{K \times K}, \quad (10)$$

where the square of $\rho_k, k = 0, 1, \dots, K - 1$ represents the target transmit power for user k . For the simulation, we consider $\rho_k = \rho_{DL}, \forall k$. Consequently, $\mathbf{P} = \rho_{DL} \mathbf{I}_K$. Two different precoding strategies are considered. The first one is the maximum ratio (MR) processing, in this case

$$\mathbf{W}_{MR} = (\mathbf{H}^{\text{norm}})^*, \quad (11)$$

where \mathbf{H}^{norm} is obtained as (7). The underlying idea of the MR processing is to amplify the signal of interest maximally and neglect the effect of interference [13]. The second is zero-forcing (ZF) processing which aims to mitigate interference among users, by the utilization of (7)

$$\mathbf{W}_{ZF} = (\mathbf{H}^{\text{norm}})^* \left((\mathbf{H}^{\text{norm}})^T (\mathbf{H}^{\text{norm}})^* \right)^{-1}. \quad (12)$$

In (12) the requirement of the inversion is fulfilled if the user channels are orthogonal, which holds if the base station is equipped with a sufficient number of antennas [15]. (11) and (12) are almost identical to (3.57) and (3.49) in [13], the multiplicative constants is removed because of the used power control strategy.

It can be concluded from (9) that in order to transmit data x_k which is dedicated to the k^{th} MS, x_k is multiplied by $[\mathbf{W}]_{m,k}$ before it is being transmitted at the m^{th} BS antenna. As a consequence, in a distributed system with one antenna, it is enough to store a single row of \mathbf{W} . The maximum ratio precoding has a considerable advantage that it can be deployed in a distributed system because each row of \mathbf{W}_{MR} can be obtained by knowing the corresponding row of \mathbf{H}^{norm} . In contrast, ZF processing requires centralized control because of the calculation of \mathbf{W}_{ZF} . On the other hand, zero-forcing will deliver higher SE than maximum ratio processing.

The evaluation of the downlink spectral efficiency simplifies owing to the simulated \mathbf{H} , which provides a perfect channel state information. Therefore, the expectations in (4.26) from

[11] simplifies and the signal-to-interference-noise can be expressed as

$$\text{SINR}_k = \frac{\left| [\mathbf{H}^T \mathbf{W} \rho_{DL}]_{k,k} \right|^2}{\sum_{j=0, j \neq k}^{K-1} \left| [\mathbf{H}^T \mathbf{W} \rho_{DL}]_{k,k} \right|^2 + \sigma_{DL}^2}, \quad (13)$$

where $\mathbf{P} = \rho_{DL} \mathbf{I}_K$ and continuous downlink transmission is assumed. Thus, the lower bound of the sum ergodic downlink spectral efficiency is

$$\text{SE} = \sum_{k=0}^{K-1} \log_2 (1 + \text{SINR}_k). \quad (14)$$

In the simulation, \mathbf{H} is known explicitly based on a particular realization. Therefore in (13) and (14) all the variables can be considered as deterministic. In order to simulate the random behavior of the users, spectral efficiency is calculated in 1000 different scenarios, with equally distributed random user positions within the cell. The average SE is visible in Figure 7. The parameters of the simulation are considered as for the evaluation of condition number, described in Section V-B. The only differences are the array geometry and postprocessing, since spectral efficiency is calculated, with $\rho_{DL} = \sigma_{DL} = 1$. The changing parameters $\sigma_{D_s}, R_{min}, R_{max}$ are denoted on the obtained curves, whereas $N_{turn} = 4$ is constant.

The first observation is that the ZF precoding significantly outperforms the MR precoding, independent of array geometry and aperture size. Therefore, the core concept of ZF precoding is realized here, since it has successfully suppressed all the interference between the users. Thus the curves corresponding to ZF precoding overlap. Also, ZF is more complex to implement because of its centralized fashion. Therefore, the comparison based on MR precoding is more relevant from practical perspectives.

It is important to note that in Figure 7 the cumulative spectral efficiency is plotted, thus in case of the MR precoding, spectral efficiency of a single user is a decreasing function of K . Therefore, the size of the system is limited by the target spectral efficiency of a single user. If higher SE is required for a single user, the number of BS antennas must be increased. However, it is essential to keep it at least an order of magnitude higher than the number of concurrently transmitting terminals.

As it was expected, increasing the size of the aperture resulted in a higher spectral efficiency, if we are considering MR precoding. This increment is significant if $D_s = 0.1 \text{ m}$ and $D_s = 1 \text{ m}$ are compared. However, the difference between the $D_s = 1 \text{ m}$ and $D_s = 10 \text{ m}$ is negligible. Furthermore, in case of the spiral array, $r_{min} = 10 \text{ m}$ array is outperformed by the $r_{min} = 1 \text{ m}$ array. The results corresponds with the $\text{CN}(D_s)$ curves in Figure 6, since the condition number does not vary significantly for $D_s \gg 1 \text{ m}$.

Finally, if large apertures are considered, there is no significant difference between the different array geometries. Even though the random and equidistant arrays outperform the spiral array for small apertures, as increasing the distance between the antennas, this difference diminishes. Consequently, the positions of the array elements of a realized ELAA can almost be arbitrary, which is beneficial from a practical perspective.

Modeling the near-field of extremely large aperture arrays in massive MIMO systems

VI. CONCLUSION

In the presented work, we analyzed the effect of modeling accuracy, aperture geometry and different antenna implementations in typical near-field ELAA scenarios. We demonstrated that simple line-of-sight propagation models overestimate inter-user correlation, whereas a more accurate model that considers ground reflections yields improved user separation capability, thus emphasizing the need for more detailed, physically motivated channel modeling approaches. Furthermore, it has been shown that the performance of the system only weakly depends on the actual implementation of the antenna elements. The condition number of the multi-user channel matrix will show similar statistics irrespective of the accuracy of the field strength calculation (simple ray-based vs. analytical calculation of the electromagnetic field). Finally, we demonstrated that increasing the size of the aperture, at least to some extent, while keeping the number of antennas identical, will yield higher spectral efficiency. On the other hand, the results are relatively independent on the actual array geometry. Therefore, antenna elements can be placed almost arbitrarily, which is beneficial from a practical implementation perspective. In conclusion, the size of the aperture can be identified as a key design parameter, with spectral efficiency being the design objective.

ACKNOWLEDGMENT

The research presented in this paper was supported by the EFOP-3.6.2-16-2017-00013 project.

REFERENCES

[1] T. L. Marzetta, "Massive MIMO: an introduction," *Bell Labs Technical Journal*, vol. 20, pp. 11–22, 2015, doi: 10.15325/BLTJ.2015.2407793.

[2] E. Björnson, J. Hoydis, and L. Sanguinetti, "Massive MIMO has unlimited capacity," *IEEE Transactions on Wireless Communications*, vol. 17, no. 1, pp. 574–590, 2017, doi: 10.1109/TWC.2017.2768423.

[3] Björnson, Emil and Sanguinetti, Luca and Wymeersch, Henk and Hoydis, Jakob and Marzetta, Thomas L, "Massive MIMO is a reality—What is next?: Five promising research directions for antenna arrays," *Digital Signal Processing*, 2019, doi: 10.1016/j.dsp.2019.06.007.

[4] A. Amiri, M. Angjelichinoski, E. De Carvalho, and R. W. Heath, "Extremely large aperture massive MIMO: Low complexity receiver architectures," in *2018 IEEE Globecom Workshops*. 9-13 Dec. 2018, Abu Dhabi, United Arab Emirates: IEEE, 2018, pp. 1–6, doi: 10.1109/GLOCOMW.2018.8644126.

[5] D. Pinchera, M. D. Migliore, F. Schettino, and G. Panariello, "Antenna arrays for line-of-sight massive MIMO: Half wavelength is not enough," *Electronics*, vol. 6, no. 3, p. 57, 2017, doi: 10.3390/electronics6030057.

[6] S. Pratschner, E. Zöchmann, H. Groll, S. Caban, S. Schwarz, and M. Rupp, "Does a large array aperture pay off in line-of-sight massive MIMO?" in *2019 IEEE 20th International Workshop on Signal Processing Advances in Wireless Communications*. 2-5 July 2019, Cannes, France: IEEE, 2019, pp. 1–5, doi: 10.1109/SPAWC.2019.8815590.

[7] Z. Zhou, X. Gao, J. Fang, and Z. Chen, "Spherical wave channel and analysis for large linear array in LoS conditions," in *2015 IEEE Globecom Workshops*. 6-10 Dec. 2015, San Diego, CA: IEEE, 2015, pp. 1–6, doi: 10.1109/GLOCOMW.2015.7414041.

[8] C. A. Balanis, *Antenna theory: analysis and design*, 3rd ed. John Wiley & Sons, 2005, ISBN: 9780471667827.

[9] E. Björnson, "A look at an LTE-TDD massive MIMO product," accessed: 2020-10-05. [Online]. Available: <http://ma-mimo.ellintech.se/2018/08/27/a-look-at-an-lte-tdd-massive-mimo-product/>

[10] À. O. Martínez, E. DeCarvalho, and J. Ø. Nielsen, "Towards very large aperture massive MIMO: A measurement based study," in *2014 IEEE Globecom Workshops*. 8-12 Dec. 2014, Austin, TX: IEEE, 2014, pp. 281–286, doi: 10.1109/GLOCOMW.2014.7063445.

[11] E. Björnson, J. Hoydis, and L. Sanguinetti, "Massive MIMO networks: Spectral, energy, and hardware efficiency," *Foundations and Trends in Signal Processing*, vol. 11, no. 3-4, pp. 154–655, 2017, doi: 10.1561/20000000093.

[12] B. Sklar, "Rayleigh fading channels in mobile digital communication systems. i. characterization," *IEEE Communications magazine*, vol. 35, no. 7, pp. 90–100, 1997, doi: 10.1109/35.601747.

[13] T. L. Marzetta, *Fundamentals of massive MIMO*, 1st ed. Cambridge University Press, 2016, doi: 10.1017/CBO9781316799895.

[14] X. Gao, O. Edfors, F. Rusek, and F. Tufvesson, "Massive MIMO performance evaluation based on measured propagation data," *IEEE Transactions on Wireless Communications*, vol. 14, no. 7, pp. 3899–3911, 2015, doi: 10.1109/TWC.2015.2414413.

[15] H. Prabhu, J. Rodrigues, O. Edfors, and F. Rusek, "Approximative matrix inverse computations for very-large mimo and applications to linear precoding systems," in *2013 IEEE Wireless Communications and Networking Conference*. 7-10 April 2013, Shanghai: IEEE, 2013, pp. 2710–2715, doi: 10.1109/WCNC.2013.6554990.



Botond Tamás Csathó is an MSc student at the Budapest University of Technology and Economics specialized in Wireless Networks and Applications. He received his BSc in 2019 at the same institute. His research interest focuses on massive MIMO networks, channel modeling and channel estimation. He is the member of the BME Balatonfűredő Student Research Group.



Bálint Péter Horváth received his M.Sc. (2013) and Ph.D. (2018) degrees in Electrical Engineering from the Budapest University of Technology and Economics where he is currently a senior lecturer at the Department of Broadband Infocommunications and Electromagnetic Theory. His research interests include signal processing in communications systems, software defined radio and computational model validation of portable wireless devices.



Péter Horváth obtained his Diploma degree at Budapest University of Technology and Economics (BME) and at Technical University of Karlsruhe, Germany. He received his PhD at BME in 2010, then he was a postdoctoral researcher at Vanderbilt University, USA. He is currently an associate professor in the Department of Broadband Infocommunications and Electromagnetic Theory at BME. His research interests include mobile wireless communications, cognitive radio and dynamic spectrum access technologies, channel modeling in multiple-antenna systems and signal design for satellite communications.

DRCN 2021

Design of Reliable Communication Networks
 19-22 April 2021 - Milan, Italy



Call for Papers

SCOPE

Since its creation in 1998, the *International Conference on the Design of Reliable Communication Networks (DRCN)* has become over the years a well-established forum for scientists from both industry and academy who have interest in reliability and availability of communication networks, and related resilience topics. The aim of the conference is to bring together people from various disciplines, ranging from engineering of survivable equipment and network technologies to network management and monitoring, through methods and models for survivable and robust network design. As such, DRCN is a well-known forum for presenting excellent results and new challenges in the field of reliable communication networks and services.

We are pleased to invite you to contribute and participate in the 17th edition of DRCN in Milan, Italy, on April 19-22, 2021.

Topics of interest for submission include, but are not limited to:

- Resilience in 5G networks and services
- Ultra-Reliable Low-Latency Communications (URLLC)
- Design of resilient and reliable IoT systems
- Resilience in Software-Defined Networking (SDN)
- Secure and reliable quantum communications
- Resilience in satellite communication networks
- High availability for Network Functions Virtualization (NFV) infrastructures
- Network dependability in cloud networking
- Dependability and reliability of wireless/cellular/mobile networks
- Resilience in FSO/VLC communications
- Survivability and traffic engineering for optical, IP and multi-layer networks
- Robustness of multi-domain networks
- Survivability in grid and distributed computing
- Reliability and resiliency of data center networks
- Recovery of overlay and peer-to-peer networks
- Risk and reliability in the Internet and enterprise networks
- Communication reliability for smart city applications and intelligent transport systems
- Methods for survivable network and systems design, analysis, and operation
- Planning and optimization of reliable networks, systems, and services
- Network reliability analysis
- Reliability and robustness of networks optimized and managed based on AI/ML techniques
- Data analytics and Machine Learning for fault diagnosis
- Network coding techniques to improve resilience
- Service differentiation based on recovery methods
- Simulation techniques for network resilience
- Quality of Experience (QoE) and network service availability assessments
- Reliability requirements and metrics for users, businesses, and the society
- Robustness of compound services
- Resilience and security of networked critical infrastructures
- Network robustness to natural disasters
- Robust network design for hostile environments
- Security issues in networks and their relation to survivability
- Network dependability and energy consumption trade-offs
- Network resilience combined with economics and commercial issues
- Standardization of network resilience and reliability
- Public policy issues for survivability and resilience
- Design and test of reliable operational technology (OT) networks



IMPORTANT DATES

Submission deadline: **November 10, 2020**

Notification to authors: **January 15, 2021**

Camera Ready Papers: **February 7, 2021**

For more information, visit: <http://www.drcn2021.polimi.it>

Guidelines for our Authors

Format of the manuscripts

Original manuscripts and final versions of papers should be submitted in IEEE format according to the formatting instructions available on

<https://journals.ieeeauthorcenter.ieee.org/>
Then click: "IEEE Author Tools for Journals"
- "Article Templates"
- "Templates for Transactions".

Length of the manuscripts

The length of papers in the aforementioned format should be 6-8 journal pages.

Wherever appropriate, include 1-2 figures or tables per journal page.

Paper structure

Papers should follow the standard structure, consisting of *Introduction* (the part of paper numbered by "1"), and *Conclusion* (the last numbered part) and several *Sections* in between.

The Introduction should introduce the topic, tell why the subject of the paper is important, summarize the state of the art with references to existing works and underline the main innovative results of the paper. The Introduction should conclude with outlining the structure of the paper.

Accompanying parts

Papers should be accompanied by an *Abstract* and a few *index terms* (*Keywords*). For the final version of accepted papers, please send the short cvs and *photos* of the authors as well.

Authors

In the title of the paper, authors are listed in the order given in the submitted manuscript. Their full affiliations and e-mail addresses will be given in a footnote on the first page as shown in the template. No degrees or other titles of the authors are given. Memberships of IEEE, HTE and other professional societies will be indicated so please supply this information. When submitting the manuscript, one of the authors should be indicated as corresponding author providing his/her postal address, fax number and telephone number for eventual correspondence and communication with the Editorial Board.

References

References should be listed at the end of the paper in the IEEE format, see below:

- a) Last name of author or authors and first name or initials, or name of organization
- b) Title of article in quotation marks
- c) Title of periodical in full and set in italics
- d) Volume, number, and, if available, part
- e) First and last pages of article
- f) Date of issue
- g) Document Object Identifier (DOI)

[11] Boggs, S.A. and Fujimoto, N., "Techniques and instrumentation for measurement of transients in gas-insulated switchgear," *IEEE Transactions on Electrical Installation*, vol. ET-19, no. 2, pp.87–92, April 1984. DOI: 10.1109/TEI.1984.298778

Format of a book reference:

[26] Peck, R.B., Hanson, W.E., and Thornburn, T.H., *Foundation Engineering*, 2nd ed. New York: McGraw-Hill, 1972, pp.230–292.

All references should be referred by the corresponding numbers in the text.

Figures

Figures should be black-and-white, clear, and drawn by the authors. Do not use figures or pictures downloaded from the Internet. Figures and pictures should be submitted also as separate files. Captions are obligatory. Within the text, references should be made by figure numbers, e.g. "see Fig. 2."

When using figures from other printed materials, exact references and note on copyright should be included. Obtaining the copyright is the responsibility of authors.

Contact address

Authors are requested to submit their papers electronically via the EasyChair system. The link for submission can be found on the journal's website:

www.infocommunications.hu/for-our-authors

If you have any question about the journal or the submission process, please do not hesitate to contact us via e-mail:

Editor-in-Chief: Pál Varga – pvarga@tmit.bme.hu

Associate Editor-in-Chief:

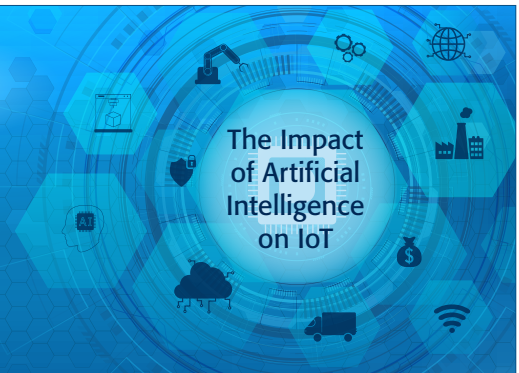
Rolland Vida – vida@tmit.bme.hu

László Bacsárdi – bacsardi@hit.bme.hu



The 7th IEEE World Forum on the Internet of Things - WFIoT2021

20-24 June 2021 // Hilton Riverside Hotel, New Orleans, Louisiana, USA



CALL FOR PAPERS

The IEEE World Forum on the Internet of Things (WFIoT2021) seeks submissions and proposals for original technical papers that address the Internet of Things (IoT), its theoretical and technological building blocks, the applications that drive the growth and evolution of IoT, operational considerations, experimentation, experiences from deployments, and the impacts of IoT on consumers, the public sector, and industrial verticals. The theme for the World Forum is “The Impact of Artificial Intelligence on IoT”. In recognition of the rapid growth of IoT across the world and adoption across almost all verticals we encourage the submission of multi-disciplinary content. Papers should address, but are not limited to, the high-level topics below and a more detailed list found on the WFIoT2021 website that can be downloaded as a PDF document:

- Applications, Processes, and Services
- Artificial Intelligence, Machine Learning, and Analytics
- Basic and Enabling Technologies
- Communication, Connectivity, and Networking
- Computing – from Edge to Cloud
- Cybersecurity, Security, and Privacy
- Infrastructure, Devices, and Components
- Information Processing from Multimedia and Heterogenous Sources
- Results from Experiments, Demonstrations and Trials, and Deployment Experiences
- Social and Societal Impacts
- Systems Engineering, Integration Methods, and Operation Technologies
- Theoretical foundations, design methods, and architectural considerations

In addition, the World Forum is also seeking proposals for: (1) Special Sessions consisting of peer reviewed papers focused on research topics of importance to IoT; (2) Workshops consisting of peer reviewed papers, discussions, and summary results about advanced topics relevant to IoT. The summary results will be edited and published as part of the WFIoT2021 Proceedings; and (3) Industry Panels aimed at research topics important to industrial IoT issues. Each, Special Session, Workshop, and Industry Panel, once selected will issue an individual call for papers.

IMPORTANT DEADLINES

Paper Submission Due Date:
15 January 2021

Acceptance Notification:
15 March 2021

Camera-Ready Submission:
19 April 2021

Sponsored by the IEEE Multi-Society IoT Initiative
Hosted by The University of Louisiana at Lafayette
Held in conjunction with the IoT Community Slam



For more information, visit wfiot2021.iot.ieee.org

SCIENTIFIC ASSOCIATION FOR INFOCOMMUNICATIONS



Who we are

Founded in 1949, the Scientific Association for Infocommunications (formerly known as Scientific Society for Telecommunications) is a voluntary and autonomous professional society of engineers and economists, researchers and businessmen, managers and educational, regulatory and other professionals working in the fields of telecommunications, broadcasting, electronics, information and media technologies in Hungary.

Besides its 1000 individual members, the Scientific Association for Infocommunications (in Hungarian: HÍRKÖZLÉSI ÉS INFORMATIKAI TUDOMÁNYOS EGYESÜLET, HTE) has more than 60 corporate members as well. Among them there are large companies and small-and-medium enterprises with industrial, trade, service-providing, research and development activities, as well as educational institutions and research centers.

HTE is a Sister Society of the Institute of Electrical and Electronics Engineers, Inc. (IEEE) and the IEEE Communications Society.

What we do

HTE has a broad range of activities that aim to promote the convergence of information and communication technologies and the deployment of synergic applications and services, to broaden the knowledge and skills of our members, to facilitate the exchange of ideas and experiences, as well as to integrate and

harmonize the professional opinions and standpoints derived from various group interests and market dynamics.

To achieve these goals, we...

- contribute to the analysis of technical, economic, and social questions related to our field of competence, and forward the synthesized opinion of our experts to scientific, legislative, industrial and educational organizations and institutions;
- follow the national and international trends and results related to our field of competence, foster the professional and business relations between foreign and Hungarian companies and institutes;
- organize an extensive range of lectures, seminars, debates, conferences, exhibitions, company presentations, and club events in order to transfer and deploy scientific, technical and economic knowledge and skills;
- promote professional secondary and higher education and take active part in the development of professional education, teaching and training;
- establish and maintain relations with other domestic and foreign fellow associations, IEEE sister societies;
- award prizes for outstanding scientific, educational, managerial, commercial and/or societal activities and achievements in the fields of infocommunication.

Contact information

President: **FERENC VÁGUJHELYI** • elnok@hte.hu

Secretary-General: **ISTVÁN MARADI** • istvan.maradi@gmail.com

Operations Director: **PÉTER NAGY** • nagy.peter@hte.hu

International Affairs: **ROLLAND VIDA, PhD** • vida@tmit.bme.hu

Address: H-1051 Budapest, Bajcsy-Zsilinszky str. 12, HUNGARY, Room: 502

Phone: +36 1 353 1027

E-mail: info@hte.hu, Web: www.hte.hu